SYNTHESIS AND CHARACTERISATION OF SYMMETRICAL DIMER CONTAINING CHALCONE MOIETY

ELEEN DAYANA BINTI MOHAMED ISA

BACHELOR OF SCIENCE (HONS) CHEMISTRY

FACULTY OF SCIENCE

UNIVERSITI TUNKU ABDUL RAHMAN

MAY 2014

ABSTRACT

SYNTHESIS AND CHARACTERIZATION OF SYMMETRICAL DIMER CONTAINING CHALCONE MOIETY

ELEEN DAYANA BINTI MOHAMED ISA

This study mainly focuses on synthesis and characterization of symmetrical dimer containing chalcone moiety, α,ω-bis(3-(4-dodecyloxyphenyl)-1-(phenyl-4-oxy)prop-2-en-1-one)alkane, (DCnC), where n = 3 (**DC3C),** n = 4 (**DC4C**), n = 5 (**DC5C**) and n = 6 (**DC6C)**. The project started with the synthesis of intermediate compound, 4-dodecyloxybenzaldehyde (**DDB**) and followed by 3-(4-dodecyloxyphenyl)-1-(4-hydroxyphenyl)prop-2-en-1-one (**DHP**). Then **DHP** is etherified using α,ω-dibromoalkane in order to obtain **DCnC**. The structure of **DCnC** were confirmed by using FTIR, ^{1}H NMR and ^{13}C NMR spectroscopic techniques. The thermal and optical properties were studied using DSC and UV-Vis spectrophotometry. From DSC analysis, all compounds in **DCnC** series show direct isotropization without exhibiting liquid crystalline phase. UV-Vis results show that all compounds undergo π-π* transition with strong intramolecular charge transfer character.

ABSTRAK

SINTESIS AND PENCIRIAN CHALCONE DERIVATIF

ELEEN DAYANA BINTI MOHAMED ISA

Kajian in tertumpu kepada sintesis dan pencirian dimer simetri mangandungi chalcone, α,ω-bis(3-(4-dodecyloxyphenyl)-1-(phenyl-4-oxy)prop-2-en-1-one)alkana, (DCnC), di mana n = 3 (**DC3C),** n = 4 (**DC4C**), n = 5 (**DC5C**) and n = 6 (**DC6C)**. Projek ini dimulakan dengan tindak balas sebatian pertengahan, 4-dodecyloxybenzaldehide (**DDB**) dan seterusnya 3-(4-dodecyloxyphenyl)-1-(4-hydroxyphenyl)prop-2-en-1-one (**DHP**). Kemudian sebatian **DHP** dieterkan menggunakan α,ω-dibromoalkana untuk mendapatkan **DCnC.** Struktur **DCnC** ditentukan menggunakan teknik spektroskopi FTIR, ^{1}H dan ^{13}C resonans magnetik nuklear. Ciri-ciri thermal dan optikal dikaji menggunakan DSC dan UV-Vis foto-spektrometer. Daripada DSC analisis, sebatian **DCnC** menunjukkan isotropasi terus tanpa melalui fasa kristal cecair. Berdasarkan keputusan dari UV-Vis, semua sebatian **DCnC** mangalami π-π* peralihan dengan alihan cas intramolekular yang kuat.

ACKNOWLEDGEMENT

I would like to thank my supervisor, Asst. Prof. Dr. Ha Sie Tiong for giving me the opportunity and always guide as well as supervise me during the final year project in order for the project to complete as scheduled.

I would also like to express my gratitude to Seou Chi Kien for always help me and guide me when I faced some problem with my project.

I would also like to express my appreciation to Universiti Tunku Abdul Rahman (UTAR) for giving me the chance to carry out my final year project in a conducive environment

Besides that, I would also like to take this opportunity to thank the UTAR laboratory officers for their guidance and effort in helping me to carry out the analysis required.

Last but not least, I will to express my gratitude to my friends and lecturers for providing useful information and guide me throughout the project

Thank you

DECLARATION

I hereby declare the project report is based on my original work except for quotations and citations which have been duly acknowledge. I also declared that it has not been previously or concurrently submitted for any other degree at UTAR or other institutions

_____

(Eleen Dayana Binti Mohamed Isa)

APPROVAL SHEET

This project report entitled **"SYNTHESIS AND CHARACTERISATION OF SYMMETRICAL DIMER CONTAINING CHALCONE MOIETY"** was prepared by Eleen Dayana Binti Mohamed Isa and submitted as partial fulfilment of the requirements for degree of Bachelor of Science (Hons) Chemistry at Universiti Tunku Abdul Rahman

Approved By:

_____

(Asst. Prof. Dr. Ha Sie Tiong) Date:……

Supervisor

Department of Chemical Science

Faculty of Science

Universiti Tunku Abdul Rahman

FACULTY OF SCIENCE

UNIVERSITI TUNKU ABDUL RAHMAN

Date:_____

PERMISSION SHEET

It is hereby certified that **ELEEN DAYANA BINTI MOHAMED ISA** (ID No: **11ADB01911)** has completed this final year project **"SYNTHESIS AND CHARACTERISATION OF SYMMETRICAL DIMER CONTAINING CHALCONE MOIETY"** supervised by **ASST. PROF. DR. HA SIE TIONG** from the Department of Chemical Science, Faculty of Science

I hereby give permission to my supervisor to write and prepare manuscripts of these research findings for publishing in any form, if I do not prepare it within six (6) months from this date, provided that my name is included as one of the authors for this article. The arrangement of the name depends on my supervisor.

Yours truly,

_____

(Eleen Dayana Binti Mohamed Isa)

TABLE OF CONTENTS

LIST OF TABLES

LIST OF FIGURES

LIST OF ABBREVIATION

4ACE	4-hydroxyacetophenone
4OH	4-hydroxybenzaldehyde
$CDCl_3$	Deuterated chloroform
Cr	Crystal
DC3C	1,3-Bis(3-(4-dodecyloxyphenyl)-1-(phenyl-4-oxy)prop-2-en-1-one)propane
DC4C	1,4-Bis(3-(4-dodecyloxyphenyl)-1-(phenyl-4-oxy)prop-2-en-1-one)butane
DC5C	1,5-Bis(3-(4-dodecyloxyphenyl)-1-(phenyl-4-oxy)prop-2-en-1-one)pentane
DC6C	1,6-Bis(3-(4-dodecyloxyphenyl)-1-(phenyl-4-oxy)prop-2-en-1-one)hexane
DCM	Dichloromethane
DCnC	α,ω-Bis(3-(4-dodecyloxyphenyl)-1-(phenyl-4-oxy)prop-2-en-1-one)alkane
DDB	4-dodecyloxybenzaldehyde
DHP	3-(4-dodecyloxyphenyl)-1-(4-hydroxyphenyl)prop-2-en-1-one
DSC	Differential Scanning Calorimetery
FTIR	Fourier transform infrared
HCl	Hydrochloric acid
I	Isotropic
J	Coupling constant in Hz
K_2CO_3	Potassium carbonate
KBr	Potassium bromide
KOH	Potassium hydroxide
MEK	Methylethylketone

NMR	Nuclear Magnetic Resonance
NOE	Nuclear Overhouser Enhancement
R_f	Retention factor
TBAB	Tetrabutylammonium bromide
TLC	Thin layer chromatography
TMS	Tetramethylsilane
UV – Vis	Ultraviolet/Visible

CHAPTER 1

INTRODUCTION

1.1 Introduction to Chalcone

Benzylideneacetophenone which is also commonly known as chalcone is a compound consist of two aromatic rings linked by unsaturated α,β-ketone (Song, Jung and Shin, 2002). It can be synthesised through numerous ways but the most common way is through Claisen-Schmidt condensation using different type's catalyst. Besides that, it is found that the Claisen-Schmidt reaction increases in the presence of $KOH.Al_2O_3$ as a catalyst under ultrasound irradiation (Rateb and Zohdi, 2009). Recently, with an approach to green chemistry, solvent free chalcone synthesis has been developed (Kumar, Suresh and Sandhu, 2010). Figure 1.1 illustrates the general structure of chalcone.

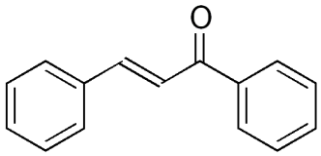

Figure 1.1: General structure of chalcone.

Based on general structure of chalcone (Figure 1.1), it is observed that this compound is highly conjugated due to presence of carbonyl group and aliphatic double bond. Due to these functional groups, a system with complete delocalization of π-electrons is generated thus this compound has relatively

low redox potential and higher chances of undergoing electron transfer process (Patil, Mahajan and Katti, 2009).

Chalcone is easily found in plants and it is one of the main as precursors for synthesis of flavonoids (Yong, et al., 2013). It has been reported that compound containing chalcone as backbone has various biological activities such as antimicrobial, anti-inflammatory, antiplatel, antimalarial, anticancer, antiviral, and antihyperglycemic. The key functional groups that are responsible for all these activities are the reactive and unsaturated keto group especially for antimicrobial activity (Prachar, et al., 2012). Besides that, chalcone derivatives also play important role in crystallography, liquid crystalline polymers, dye industries and solar cells (Ramkumar, et al., 2013).

1.2 Introduction to Liquid Crystal

"Liquid crystal is quite a mysterious field to study" said by one of famous scientist. From the name itself defined it uniqueness because how can a substance be liquid and crystalline at the same time? Through further understanding of liquid crystal, it is understandable how the term liquid crystal applied to certain substance and it is even shocking to witness that this term compromise the situation perfectly. Besides that, that liquid crystals exist in many forms thus create an interesting and exciting phenomenon (Collings, 2002).

To understand how liquid crystals exist, an in depth understanding regarding states of matter. There are three states of matter which are solid, liquid and gas and these three different states differ from each other due to configuration of particles in that particular state. In solid state, the molecules are in fixed arrangement and they are not free to move while in liquid and gas, the molecules are free to move around. However, in gas the distance between molecules are further apart compared to liquid. Contradictory to education syllabus, these three states of matter is not the only state that existed in reality (Collings, 2002). The extra phase that present is liquid crystal phase and it also known as intermediate or mesomorphic phases (Fisch, 2006). For a compound to be classified as liquid crystals, it must fulfil the properties of liquid and crystal (Andrienko, 2006).

Mesomorphic phase lays in between solid crystalline and liquid thus the best way to understand the differences in through molecules arrangement. In solid crystalline state, the molecules are arranged in regular with repeating pattern (Shakhashiri, 2007). All the molecules in the crystalline structure fixed in position through intermolecular forces. These forces are broken as the molecules vibrate vigorously as temperature increase and the molecules will move into random position. However, for liquid crystalline substances, the intermolecular forces in solid is unequal in all direction thus as temperature increases, the weaker bonds break first then the stronger bonds. This phenomenon resulted in random and regular arrangement in certain places this

liquid crystalline is produced. Figure 1.2 depicts the molecular arrangement of solid, liquid crystal and liquid.

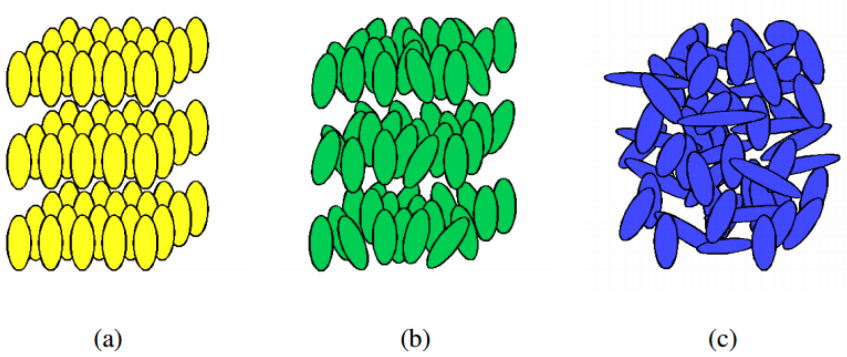

Figure 1.2: Molecular arrangement of solid (a), liquid crystal (b) and liquid (c) (Shakhashiri, 2007).

1.3 History of Liquid Crystals

Liquid crystal was first discovered in 1888 by an Austrian botanist, Friedrich Reinitzer and his research is about the melting behaviour of compound related to cholesterol (Fisch, 2006). Through an experiment, he observed that a compound, cholesteryl benzoate had two distinct melting points. From solid, the compound form hazy liquid at 145.5 ℃ and at 178.5 ℃ (Figure 1.3), the solution becomes completely clear. To study this phenomenon, Reinitzer send samples of this compound to Lehmann, a physicist that studies the crystallization properties. Through polarising microscope, Lehmann observed similarity of the sample to his own samples whereby the sample shows both liquid and crystal properties. Besides that, the mechanical and symmetry properties of these phases lie in between crystalline solid and isotropic liquid

(Singh, 2002). Combination of flow properties like a liquid and optical properties like solid led Lehmann to label these compounds as liquid crystals (Collings, 2002).

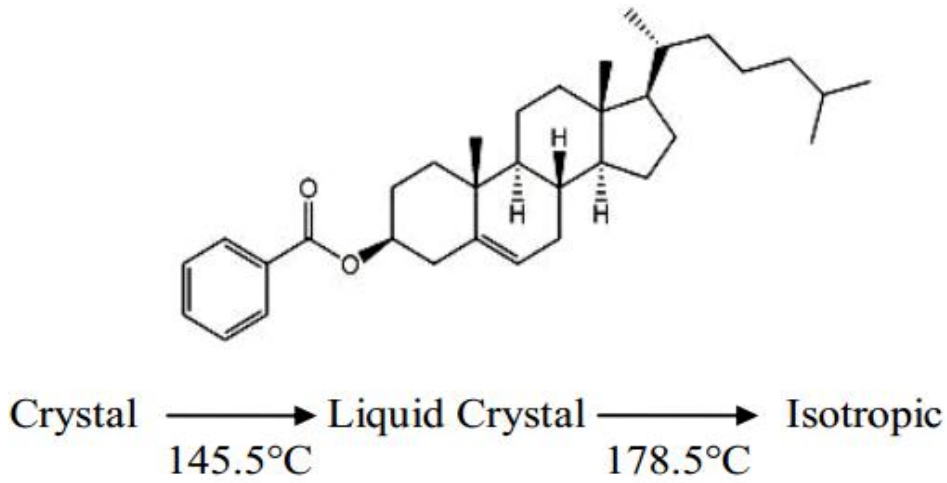

Figure 1.3: Structure of cholestryl benzoate and its two melting points (Fisch, 2006).

1.4 Classification of Liquid Crystal

Mesogen can be broadly classified into two groups viz thermotropic and lyotropic depending by which the intermediate phases occur (Devi and Bharracharjee, 2010). Thermotropic liquid crystals exist through thermal process while lyotropic liquid crystals exist through the influence of solvents. This type of phase can be easily observed in daily life especially during dish washing (Fisch, 2006). Typical lyotropic mesogen are amphilic which mean that the molecule consist of hydrophilic and hydrophobic groups. The best example of lyotropic liquid crystal is soap (Collings, 2002).

Thermotropic liquid crystal can be further classified into three categories based on geometrical structure. Those three are calamitic for rod-like, discotic for dics-like and sanidic for brick- or lath-like species (Singh, 2002). Calamitic liquid crystals made out of rod-like molecules where one of the axes is longer than the other two. Typical calamitic mesogen consist of rigid core unit and flexible side chain (Devi and Bharracharjee, 2010). Discotic liquid crystal was first discovered by an Indian researcher, Sivaramkrishna Chandrasekhar. The researcher found that disc-like molecule able to form liquid crystal in which axis perpendicular to the plane of the molecule tends to orient along a specific direction (Collings, 2002). In discotic liquid crystal, the most important part is the central part of the molecule which is rigid. In a typical discotic mesogen, the core usually made out of aromatic rings with six or eight side chain each resembling a typical calamitic mesogen (Gan, 2011). Classification of liquid crystal is being summarised in Figure 1.4.

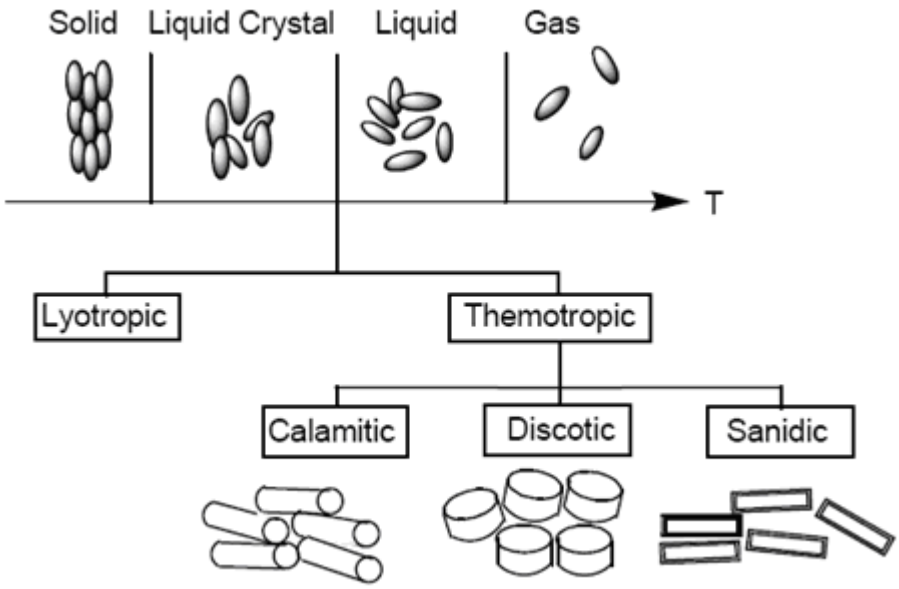

Figure 1.4: Classification of liquid crystals (Morris, 2006).

1.5 Liquid crystals phases

Mesophases can be characterised by many physicals parameters. However, the easiest way to distinguish each mesophases is in term of their molecular arrangement (Khoo, 2007). There are three general phases in liquid crystals which are nematic phase, smectic phase and cholesteric phase or also known as chiral nematic phase.

1.5.1 Nematic phase

Molecules with the least positional order but has the highest symmetry is known as nematic phase (Dierking, 2003). The molecules positions are random which is similar to liquid. However, these molecules are related in terms of direction where they are aligned in general direction known as director axis (Khoo, 2007). It appears that the molecules able to rotate about their axis and there are no preferential arrangement of the two ends of the molecules if they differ. Therefore, the sign of the director has no physical significance (Andrienko, 2006). The molecular arrangement of nematic phase is shown in Figure 1.5.

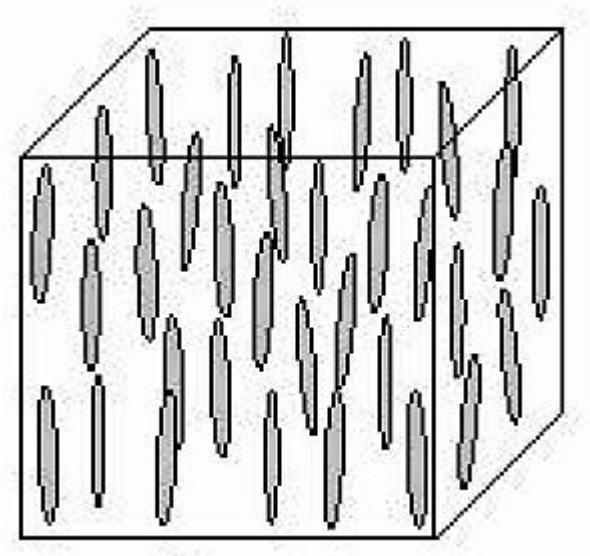

Figure 1.5: Molecular arrangement of nematic phase (Devi and Bharracharjee, 2010).

1.5.2 Cholesteric Phase

Cholesteric which is also known as chiral nematic liquid crystal has similar physical properties to nematic phase except the molecules tend to align in helical manner. Arises of this property is due to synthesis whereby addition of chiral molecule to nematic mesophase (Khoo, 2007). Cholesteric also differ from nematic as the director of cholesteric phase varies in direction throughout the medium in a regular way (Andrienko, 2006). Another unique property of this type of liquid crystal is that the colour change according to the temperature (Walcott, 2013).

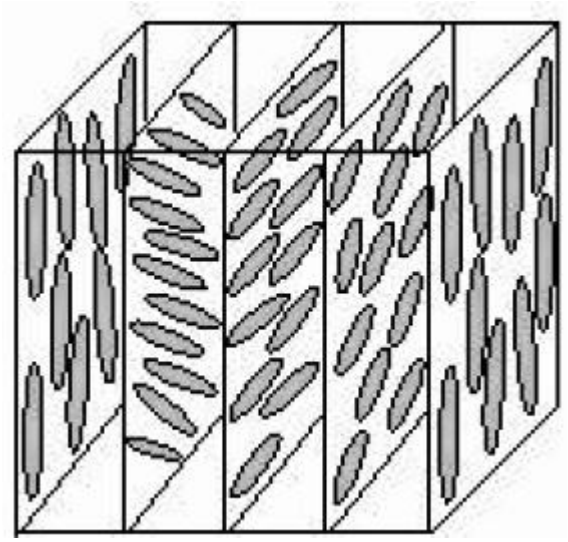

Figure 1.6: Molecular arrangement of cholesteric phase (Devi and Bharracharjee, 2010).

1.5.3 Smectic Phase

The word smectic is derived from the Greek word for soap, because at first such liquid crystal phase was observed on ammonium and alkali soaps (Fisch, 2006). Through lowering the temperature of nematic material, positional order of molecules may appear and this is known as smectic phase (Dierking, 2003). The important feature of smectic phase that distinguish it from nematic phase is its stratification (Andrienko, 2006). Smectic phase possesses positional order and the molecules position correlated in some ordered pattern (Khoo, 2007). There are many types of smectic phase but the most important ones are Smectic A (SmA) and Smectic C (SmC). In SmA, the molecules orientation is perpendicular to the layers while in SmC, the director is tilted (Devi and Bharracharjee, 2010).

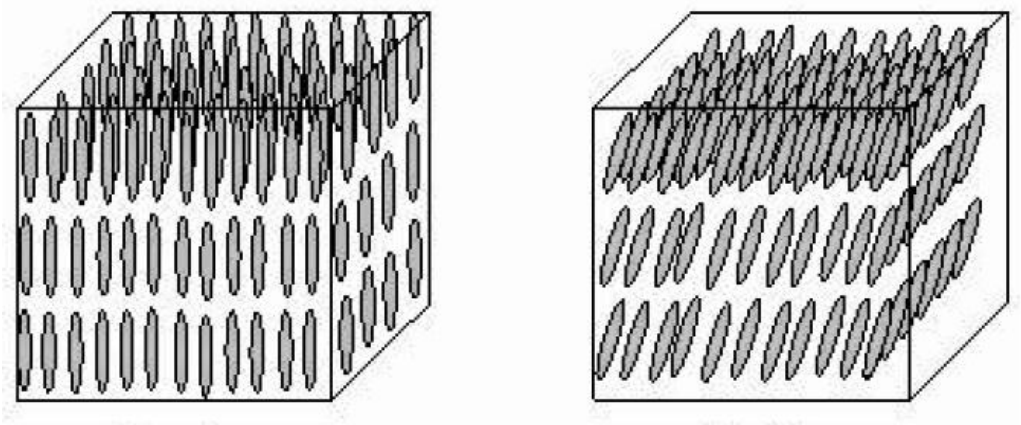

(a) (b)

Figure 1.7: The molecular arrangement of smectic A (a) and smectic C (b) (Devi and Bharracharjee, 2010).

1.6 Application of Liquid Crystal

The discovery of liquid crystal compounds has had major effect on science and engineering area as well as device technology. This unique compound has provided solution for different types of problems and it is still actively being investigated for its application in many fields due to its special properties (Andrienko, 2006).

One of major application of liquid crystal is liquid crystal displays (LCDs). LCDs were first invented in the year 1968 and it was further developed and twisted nematic display was discovered. This twisted nematic display is the basis of LCD industry ever since (Collings, 2002).

Besides LCD, liquid crystal is also found in liquid crystal thermometer. Based on researches, chiral nematic liquid crystals reflect light with a wavelength equal to pitch and pitch is dependent on temperature. Due to this factor, it is possible to used liquid crystal compound to determine temperature through the colour changes of the compound. Through combination of several compounds, device with certain temperature range can be built (Andrienko, 2006). Figure 1.8 shows the application of liquid crystal in LCDs and liquid crystal thermometer.

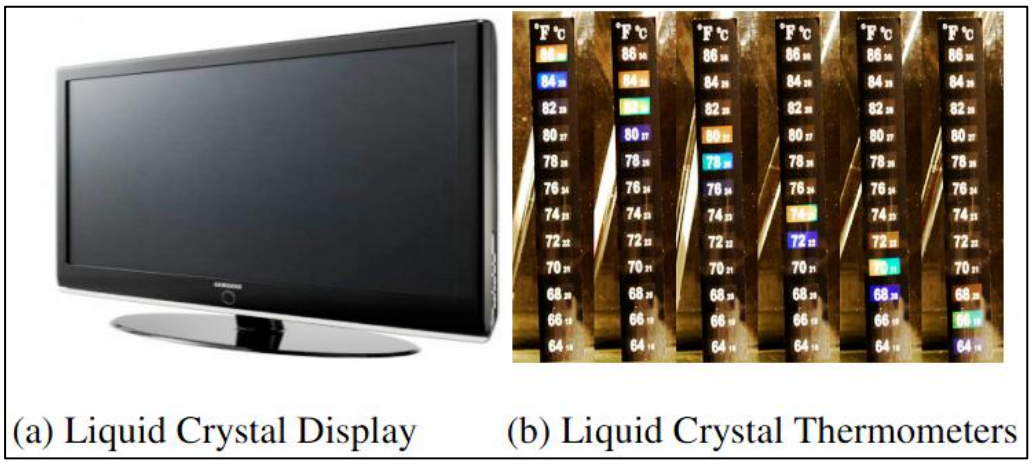

Figure 1.8: Liquid Crystal Display (a) and liquid crystal thermometers (b) (Fairchild, 2013).

1.7 Objectives

The objectives of this final year project are as follow:

1. To synthesise a series of symmetrical dimer containing chalcone moiety, α,ω-Bis(3-(4-dodecyloxyphenyl)-1-(phenyl-4-oxy)prop-2-en-1-one)alkane (**DCnC**).

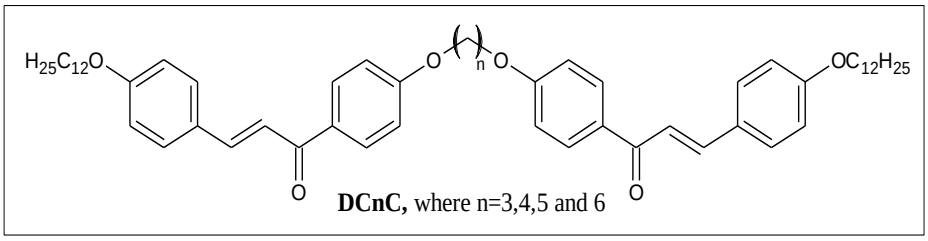

DCnC, where n=3,4,5 and 6

2. To elucidate the structure of compounds **DCnC** by using FTIR, ^{1}H NMR and ^{13}C NMR spectroscopic techniques.

3. To characterise the physical properties of compounds **DCnC** by using DSC, UV-Vis spectrophotometer.

CHAPTER 2

LITERATURE REVIEW

2.1 Liquid Crystal Dimer

Liquid crystal dimers which is also known as twin or bismesogen have received quite great attention during these past decades as they are particularly special in terms of thermal behaviour and structural features as the model compounds similar to polymeric liquid crystals (Liao, et al., 2008). The exact definition of liquid crystal dimer is a compound consists of two mesogenic units and separated or bonded to each other via a flexible spacer (Senthil, Kamalraj and Wu, 2008). This bismesogen compound can be broadly classified into two types which are symmetrical dimer and non-symmetrical dimer. In symmetrical dimer, both mesogenic units are identical while in non-symmetrical, the mesogenic units differ from one another (Figure 2.1) (Donalsdson, et al., 2010). The properties of these dimers are influenced by the length of spacer, lateral substituent, terminal substituent and linking group.

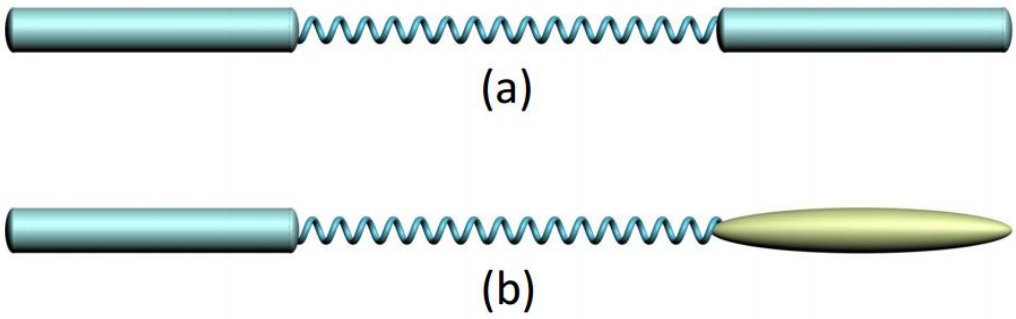

Figure 2.1: Schematic diagram of symmetrical dimer (a) and non-symmetrical dimer (b) (Kundu, 2008).

2.1.1 Effect of the length of spacer

The mesomorphic properties of liquid crystal dimers are greatly influenced by the length of spacer. It is found that twin liquid crystal exhibit a great odd-even effect on mesomorphic behaviour with spacer length. Generally, dimer with an even spacer has a more parallel orientation compared to those with odd spacer thus even spacer dimer has more stable mesophase. Most mesogenic twins formed smectic or nematic phase. As for smectic layers, there are three subtypes structure proposed which can be monolayer, interdigitated or intercalated (Figure 2.2). These conformations depended on the spacer and/or molecular length (Liao, et al., 2008). Table 2.1 illustrates the effect of changing spacer length on transition temperature.

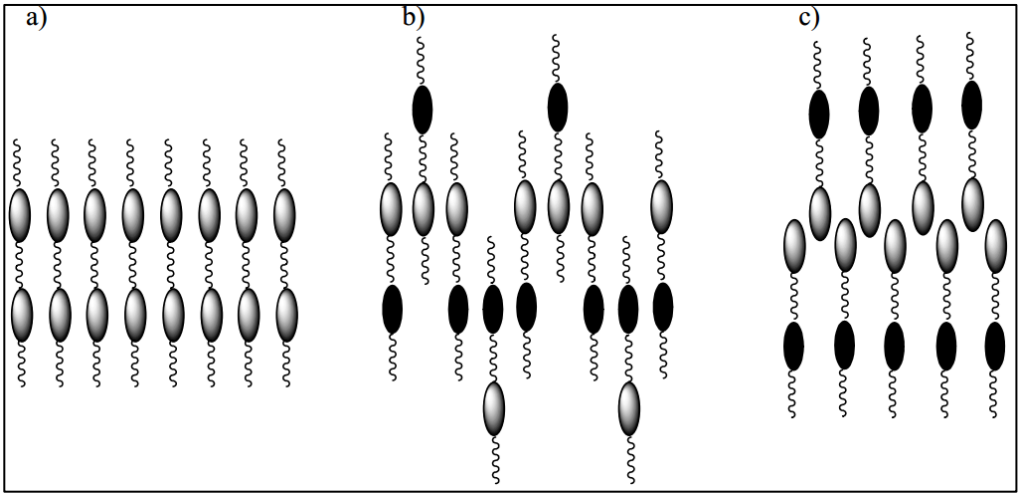

Figure 2.2: Schematic representation of monolayer (a), intercalated (b) and interdigitated (c) in Smectic phase (Kropff, 2006).

Table 2.1: Effect of changes of spacer length on transition temperature (Liao, et al., 2008).

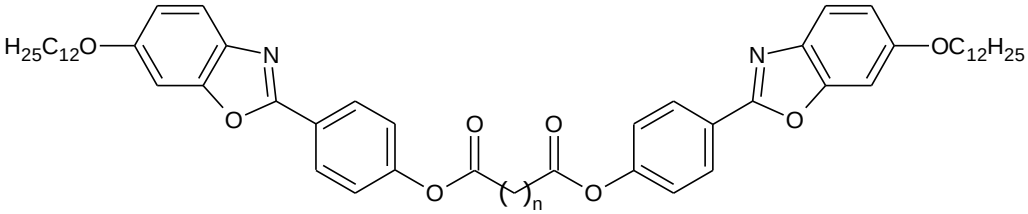

Compounds	Cycle	Transition temperature (℃)				
		Cr		SmC		I
1a, n=3	Heating	•	125.9	•	142.5	•
	Cooling	•	122.3	•	141.7	•
1b, n=4	Heating	•	124.4	•	166.8	•
	Cooling	•	122.2	•	165.0	•
1c, n=5	Heating	•	116.2	•	130.6	•
	Cooling	•	103.1	•	128.8	•
1d, n=6	Heating	•	125.4	•	147.4	•
	Cooling	•	121.6	•	143.5	•
1e, n=7	Heating	•	106.2	•	122.7	•
	Cooling	•	105.2	•	121.4	•
1f, n=11	Heating	•	105.6	-		•
	Cooling	•	95.2	•	103.1	•

From Table 2.1**,** all compounds show transition from crystal to smectic C phase due to the weak dipole induced interaction cause by heterocyclic benzoxazoles (Liao, et al., 2008). Besides that, enantiotropic liquid crystal phases are observed except for the compound 1f where it is a monotropic liquid crystal phase exhibited during the cooling cycle. Monotropic behaviour is observed when the ratio of molecule unsuitable and it is kinetically unstable (Liao, et al., 2008). There is no apparent change in the melting and clearing temperatures as the spacer length increase. However, the temperature range for mesophase is at its maximum with compound 1b and the mesophase range start to decrease as the spacer length increases. Therefore, it is concluded that compound 1b has the best ratio for the formation of mesophase. Figure 2.3 illustrates the effect of spacer length on transition temperature (Liao, et al., 2008).

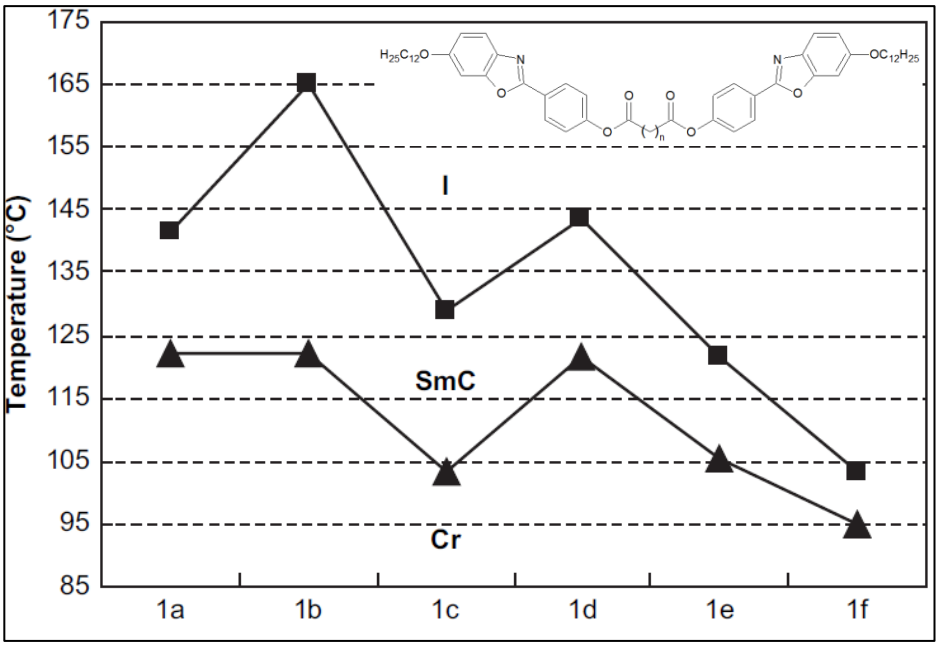

Figure 2.3: Dependence of melting and clearing temperature on the number of methylene group in the spacer of compound 1a-1f (Liao, et al., 2008).

From Figure 2.3, it is observed that compounds 1b and 1d which have even number of methylene group in the spacer exhibit the highest melting and clearing temperatures while compounds 1a, 1c and 1f which have odd number of methylene group in the spacer show lower melting and clearing temperatures. The possible reasons that the even carbon spacer exhibit higher transition temperature is due to its all-*trans* conformation. Molecules with all-*trans* conformation are likely to be linear and this resulted in better packing in mesophase. For odd number spacer, the transition temperature is lower due to it possible conformation of bent shape (Liao, et al., 2008). Besides that, as the length of spacer increased, the melting and clearing temperatures generally show decreasing trend.

2.1.2 Effect of lateral substituent

Recently, fluorinated liquid crystals gain attention especially when the lateral hydrogen is replaced by fluorine as this type of compound exhibit unique properties. Some of the unique properties of lateral fluorinated liquid crystals are negative dielectric anisotropy, low viscosities, optical and chemical stability, low melting point and low conductivity (Wei, et al., 2008).

Generally, the presence of fluorine group at the lateral position enhances the formation of nematic phase and decrease the clearing point while the presence of fluorine on the terminal position enhances the formation of smectic phases and increase the clearing points while presence of fluorine in the core will form nematic phase and lower the clearing points (Guo, et al., 2008). Normally, presence of substituents at lateral position causes the molecules to detract from linearity thus reduces the probability of the molecules to exhibit mesophases. Besides that, any group the protruded out of the mesoginic core will also disrupt the intermolecular forces as well as the mesogen packing. However, since fluorine atom is small, the linearity of the molecule is not greatly affected (Hird, 2007). Wei, et. al. (2008) tried to establish the relationship between the structures and properties of laterally fluorinated materials by synthesizing two kinds of laterally fluorinated ester mesogens with hydroquinone moiety (Table 2.2).

Table 2.2: Phase transition temperature associated with nAFBHQ and nADFBHA (Wei, et al., 2008).

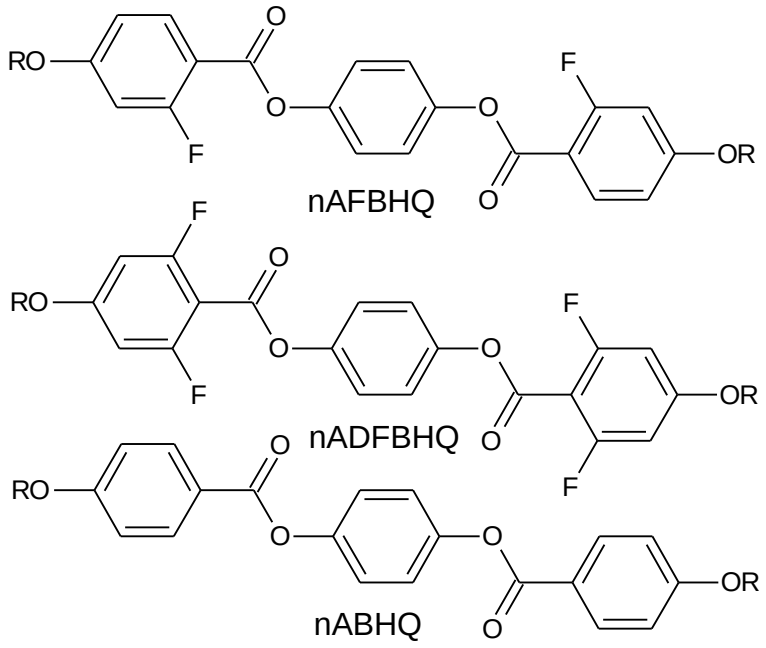

Compounds	Cycle	Transition temperature (℃)				
		Cr		N		I
6AFBHQ	Heating	•	94.0	•	184.6	•
	Cooling	•	58.5	•	183.1	•
5AFBHQ	Heating	•	116.8	•	193.3	•
	Cooling	•	82.5	•	190.5	•
2AFBHQ	Heating	•	166.2	•	269.9	•
	Cooling	•	156.4	•	267.7	•
6ADFBHA	Heating	•	93.6	•	146.0	•
	Cooling	•	68.5	•	143.1	•
5ADFBHA	Heating	•	116.7	•	153.4	•
	Cooling	•	101.7	•	151.5	•
2ADFBHA	Heating	•	160.1	•	221.9	•
	Cooling	•	120.9	•	220.0	•

Table 2.2 shows that all the compounds are enantiotropic and exhibit transition from crystal to nematic phase. Besides that, the number of fluorine atoms had significant effect on the thermal stability. It is also found that the odd and even effect in both series do not show distinct effect on its melting and clearing temperatures and the numbers of carbon atoms affect the transition temperature

in reverse manner. By comparing the nAFBHQ and nADFBHA with its non-fluorinated analogue (nABHQ), it is found that the melting and clearing temperatures of fluorinated analogues is greatly reduced. This is due to the debased symmetry and lowered slenderness ratio of the molecules in the presence of fluorine atom. Furthermore, nAFBHQ has a broader mesophase range and a higher clearing temperature. It is concluded that compounds with one lateral fluorine atom much more promising for liquid crystal formation (Wei, et al., 2008).

2.1.3 Effect of terminal substituent

Most liquid crystal phase is exhibited by rod-liked molecules having long tails at *para*-position. In contrast, instability of liquid crystalline phase is observed when substituent is present at *meta*- or *ortho*- position of aromatic ring. However, compound with *ortho* hydroxyl group and azomethine group nearby, the thermal stability is increased due to hydrogen bonding (Yeap, et al., 2006). To determine the effect of length of alkyl chain on the mesomorphic properties of liquid crystal dimer, a series of compound was synthesized with varying alkyl chain length (Figure 2.4).

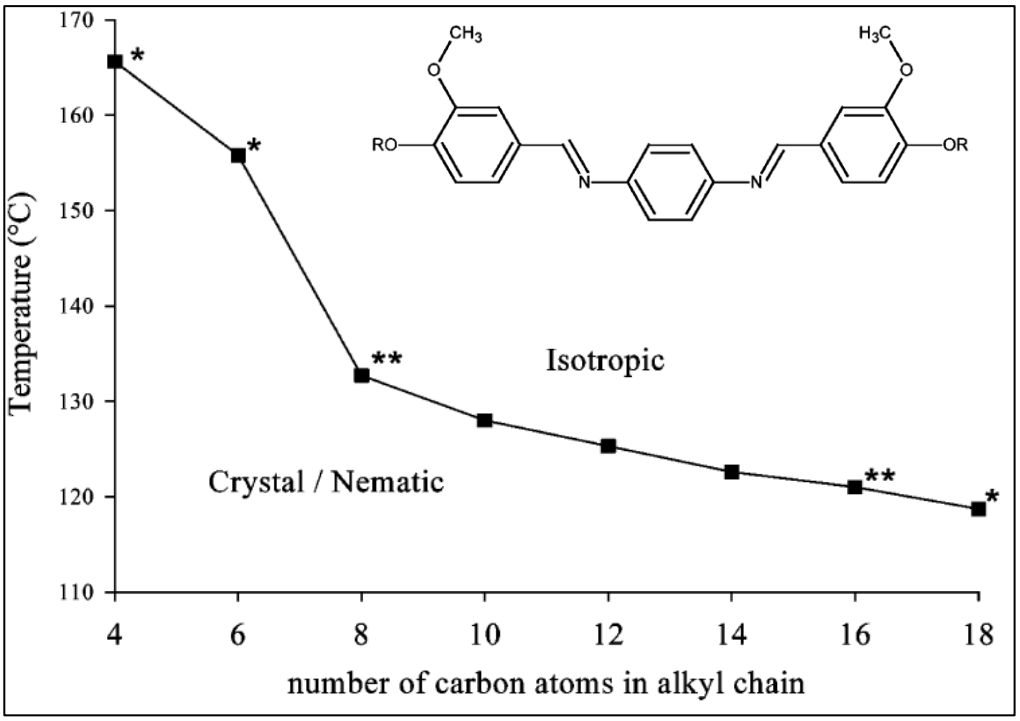

Figure 2.4: Trend of clearing points during the heating process with respective number of carbon atoms in alkyl chain: *-crystal to isotropic (non-mesogenic) and **-crystal to isotropic (monotropic) (Yeap, et al., 2006).

Figure 2.4 shows that the clearing temperature decreases as the number of carbon atoms in alkyl chain increase. Besides that, compounds with four, six and eighteen carbon atoms in the alkyl chain do not exhibit mesophase. For compounds with carbon atom of four and six, the clearing temperature is relatively high due to the strong intermolecular interaction between short chain and this also limit the formation of mesophase. However compound with eighteen carbons, has a low transition temperature because the linearity of the molecule is loss thus led to poor packing and thermal instability. A monotropic liquid crystal phase is exhibited by compound with 16 carbons in alkyl chain, and this is due to lower anisotropy that destabilizes the mesomorphic properties. (Yeap, et al., 2006).

2.1.4 Effect of linking group

Liquid crystal dimers mesomorphic properties are greatly affected by the length of spacer. However, the linkage types of the spacer are also affecting the mesogenic properties. For a meaningful comparison between the types of linkages between mesogens, the number of atoms connecting the mesogenic group must be the same. Based on this principle, it is found that nematic-isotropic transition temperature is higher for ether than methylene linked dimers and this is due to the molecular geometry. Compounds with greater linearity will exhibit a more stable mesophase. By comparing bond angles of methylene and ether which are 113.5° and 126.4° respectively, it proves that ether dimer will have more linearity than methylene dimer due to larger bond angles. To understand the effects of linking group on mesomorphic properties, a series of compound (Figure 2.5, Table 2.3) with different linkages were studied (Henderson, Niemeyer and Imrie, 2001).

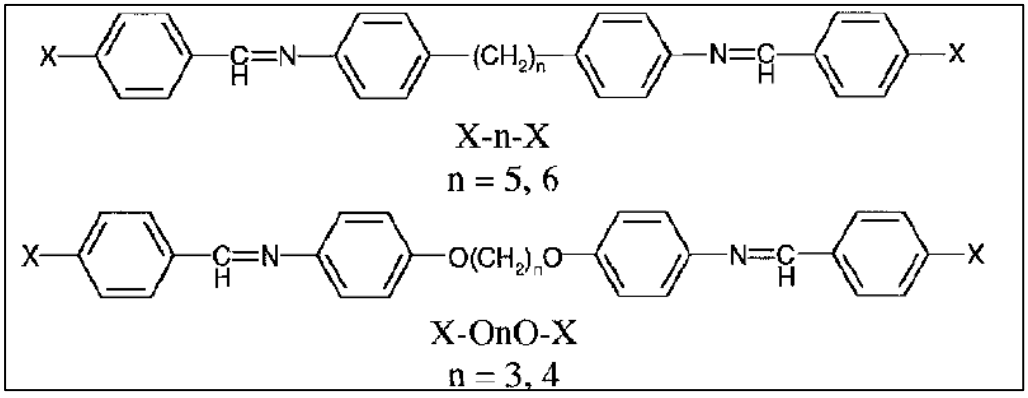

X= OCH_3 mO-n-Om, mO-OnO-Om
X= CH_3 1-n-1, 1-OnO-1

Figure 2.5: Structure of mO-n-Om, mO-OnO-Om, 1-n-1 and 1-OnO-1 (Henderson, Niemeyer and Imrie, 2001).

Table 2.3: Transition temperatures for m-OnO-m, m-n-m, mO-n-Om and mO-OnO-Om series (Henderson, Niemeyer and Imrie, 2001).

Compounds	T_{cr}/℃	$T_{Sm,N}$/℃	T_{NI}/℃
1-O3O-1	156.0	-	-
1-O4O-1	203.0	-	213.0
1-5-1	103.0	-	-
1-6-1	168.0	-	187.0
1O-O3O-O1	188.0	-	(175.0)
1O-O4O-O1	212.0	-	239.0
1O-5-O1	123.0	(83.0)	(86.0)
1O-6-O1	140.0	-	214.0

* Monotropic transition temperature is given in parentheses ()

From Table 2.3, the melting temperatures for the odd members are significantly lower compared to their even members. Based on past research, replacing the alkyl terminal chain with alkoxy chain able to increase the transition temperature of nematic-isotropic around 40 ℃. From Table 2.3, the T_{NI} increase significantly when the alkyl chain is replaced with alkoxy chain especially in odd number spacer compound. However, the increase in even number spacer is lower than expected. Based on the data collected, by replacing the terminal alkyl chain with alkoxy chain the T_{NI} increase around 30 to 40 ℃ while replacing the methylene bridge with ether bridge, the T_{NI} increase around 20 to 30 ℃. If both methylene and alkyl chain is replaced by ether bridge and alkoxy group, the T_{NI} increase significantly. Through this information, the replacement of alkyl chain with alkoxy group will significantly increase the T_{NI} while replacing the inner methylene is essentially additive (Henderson, Niemeyer and Imrie, 2001).

2.2 Liquid crystal containing chalcone moiety

Chalcone as shown in Figure 1.1 consists of two aromatic ring linked by an enone group. It is highly conjugative due to presence of aliphatic double bond and carbonyl group. Chalcone liquid crystals are relatively rare due to it linkage which is not conducive for mesomorphism. The enone bond in chalcone is non-linear due to the angle strain arising from keto group thus it become less conducive for mesomophism (Thaker, et al., 2009). Yeap, et. al (2005) have prepared a series of chalcone derivatives, 1-phenyl-3-(4'-undecylcarbonyloxyphenyl)-2-propen-1-one and studied their phase transition and Figure 2.6 depicts its structure.

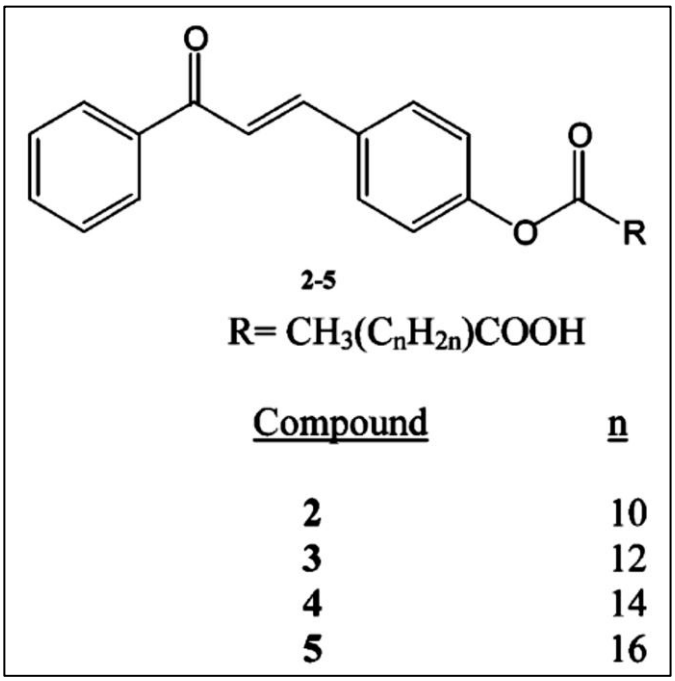

Figure 2.6: Structure of 1-phenyl-3-(4'-undecylcarbonyloxyphenyl)-2-propen-1-one (Yeap, et al., 2005).

All compounds, **2-5** were found to undergo isotropization process only. As the alkyl chain increases, the transition temperature increases. One of the factors that cause this observation is the increase in the van der Waals attraction among the alkyl chain. However, the transition temperature for compound **5** is lower than compounds **2-4** and this probably due to the repulsion which lead to further intermolecular distance. With these repulsions, the molecule distort from linearity thus lead to lower transition temperature as it cannot pack nicely. Through investigation using POM, the transition of Cr_1-Cr_2 in compound **3-5** show smectic-like texture in Cr_2 region (Yeap, et al., 2005). Transition temperatures for compound **2-5** is shown in Table 2.4**.**

Table 2.4: Transition temperature of compound **2-5** (Yeap, et al., 2005).

Compound	Cycle	Transition	Temperature (˚C)
2	Heating	Cr-I	94.6
	Cooling	I-Cr	77.0
3	Heating	Cr_1-Cr_2	86.2
		Cr_2-I	97.7
	Cooling	I-Cr	76.8
4	Heating	Cr_1-Cr_2	85.5
		Cr_2-I	99.9
	Cooling	I-Cr	83.0
5	Heating	Cr_1-Cr_2	83.7
		Cr_2-I	92.6
	Cooling	I-Cr	79.8

There are many different types of linkages reported. However, most of them has even number of linking groups. Odd number linkages like enone is relatively rare because most mesogenic unit required to be linear along molecular axis and this cannot be achieved using odd number atom of linking group. Even though enone group is not conducive to mesomorphism, it can be changed by including other central linkages such as azomethine, ester or azo

groups (Thaker and Kanojiya, 2011). To investigate the influence of terminal group and central linkages, a series of chalcone derivatives (Figure 2.7 and 2.8) were prepared by Thaker and Kanojiya (2011).

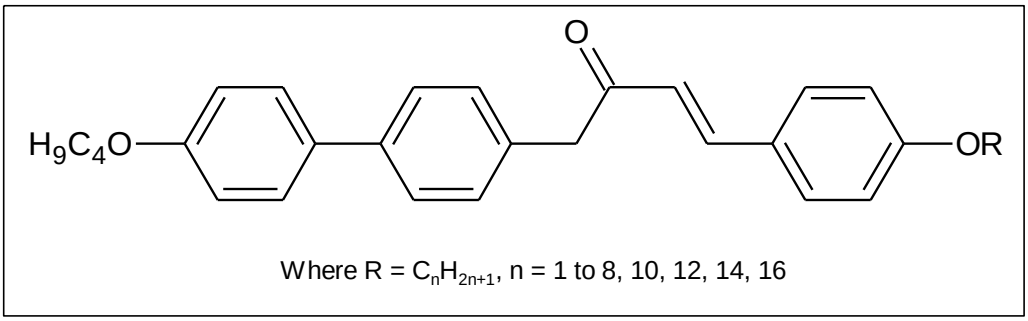

Figure 2.7: Structure of 1-(4'-butoxybiphenyl-4-yl)-3-(4-alkoxyphenyl)prop-2-en-1-one (Series I) (Thaker and Kanojiya, 2011).

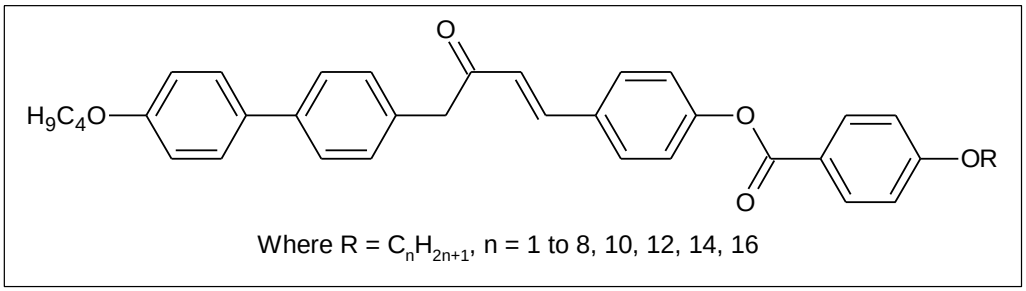

Figure 2.8: Structure of 4-[3-(4'-butoxybiphenyl-4-yl)-3-oxoprop-1-en-1-yl]phenyl-4-alkoxybenzoate (Series II) (Thaker and Kanojiya, 2011).

In general, compounds synthesized in these two series exhibited liquid crystal mesophases, nematic and/or smectic phase. For Series I, it have biphenyl central core which is more polar than benzene and this increase the liquid crystalline properties. This is because the biphenyl ring increases the rigidity and linearity of the molecule which further lead to the thermal stability. In fact, due to presence of terminal butoxy biphenyl ring in addition to chalcone linkage, the compound became conducive to mesomorphism. For Series II,

there is addition ester group and benzene ring. The presence of these two groups enhances the liquid crystalline properties the most as it increase the polarisability of the molecules. However, there is a decrease in thermal stabilities in liquid crystalline phase. This is due to the decrease in interaction of molecule as the breadth forces increases. Figures 2.9 and 2.10 show the effect of terminal chain and linkage group on the transition temperature of Series I and Series II (Thaker and Kanojiya, 2011).

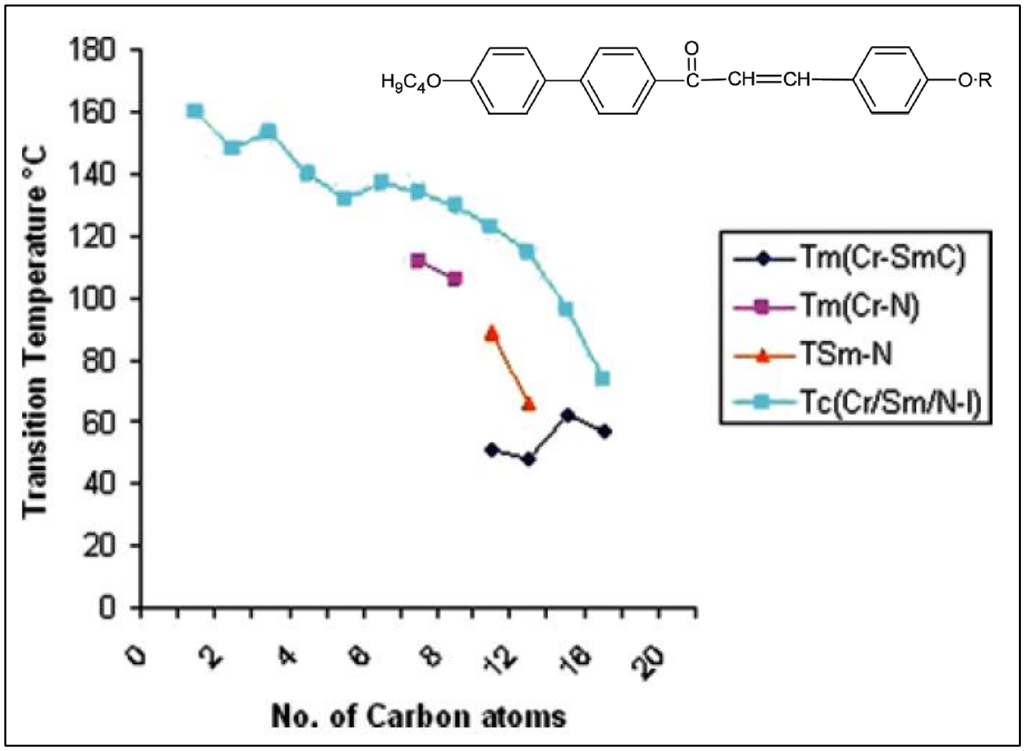

Figure 2.9: Mesomorphic behaviour as a function of the number of carbon atoms (n) in the terminal alkoxy chain for Series I (Thaker and Kanojiya, 2011).

From Figure 2.9, it is found that early members (n = 1 – 7) did not exhibit liquid crystal phase. As the number of carbon atoms increases to n = 8, the compounds started to exhibit liquid crystal phases. The possible reason for this observation is the molecule is non-linear due to enone group. However, as the number of carbon increases, the linearity increases.

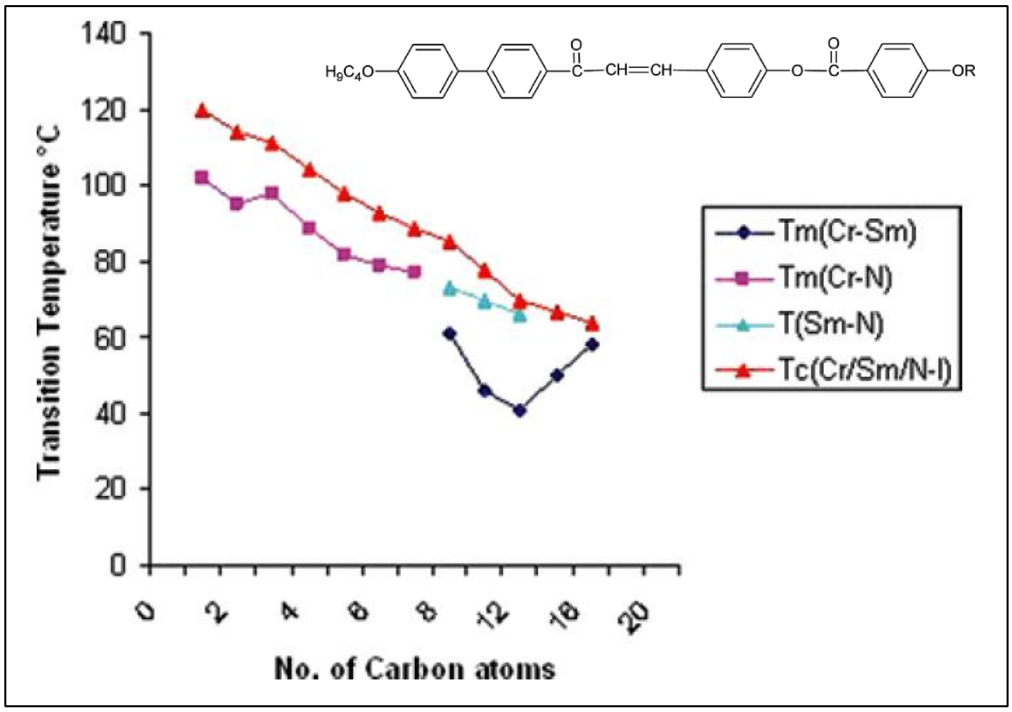

Figure 2.10: Mesomorphic behaviour as a function of the number of carbon atoms (n) in the terminal alkoxy chain for Series II (Thaker and Kanojiya, 2011).

From Figure 2.10, it is observed that the Series II molecules exhibit liquid crystal phase from lower number of carbon to higher number of carbon. This is due to the presence of ester group and benzene ring. The presence of this two functional group increases the polarisability of the compound thus enhances the liquid crystalline properties. However, it is observed that the thermal stability of Series II is lower than Series I and this is due to ester and alkoxy benzene ring as terminal substitution. The presence of both groups increases the breadth forces which decreases the interaction and consequently, lower the thermal stability (Thaker and Kanojiya, 2011).

2.3 Other applications of chalcone

Chalcone is mostly studied for medicinal purposes due to its biological activities. Most research done on chalcone is about its antimicrobial activity. It is claimed that hydroxylated chalcone has good antimicrobial activity. In plants, chalcone is normally found is its hydroxylated formed and many reports show that they are biologically active. Besides that, presence of alkyl chain also shows significant biological activities because the long alkyl chain able to disrupt the microorganism cell walls. Figure 2.11 shows chalcone with variable alkyl chain length which possessed antimicrobial activity (Ngaini, Fadzillah and Hussain, 2012).

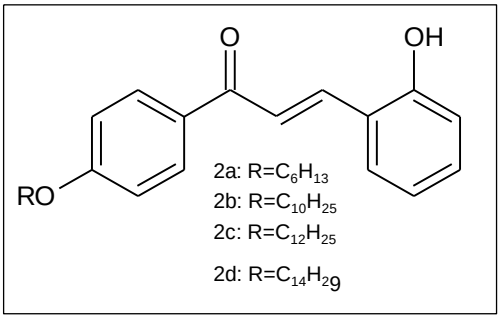

Figure 2.11: Chalcone with variable alkyl chain length (Ngaini, Fadzillah and Hussain, 2012).

For antibacterial studies, it shows that compound in Figure 2.11 exhibits bacteriostatic acitivities against E. coli. It is found that the inhibition activities increase as the concentration of chalcone increases and this proves that bacteriostatic activities is dependent on concentration of chalcone. It is also observed that compound **2a** shows a complete inhibition at 100 ppm compared to the other compounds. However, as the alkyl chain increase, the bacteriostatic

activity decreases. Figure 2.12 shows the inhibition activities of chalcone **2a-2d** (Ngaini, Fadzillah and Hussain, 2012).

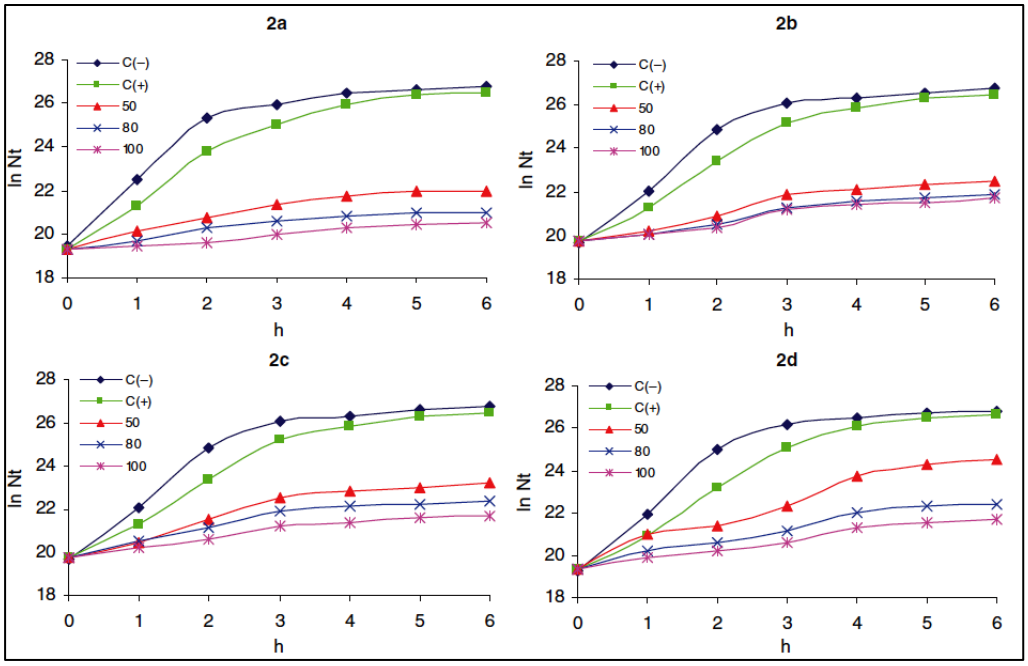

Figure 2.12: Inhibition activities of chalcones **2a-d** towards *E. coli* shown as ln N_t for *E. coli* growth vs. time (Ngaini, Fadzillah and Hussain, 2012).

CHAPTER 3

MATERIALS AND METHODOLOGY

3.1 Chemicals

The chemicals used in this project with its manufacturers were listed in Table 3.1. All chemicals were used without further purification unless it is stated in the synthesis section.

Table 3.1: Chemicals and its manufacturers.

Chemicals	Manufacturers
1-Bromododecane	Merck
1,3-Dibromopropane	Merck
1,4-Dibromobutane	Merck
1,5-Dibromopentane	Merck
1,6-Dibromohexane	Merck
4-Hydroxybenzaldehyde	Acros Organics
4'-Hydroxyacetophenone	Merck
Acetone	Fischer Scientific
Chloroform	Fischer Scientific
Deuterated Chloroform	Merck
Dichloromethane (DCM)	Merck
Ethyl acetate	ChemSoln
Hexane	R & M Chemicals
Methanol	R & M Chemicals
Methylethylketone (MEK)	Merck
Potassium bromide	Merck
Potassium carbonate (anhydrous)	R & M Chemicals
Potassium hydroxide	R & M Chemicals
Tetrabutylammonium bromide (TBAB)	Sigma-Aldrich
TLC aluminium sheet silica gel 60 F_{254}	Merck

3.2 Instruments

Models of the instruments involved in this project were listed in Table 3.2

Table 3.2: Models of instruments.

Models of Instruments
Stuart SMP10 Melting Point Apparatus
Perkin Elmer – FT-IR Spectrometer Spectrum R X 1
Jeol JNM ECP 400MHz Nuclear Magnetic Resonance (NMR) spectrometer
Differential Scanning Calorimeter (DSC) Mettler Toledo DSC823[e]
Perkin Elmer Lambda 35 – UV/Vis Spectrometer

3.3 Synthesis

Synthesis route of compounds **DDB**, **DHP** and **DCnC** is shown in Figure 3.1.

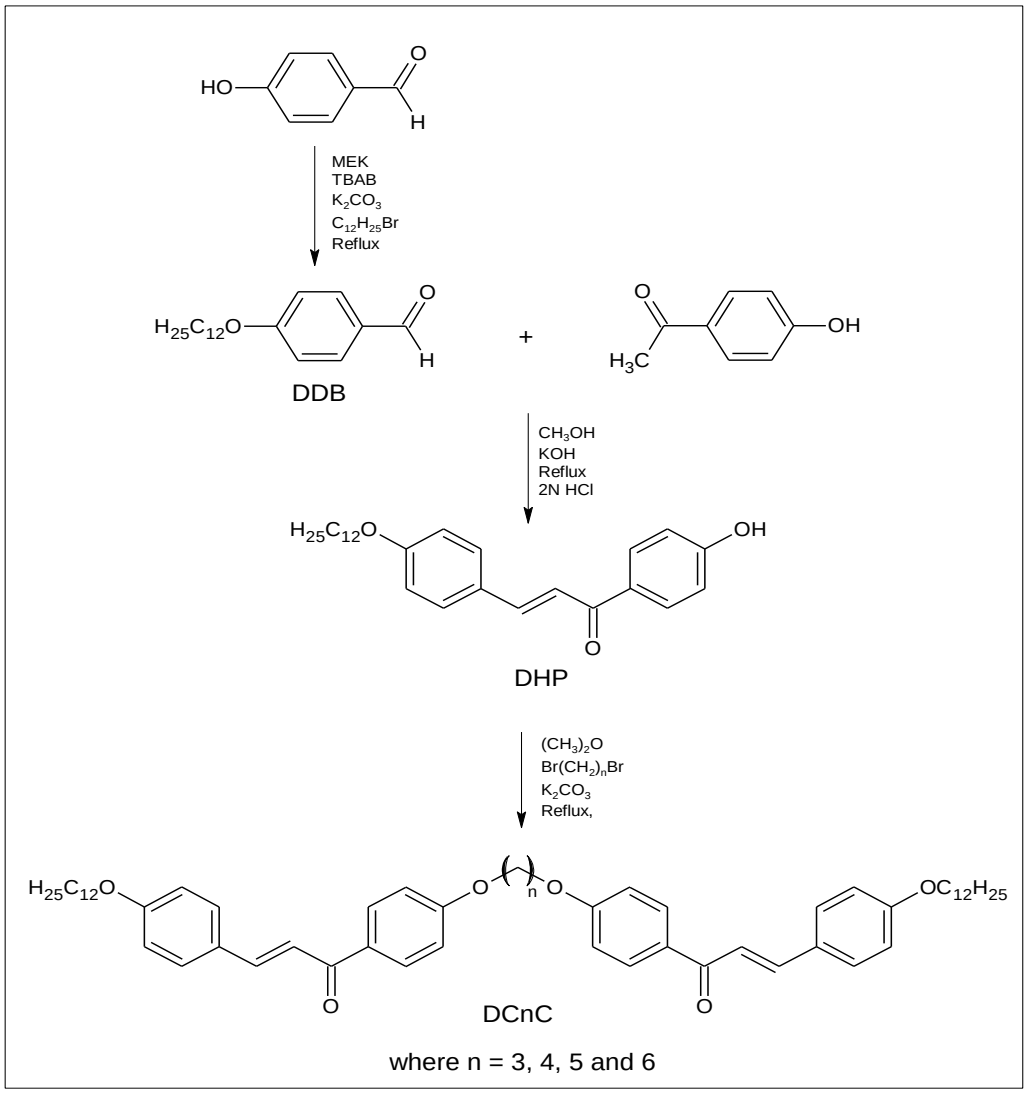

Figure 3.1: Reaction scheme for preparing compound **DDB**, **DHP** and **DCnC.**

3.3.1 Synthesis of 4-dodecyloxybenzaldehyde (DDB)

The synthesis route was modified from the method reported by Ngaini, Chee and Chin (2013). A mixture of 1-bromododecane (4.98g, 20mmol), 4-hydroxybenzaldehyde (3.05g, 25mmol), K_2CO_3 (2.76g, 20mmol), TBAB (0.64g, 2mmol) in MEK (30 to 40mL) were refluxed for 6-10 hours. The mixture was filtered and cooled to room temperature. Water (20mL) was added to the filtrate and the layers were separated. The organic layer was washed with dichloromethane (DCM) (2 x 15mL). The combined organic layer was washed with water (2 x 20mL) then dried over anhydrous magnesium sulphate and excess solvent was evaporated to give brownish oil product.

3.3.2 Synthesis of 3-(4-dodecyloxyphenyl)-1-(4-hydroxyphenyl)prop-2-en-1-one (DHP)

The synthesis route was modified from the method reported by Ngaini, Chee and Chin (2013). A mixture of 4-hydroxyacetophenone (2.73g, 20mmol) and compound **DDB** (5.80g, 20mmol) in 40mL methanol was added under stirring to a solution of KOH (4.04g, 72mmol) in methanol (10mL). The mixture was refluxed for 6-10 hours. The reaction was cooled to room temperature and acidified with cold HCl (2N) until the precipitate stop forming from the mixture. The resulting precipitate was filtered, washed and dried. The crude was recrystallized using hexane:ethanol (7:1) to give yellow crystal.

3.3.3 Synthesis of α,ω-Bis(3-(4-dodecyloxyphenyl)-1-(phenyl-4-oxy)prop-2-en-1-one)alkane, DCnC

3.3.3.1 Synthesis of 1,3-Bis(3-(4-dodecyloxyphenyl)-1-(phenyl-4-oxy)prop-2-en-1-one)propane DC3C

The synthesis route was modified from the method reported by Cook et. al. (2012) and Yeap, et. al. (2006). In a round bottom flask, **DHP** (0.409g, 1mmol) was dissolved in acetone (30-40 mL) containing potassium carbonate (1.38g, 10mmol) and the solution was heated with stirring. 1,3-Dibromopropane (0.101g, 0.5mmol) was then added dropwise and the mixture was refluxed for 6-8 hours. The reaction was cooled to room temperature. The resulting solution was poured into 70mL of cold water and the precipitate formed was filtered off and dried. The precipitate was recrystallized with hexane:dcm (3:1) to yield desired product.

3.3.3.2 Synthesis of 1,4-Bis(3-(4-dodecyloxyphenyl)-1-(phenyl-4-oxy)prop-2-en-1-one)butane, DC4C

1,4-Bis(3-(4-dodecyloxyphenyl)-1-(phenyl-4-oxy)prop-2-en-1-one)butane, **DC4C** was synthesized according to the method described for compound **DC3C**, except replacing 1,3-dibromopropane (0.101g, 0.5mmol) with 1,4-dibromobutane (0.108g, 0.5mmol).

3.3.3.3 Synthesis of 1,5-Bis(3-(4-dodecyloxyphenyl)-1-(phenyl-4-oxy)prop-2-en-1-one)pentane, DC5C

1,5-Bis(3-(4-dodecyloxyphenyl)-1-(phenyl-4-oxy)prop-2-en-1-one)pentane, **DC5C** was synthesized according to the method describe for compound **DC3C**, except replacing 1,3-dibromopropane (0.101g, 0.5mmol) with 1,4-dibromopentane (0.116g, 0.5mmol).

3.3.3.4 Synthesis of 1,6-Bis(3-(4-dodecyloxyphenyl)-1-(phenyl-4-oxy)prop-2-en-1-one)hexane, DC6C

1,6-Bis(3-(4-dodecyloxyphenyl)-1-(phenyl-4-oxy)prop-2-en-1-one)hexane, **DC6C** was synthesized according to the method described for compound **DC3C**, except replacing 1,3-dibromopropane (0.101g, 0.5mmol) with 1,6-dibromohexane (0.122g, 0.5mmol).

3.4 Characterisation

The compounds synthesised were characterized using melting point instrument, thin layer chromatography, Fourier Transform Infrared spectroscopy (FTIR), NMR spectroscopy, differential scanning calorimeter (DSC) and ultraviolet/visible spectral spectrometry.

3.4.1 Melting point determination

Homologous series of α,ω-bis(3-(4-dodecyloxyphenyl)-1-(phenyl-4-oxy)prop-2-en-1-one)alkane, **DCnC** and compound **DHP** were analysed using Stuart SMP10 Melting Point Apparatus to determine the melting point of the compounds.

3.4.2 Thin Layer Chromatography

The purity of the **DHP** and **DCnC** are tested with TLC anaylsis. Mixture of solvent of ethyl acetate and hexane with ratio of 1:1 was used as eluent. The numbers of spots were recorded and their R_f values were calculated.

3.4.3 Infrared Spectroscopy Analysis

Infrared (IR) spectra of **DDB**, **DHP** and final products of α,ω-bis(3-(4-dodecyloxyphenyl)-1-(phenyl-4-oxy)prop-2-en-1-one)alkane, **DCnC** were recorded using a Perkin Elmer 2000 FT-IR spectrometer via KBr disc procedure in the frequency of 4000-400 cm^{-1}.

3.4.4 ^{1}H and ^{13}C Nuclear Magnetic Resonance Spectroscopy Analysis

^{1}H and ^{13}C NMR spectra were recorded using a Jeol JNM ECP 400 MHz NMR spectrometer. About 25 to 50 mg of sample was dissolved in deuterated chloroform solvent at room temperature. Tetramethylsilane (TMS) was used as the internal standard. The spectra were recorded in the chemical shift range of 0 to 10 ppm and 0 to 200 ppm for ^{1}H and ^{13}C NMR respectively.

3.4.5 Differential Scanning Calorimetry

Mettler Toledo DSC823^{e} was used to determine the phase transition temperature and to analyse the enthalpy changes of the samples. The heating and cooling cycles were carried out at the rate of 10℃/min with flow rate of nitrogen has at 10mL/min.

3.4.6 Ultraviolet – Visible Spectral Analysis

Optical properties of α,ω-bis(3-(4-dodecyloxyphenyl)-1-(phenyl-4-oxy)prop-2-en-1-one)alkane, **DCnC** were studied using UV-Vis analysis. All of the compounds were prepared in chloroform with the concentration of 10 μM and scanned in the wavelength region of 260-410 nm at room temperature.

CHAPTER 4

RESULTS AND DISCUSSION

4.1 Physical characteristic of 4-dodecyloxybenzaldehyde (DDB), 3-(4-dodecyloxyphenyl)-1-(4-hydroxyphenyl)prop-2-en-1-one (DHP) and α,ω-Bis(3-(4-dodecyloxyphenyl)-1-(phenyl-4-oxy)prop-2-en-1-one)alkane (DCnC)

The physical characteristic of **DDB, DHP** and **DCnC** are tabulated in Table 4.1. The percentage of yields for each compound is tabulated in Table 4.1.

Table 4.1: Physical characteristic and yield for **DDB**, **DHP** and **DCnC.**

Compounds	Physical Appearance	Yield (%)
DDB	Reddish brown liquid	89.72%
DHP	Yellowish crystal	46.78%
DC3C	Pale yellow crystal	15.76%
DC4C	Pale yellow crystal	20.45%
DC5C	Pale yellow crystal	17.28%
DC6C	Pale yellow crystal	23.63%

4.2 Synthesis of DDB, DHP and DCnC

DDB, DHP and **DCnC** were synthesised through Williamson etherification process and Claisen Schmidt condensation process.

4.2.1 Williamson Etherification between 4-Hydroxybenzaldehyde and 1-Bromododecane

In the formation of **DDB**, Williamson etherification was used in the reaction of 4-hydroxybenzaldehyde (**4OH**) and 1-bromododecane. This reaction occurs in two steps. In the first step, a base which is potassium carbonate (**K_2CO_3**) is used to abstract the hydrogen from the hydroxyl group of **4OH** and alkoxide ion is formed. In the second step, this alkoxide ion then act as a nucleophile and attack the carbon bonded with the halogen group of 1-bromododecane through S_N2 mechanism. In this reaction, the catalyst used is tetrabutylammonium bromide (**TBAB).** The general mechanism of etherification process is shown in Figure 4.1 and percentage yield of **DDB** is tabulated in Table 4.1.

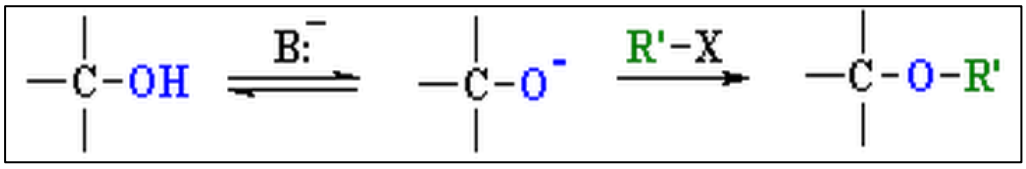

Figure 4.1: General mechanism of etherification.

4.2.2 Claisen Schmidt Condensation between DDB and 4 - Hydroxyacetophenone

The second intermediate, **DHP** was formed by reacting the first intermediate, **DDB** with 4-hydroxyacetophenone (**4ACE)** through Claisen Schmidt condensation. This reaction is done with a presence of basic a catalyst, potassium hydroxide (KOH). This base will abstract the α-hydrogen from

4ACE and an enolate ion is the product. This enolate ion is then stabilised by resonance. The electrons of the double bond will then attack the carbonyl carbon of **DDB** followed by abstraction of H^+ ion from the water and give rise to aldol compound. This aldol compound would then undergo dehydration process catalyse by hydroxide ion. This hydroxide ion will attack the α-hydrogen followed by the expulsion of hydroxide at β-carbon. A double bond is then formed between the α and β carbon. A detailed mechanism of the reaction is shown in Figure 4.2 and the percentage of yield of **DHP** is shown in Table 4.1.

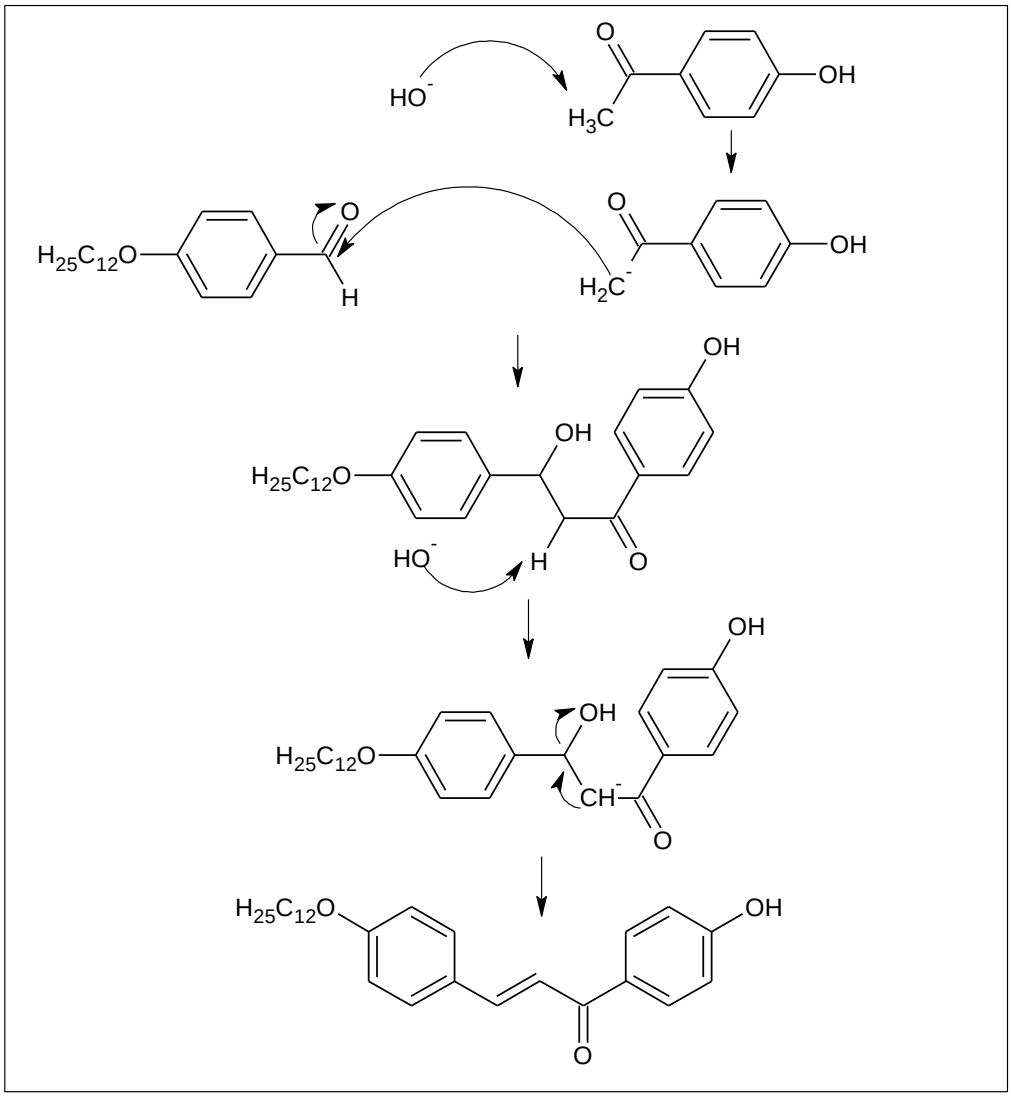

Figure 4.2: Mechanism of Claisen-Schmidt condensation.

4.2.3 Williamson Etherification between DHP and α,ω-Dibromoalkane

The final product, **DCnC** were formed by reacting the second intermediate, **DHP** with α,ω-dibromoalkane through Williamson etherification reaction. The mechanism of the reaction is the same as section 4.2.1 except for this reaction, the base used serves dual purposes which act as a base as well as a catalyst. The percentage yields of **DCnC** were tabulated in Table 4.1.

4.3 Structural Elucidation of 3-(4-dodecyloxyphenyl)-1-(4-hydroxyphenyl)prop-2-en-1-one (DHP) and α,ω-Bis(3-(4-dodecyloxyphenyl)-1-(phenyl-4-oxy)prop-2-en-1-one)alkane (DCnC)

4.3.1 Thin Layer Chromatography (TLC)

DHP and **DCnC** were analysed using TLC plates to determine the purity of the compounds. The TLC plates were spotted and developed in hexane : ethyl acetate, 1 : 1 solvent system and it was visualised under 254 nm UV light lamp. Table 4.2 illustrates the data collected from the TLC analysis.

Table 4.2: Retention factors for **DHP** and **DCnC**

Compounds	R_f Value
DHP	0.714
DC3C	0.857
DC4C	0.857
DC5C	0.857
DC6C	0.857

4.3.2 Infrared Spectral Analysis

DHP was formed by reaction of **DDB** and **4ACE** while **DCnC** is formed from the reaction of **DHP** and α,ω-dibromoalkane. Therefore, the FTIR spectrum of **DHP** will be discussed and compared with spectra of **4ACE** and **DDB**, while for **DCnC** homologous series, **DC3C** is chosen as representative and its FTIR spectrum will be discussed and compared with the spectrum from **DHP**. Selected IR data are shown in Table 4.3.

In **4ACE**, the ν(O-H) is indicated by broad peak centred at 3136 cm^{-1} while **DDB** does not show any ν(O-H). This is in agreement as there is phenol group in **4ACE** but hydroxyl group is absent in **DDB**. Upon the formation of **DHP**, ν(O-H) has been shifted to a lower frequency which is 3072 cm^{-1}. Similar ν(O-H) frequency has been reported by Yelamaggad, et. al. (2007) for the same compound. Lowering of the ν(O-H) frequency might be due to the increased intermolecular hydrogen bonding which would weakens the O-H bond.

In **DDB** and **DHP**, strong absorption bands are observed around 2950-2850 cm^{-1} and these peaks are due to aliphatic ν(C-H) asymmetrical and symmetrical stretching vibration of methyl and methylene group of long alkyl chain (Bhagvatiprasad, 2011). These signals are in agreement with both **DDB** and **DHP** as both has long alkyl chain as part of the compounds.

The v(C=O) frequencies for **DDB** and **4ACE** are 1690 and 1646 cm^{-1} respectively. These values are in agreement as **DDB** has carbonyl aldehyde and **4ACE** has carbonyl ketone. In **DHP**, v(C=O) is observed at 1644 cm^{-1} which is lower than **4ACE** and **DDB**. Similar value for v(C=O) was reported by Ngaini, et.al (2012) for (E)-1-(4-dodecyloxyphenyl)-3-(4-hydroxyphenyl)-prop-2-en-1-one. It is observed that the v(C=O) shifted to lower frequency from **DDB** to **DHP**. This indicates that the reaction has taken place whereby the carbonyl aldehyde reacted to form **DHP**. Besides that, the lowering frequency of carbonyl group in **DHP** is due to the conjugation of unsaturated alkene with two benzene rings. Therefore, the carbonyl group has more singly characteristic thus showed at lower frequency.

The v(C=C) frequencies for **4ACE** and **DDB** are observed around 1610-1430 cm^{-1}. For **4ACE**, the C=C aromatic stretch are observed at 1585 and 1439 cm^{-1} while for **DDB**, the C=C aromatic stretch are observed at 1602 and 1578 cm^{-1}. However, for **DHP**, v(C=C) frequencies are observed at 1603, 1591 and 1509 cm^{-1}. Absorption bands at 1603 cm^{-1} and 1591 cm^{-1} are assigned as olefinic C=C stretch while 1509 cm^{-1} is assigned as aromatic C=C stretch. Sreedhar, et. al. (2010) reported similar values of frequencies for olefinic C=C stretch while similar values for C=C aromatic stretch reported by Ngaini, et. al. (2012).

Based on the FTIR data, the olefinic C=C stretch is present at relatively lower wavenumber and the possible reason for this observation is due to the conjugation of olefinic carbon with carbonyl and phenyl group. Besides that, the intensity of the olefinic C=C peak is intensified due to strong dipole of carbonyl group, with two closely spaced peaks being observed (Pavia, et al., 2009). This is due to the formation of two possible conformations which is *cis* and *trans* conformations (Shin, et al., 2001). On the other hand, the aromatic C=C stretch frequency of **DHP** remains almost the same with **DDB** and **4ACE**. The slight decrease might be due to the conjugation effect.

In **4ACE**, there is no C-O stretch as there is no ether functional group. However, for **DDB**, the v(C-O) absorption band is observed at 1259 and 1159 cm^{-1}. Similar values of v(C-O) frequencies reported by Islam, et. al. (2012) for a similar compound. The signal at 1259 cm^{-1} represents phenyl ether while signal at 1159 cm^{-1} represenst aliphatic ether (Pavia, et al., 2009). For **DHP**, the v(C-O) frequencies are observed at 1291 and 1175 cm^{-1}. It is observed that the wavenumber shifted slightly higher than **DDB** and one of the possible reason is the ability of oxygen to conjugate with the phenyl group and ketone carbonyl group thus give the C-O bond more double bond characteristic which show the signals at higher frequencies (Ha and Low, 2013).

It is observed that **4ACE** and **DDB**, there is no signal representing v(C=C) trans while in **DHP**, v(C=C) trans is observed at 987 cm^{-1}. This shows that the formation of chalcone with trans conformation is a success. Besides that, signal representing *para*-substituted benzene for **4ACE** and **DDB** is observed at 835 cm^{-1} and 833 cm^{-1} respectively. This is in agreement as both **4ACE** and **DDB** has *para* substituent. For **DHP**, the frequency representing *para* – substituted benzene is observed at slightly lower frequency which is at 825 cm^{-1}. The main reason of this shifting is due to the conjugation effect between the phenyl ring and the enone bond in chalcone.

IR spectrum of **DC3C** is then compared to the IR spectrum of **DHP**. It is found that all the signal between **DHP** and **DC3C** is the same except the v(O-H) in **DHP** disappear in **DC3C**. This is in agreement as formation of **DC3C** from **DHP** involves the etherification of phenol group in **DHP**. Therefore, in the IR spectrum of **DC3C**, there is no O-H peak observed due to the reaction completion. Besides that, it is observed there is one new peak at 1266 cm^{-1} and this peak possibly represent the new C-O bond form through etherification process. FTIR spectrum of **DDB**, **DHP** and **DC3C** are shown in Figures 4.3, 4.4, and 4.5 respectively.

Table 4.3: IR frequencies of **4ACE, DDB, DHP** and **DC3C.**

Compounds	IR Frequencies of Compounds (cm^{-1})									
	$v(O-H)_{free}$	v(O-H)	$v(C-H)_{aro}$	$v(CH_2)$	v(C-H)	v(C=O)	v(C=C)	v(C-O)	$v(C=C)_{trans}$	$v_{para\ subs}$
4ACE	3678	3136	-	3015	2812	1646	1585 1439	-	-	835
DDB	-	-	-	2925	2854 2733	1690	1602 1578	1259 1159	-	833
DHP	-	3072	3017	2937 2870	2918 2850	1644	1603 1591 1509	1291 1175	987	825
DC3C	-	-	3017	-	2918 2849	1618	1603 1508	1295 1266 1247 1177	991	817

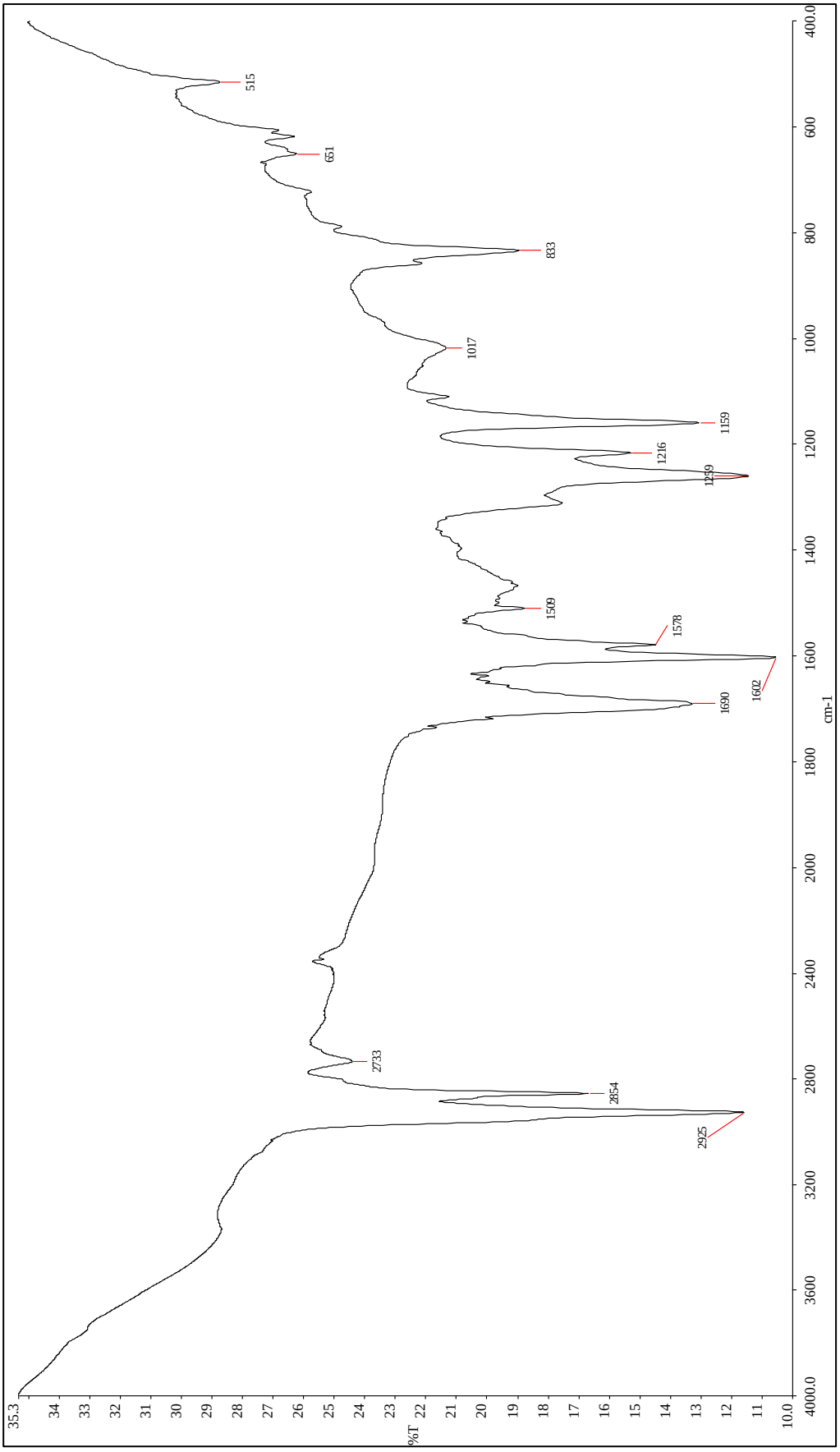

Figure 4.3: IR spectrum of **DDB**

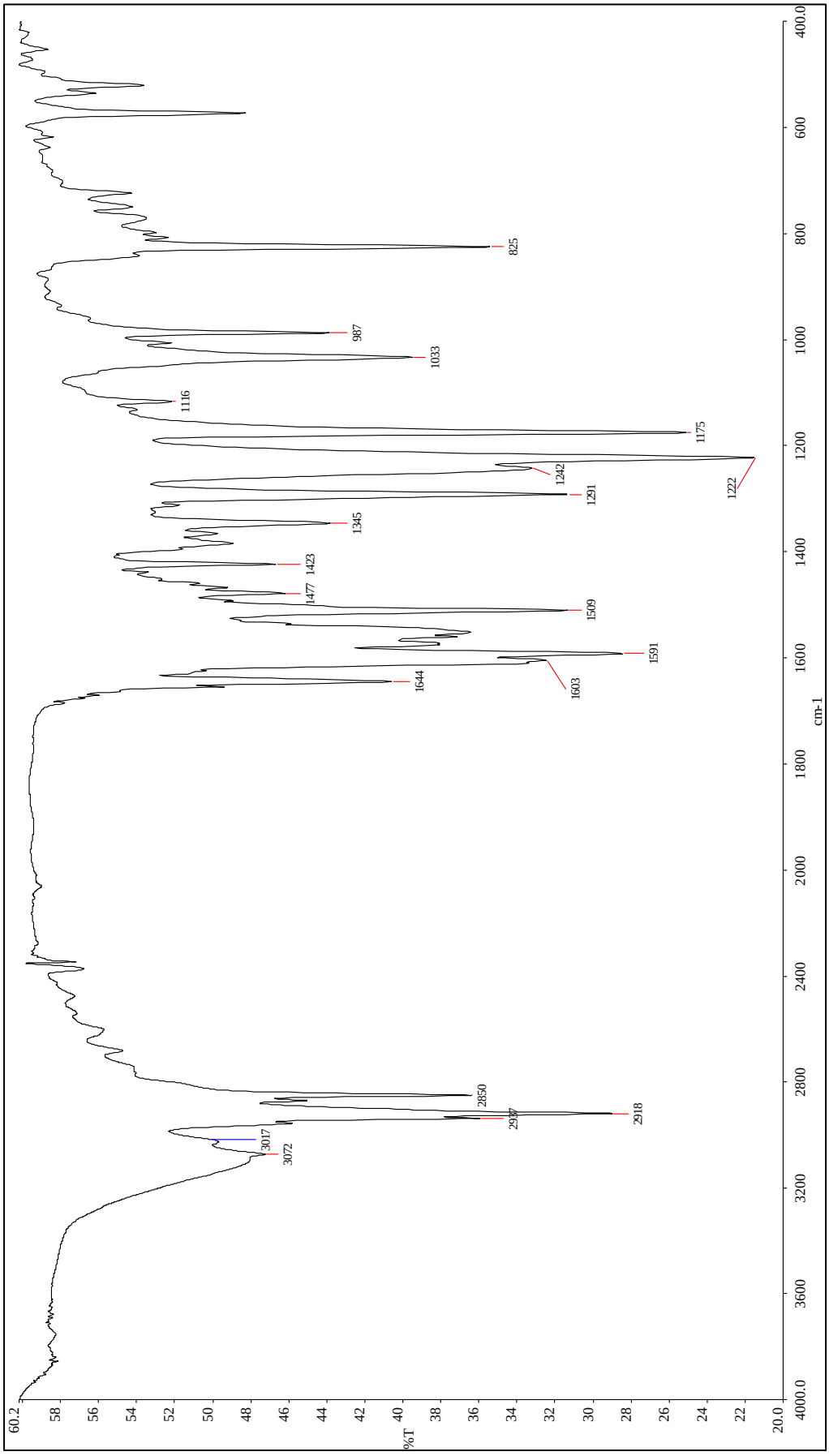

Figure 4.4: IR spectrum of **DHP**

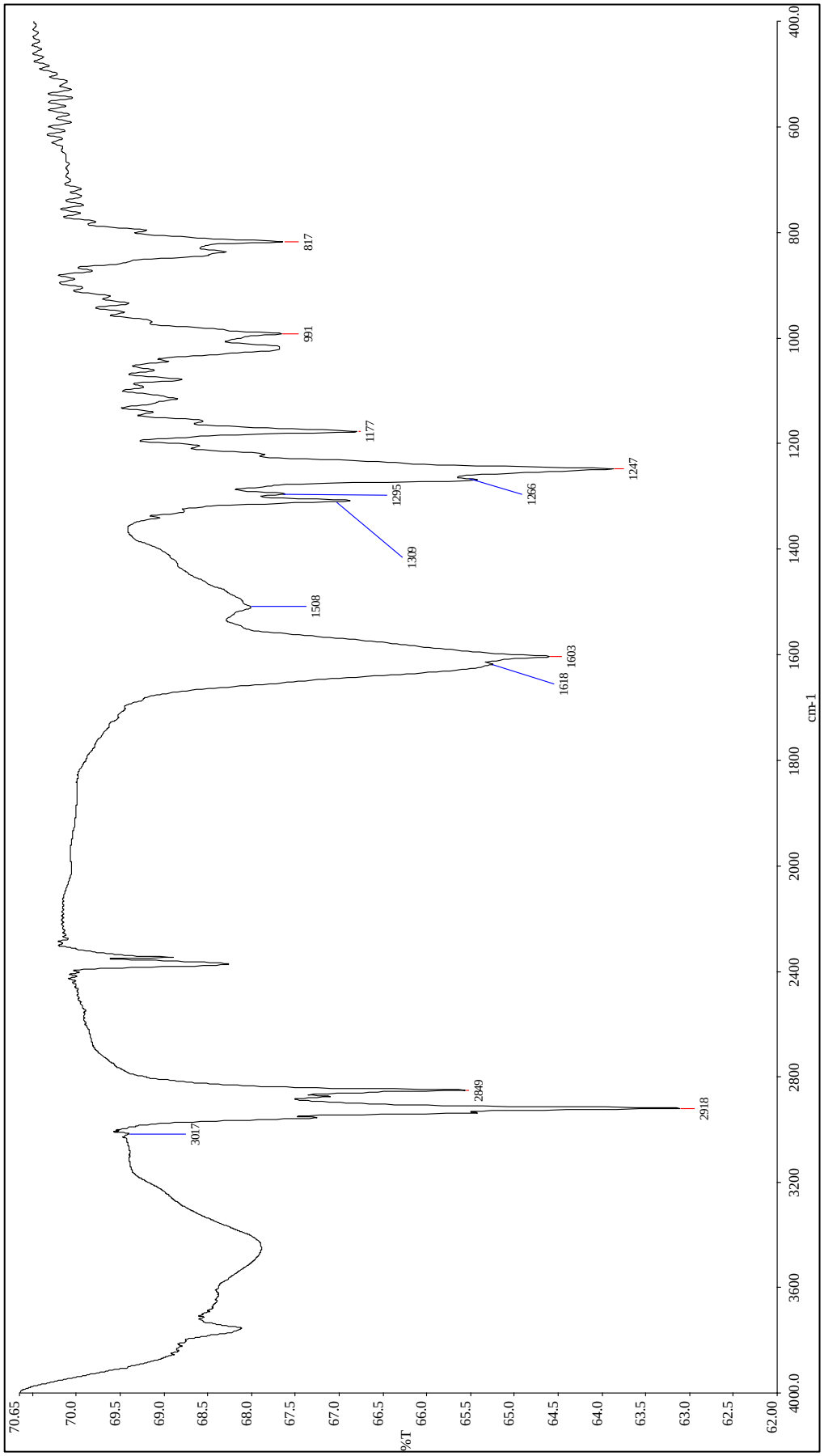

Figure 4.5: IR spectrum of **DC3C**

4.3.3 ^{1}H NMR Spectral Analysis

4.3.3.1. 3-(4-Dodecyloxyphenyl)-1-(4-hydroxyphenyl)prop-2-en-1-one (DHP)

DHP has been sent for ^{1}H NMR analysis. The structure of **DHP** is shown in Figure 4.6 with numbering scheme. All the data of chemical shift, δ (ppm) and coupling constant (*J*) for **DHP** have been tabulated in Table 4.4 and the ^{1}H NMR spectrum is shown in Figure 4.7.

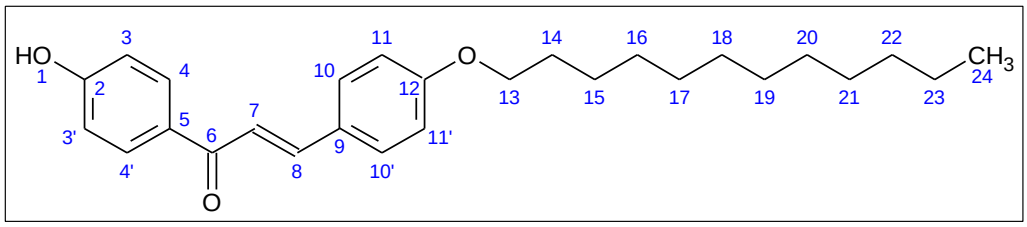

Figure 4.6: Structure of **DHP.**

Table 4.4: ^{1}H NMR data of **DHP.**

Proton(s)	Number(s) of H	Coupling constant, J (Hz)	Chemical shift, ppm	Multiplicity of signal (s)
H4 & H4'	2	8.72	7.98	d
H8	1	15.60	7.78	d
H10 & H10'	2	9.16	7.57	d
H7	1	15.12	7.41	d
H3 & H3'	2	8.68	6.94	d
H11 & H11'	2	9.16	6.91	d
H1	1	-	6.73	s
H13	2	6.88	3.99	t
H14	2	-	1.82 – 1.75	p
H15	2	-	1.48 – 1.41	m
H16 – H23	16	-	1.34 – 1.25	m
H24	3	6.88	0.88	t

* d = doublet, t = triplet, m = multiplet, p = pentet

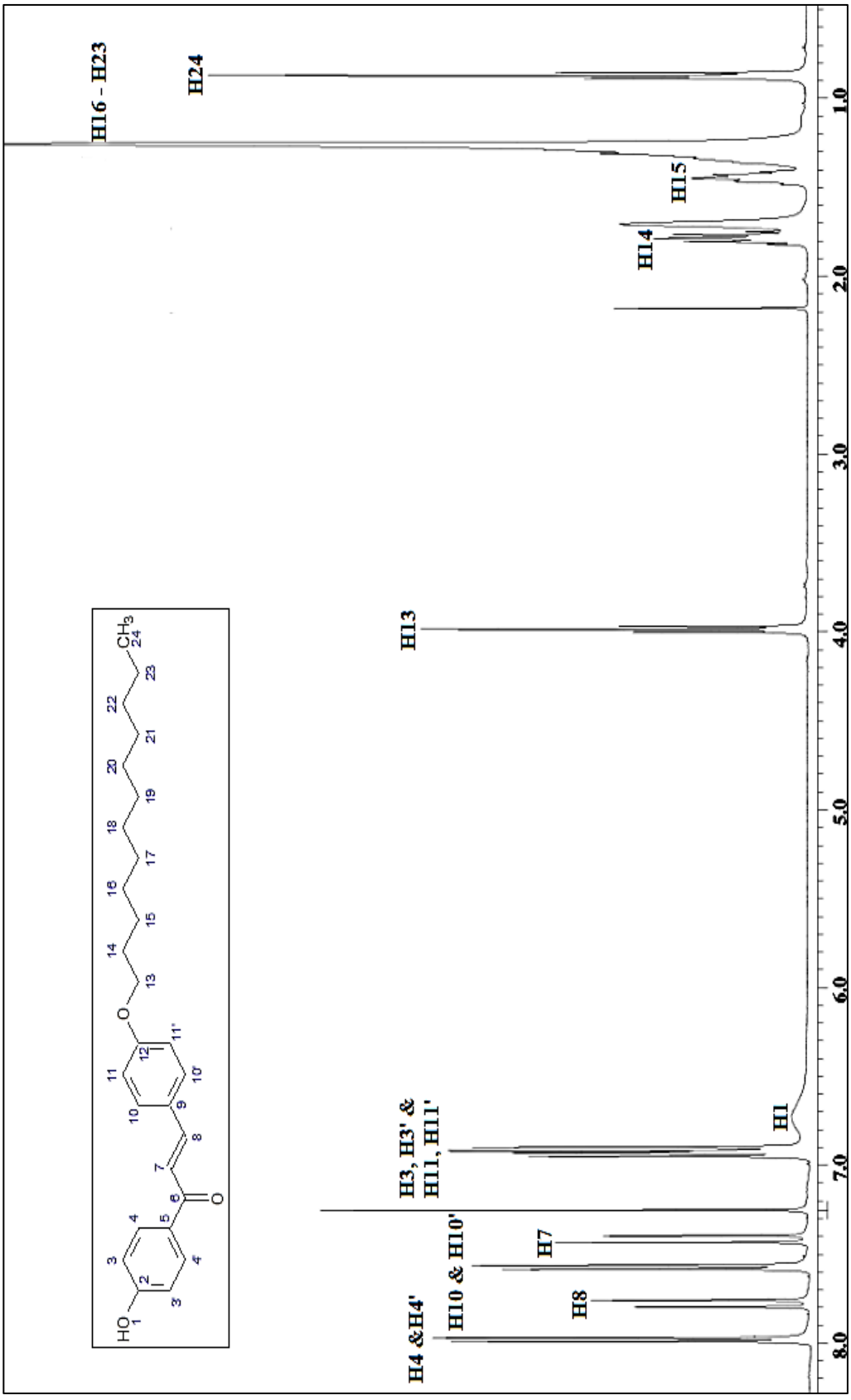

Figure 4.7: ^{1}H NMR spectrum of **DHP**

The solvent used for ^{1}H NMR analysis of **DHP** was deuterated chloroform ($CDCl_3$) thus the solvent peak is present at 7.25 ppm. Multiplet signals present in the region of δ = 7.98 – 6.91 ppm are assigned as the aromatic protons (Ar-H). Doublet signals present at δ = 7.78 and δ = 7.41 ppm are assigned as olefinic protons. Protons in O-CH_2- group are found at δ = 3.99 ppm, and the following proton on the next carbon atom in the alkyl chain have a chemical shift of δ = 1.82 – 1.75 ppm. The remaining protons in alkyl chain are found in the region of δ = 1.48 – 1.25 ppm. Protons of methyl group is found at δ = 0.88 ppm. All these values are similar to the values reported by Yelamaggad, et. al. (2007)

H4 and H4' has been shifted to the most deshielded region in Ar-H due to the strong electron withdrawing carbonyl group. This carbonyl group is directly attached to the phenyl group *ortho* to the H4 and H4' thus this electron withdrawing group undergo conjugation with the phenyl group. The resulting resonance form will have a lower electron density at *ortho* and *para* position of phenyl group. Besides that, the magnetic anisotropy effect caused by π-bond of carbonyl to the *ortho* position further deshields the *ortho* proton. This then leads to H4 and H4' signal appear at deshielded region due to lower electron density around these protons. Similar reason could be applied to the deshielding effect of H10 and H10'. H10 and H10' is slightly further away from the carbonyl group thus the deshielding effect is lower compared to H4 and H4'.

H3, H3', H11 and H11' signal appears as two doublets at δ = 6.96 – 6.92 ppm and these four protons belong to Ar-H. These four protons appeared at more shielded region compared to H4, H4', H10 and H10'. One of the reasons for this explanation is due to the electron donation effect from oxygen of ether and phenol group which is then increase the electron density around these four protons causing them to appear at slightly more shielded region. Besides that, these four protons are further away from carbonyl group thus the inductive effect is not as strong as resonance effect.

The olefinic proton found at downfield region (δ = 7.78 ppm) is assigned to the β-position (H8) of unsaturated ketone, while the upfield region (δ = 7.41 ppm) is assigned to the α-position (H7). This is due to the resonance form of α,β-unsaturated ketone. This causes lower electron density around the β-carbon thus β-hydrogen is more deshielded. Besides that, the anisotropic field generated by the π-electrons of benzene would interact with β-hydrogen which further deshield it.

H13 signal appear at moderately shielded region (δ = 3.99 ppm). Even though these protons are directly attached to the oxygen of ether, the electron density around it is highly dense. One of the possible reasons is due to the donation effect from alkyl chain. The electron withdrawing effect of ether oxygen is reduced due to the donation effect from the alkyl chain therefore, even with presence of oxygen attached directly to the carbon bonded to H13, the electron

density around H13 remain dense and the signal appear at moderately shielded region. Besides that, the oxygen of ether group can act as electron donating group thus further increase the electron density around H13.

Signals appeared at δ = 1.82 – 1.25 ppm represents the protons at the alkyl chain (H14 – H23). It appears at highly shielded region as the electron densities of the protons are very high. Another signal is observed at δ = 0.89 – 0.85 ppm and these signals represent methyl group of alkyl chain. For this compound, there is no electron withdrawing group attached directly to it thus the electron density is highly dense.

Coupling constants are calculated to determine the types of coupling proton in **DHP**. For Ar-H, H3 and H3' are coupled with H4 and H4' and show doublet coupling constant of $J_{3,4}$ = 8.68 Hz. Based on calculated coupling constant, it suggested that the interaction between H3 and H3' with H4 and H4' is *ortho* interaction. H4 and H4' are then coupled with H3 and H3' and show doublet coupling constant of $J_{4,3}$ = 8.72 Hz. There is slight difference in calculated value of $J_{3,4}$ and $J_{4,3}$ which might be cause slight differences in chemical shift. Similar reason is applied to the rest of the coupling of protons which shows slight difference in coupling constant. H11 and H11' are coupled with H10 and H10' and show doublet coupling constant of $J_{11,10}$ = 9.16 Hz. From the coupling constant calculated, the interaction between H11 and H11' with H10 and H10' is *ortho* interaction. The same coupling constant value was obtained

between H10 and H10' coupled with H11 and H11'.Through further analysis, on ^{1}H NMR spectrum, it is found that H8 coupled with H7 and show doublet with coupling constant of $J_{8,7}$ = 15.60 Hz. The coupling of H7 and H8 show slightly different value which is $J_{7,8}$ = 15.12 Hz and this might be slight differences in chemical shift. These values of coupling constant between H7 and H8 suggest that the interactions between these two protons are in *trans* position.

H13 coupled with H14 showing triplet signal with coupling constant of $J_{13,14}$ = 6.88 Hz. For H13 – H23, it show multiplet signals thus the coupling constant these protons cannot be determined. H24 coupled with H23 and show triplet with coupling constant of $J_{24,23}$ = 6.88 Hz.

4.3.3.2 α,ω-Bis(3-(4-dodecyloxyphenyl)-1-(phenyl-4-oxy)prop-2-en-1-one)alkane (DCnC)

All compounds in homologous series of **DCnC** have been sent for ^{1}H NMR analysis. **DC3C** was chosen as representative for **DCnC** series and will be discussed. The structure of **DC3C** is shown in Figure 4.8 with numbering scheme. All the data of chemical shift, δ (ppm) and coupling constant (*J*) for **DC3C** have been tabulated in Table 4.5 and the ^{1}H NMR spectrum is shown in Figure 4.9.

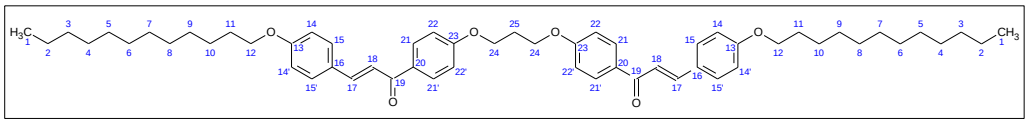

Figure 4.8: Structure of **DC3C.**

Table 4.5: ^{1}H NMR data of **DC3C.**

Proton(s)	Number(s) of H	Coupling constant, J (Hz)	Chemical shift, ppm	Peak (s)
H21 & H21'	4	9.16	8.02	d
H17	2	15.56	7.77	d
H15 & H15'	4	8.68	7.58	d
H18	2	15.60	7.41	d
H22 & H22'	4	9.20	6.99	d
H14 & H14'	4	8.68	6.91	d
H24	4	5.92	4.26	t
H12	4	6.88	3.99	t
H25	2	-	2.37 – 2.32	p
H11	4	-	1.82 – 1.75	m
H10	4	-	1.47 – 1.41	m
H2 – H9	32	-	1.31 – 1.26	m
H1	6	6.40	0.87	t

* d = doublet, t = triplet, m = multiplet, p = pentet

The solvent used to for ^{1}H NMR analysis of **DC3C** was deuterated chloroform ($CDCl_3$) thus the solvent peak is present at 7.25 ppm. Multiplet signals present in the region of δ = 8.02 – 6.91 ppm are assigned as the aromatic protons (Ar-H). Doublet signals present at δ = 7.77 and δ = 7.41 ppm are assigned as olefinic protons. Signal due to O-CH_2- protons are found at δ = 4.24 and δ = 3.99 ppm. The methylene group on the spacer where the plane of symmetry is observed has a chemical shift of δ = 2.37 – 2.32 ppm. The remaining protons in alkyl chain are found in the region of δ = 1.50 – 1.26 ppm. Protons of methyl group is found at δ = 0.89 – 0.86 ppm. All these values are similar to the values reported by Yelamaggad, et al (2007).

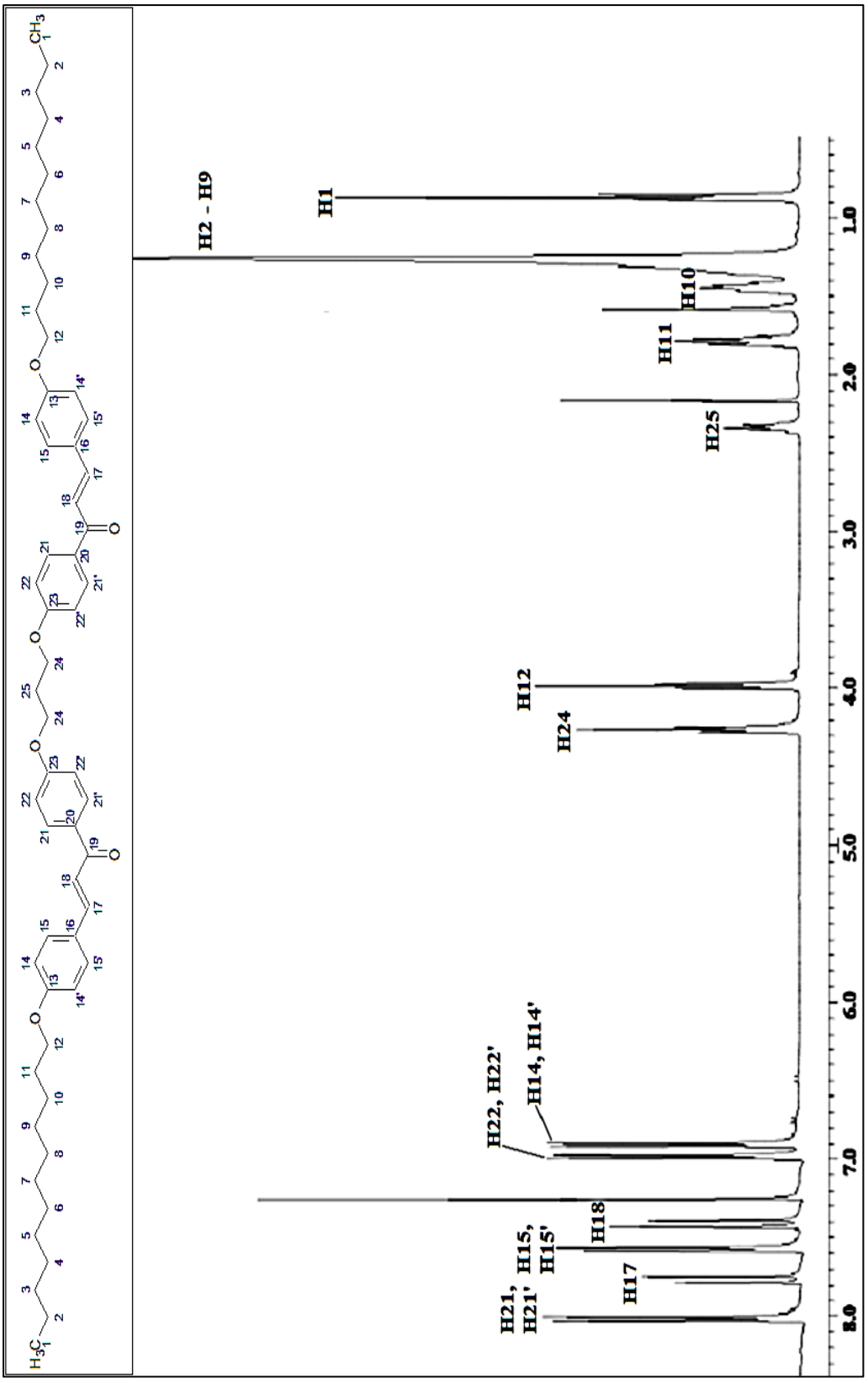

Figure 4.9: ^{1}H NMR spectrum of **DC3C**

The peaks observed in ^{1}H NMR spectrum of **DC3C** is the same as **DHP** which was explained in section 4.3.3.1**.** The only difference between these two spectra is the absence of proton representing hydroxyl group in **DC3C** spectrum. This is in agreement as to synthesise **DC3C**, **DHP** has to undergo etherification process therefore, the hydroxyl peak in **DC3C** spectrum disappear. Besides that, it is observed that in **DC3C** spectrum, there is additional one signal at δ = 4.26 ppm which represent the new ether bond that form. This signal is at slightly deshielded region compared to the other ether signal at δ = 3.99 ppm. The possible reason for this observation is due to the presence of oxygen atom which is an electron withdrawing group. H24 is more deshielded than H12 because it has two oxygen atom nearby which can withdraw electron from it thus lower the electron density around H24. Therefore, the signal representing H24 appear at more deshielded region. There is also another new signal observed at δ = 2.37 – 2.32 ppm. This signal represent the H25 which is the centre of symmetrical plane exist.

Coupling constants are calculated to determine the types of coupling proton in **DC3C**. For the new signal that present, only one new coupling constant was calculated as the rest of the new peaks show multiplet signal. H24 coupled with H25 with coupling constant of $J_{24,25}$ = 5.92 Hz.

4.3.4 ^{13}C NMR Spectral Analysis

4.3.4.1 3-(4-dodecyloxyphenyl)-1-(4-hydroxyphenyl)prop-2-en-1-one (DHP)

DHP has been sent for ^{13}C NMR analysis. The structure of **DHP** is shown in Figure 4.6 with numbering scheme. All the data of chemical shift, δ (ppm) for **DHP** have been tabulated in Table 4.6 and the ^{13}C NMR spectrum is shown in Figure 4.10.

Table 4.6: ^{13}C NMR data of **DHP**

Position of C	Chemical Shift (ppm)
C6	189.54
C5	161.37
C2	160.55
C8	144.59
C9	131.22
C4	131.15
C10	130.32
C12	127.53
C7	119.35
C3	115.63
C11	115.00
C13	68.31
C14 – C23	32.01, 29.75, 29.68, 29.46, 29.44, 29.24, 26. 09, 22.79
C24	14.22

Solvent peak at δ = 77.11 ppm represents $CDCl_3$. Carbonyl carbon was assigned at δ = 189.54 ppm. Aromatic carbon peaks are within δ = 161.37 – 115.00 ppm. Ether carbon is at δ = 68.31 ppm while olefinic carbon are found at δ = 119.35 and δ = 144.59 ppm. Other signals represent aliphatic carbon and all these values similar as reported by Ngaini, Fadzillah and Hussain, (2012).

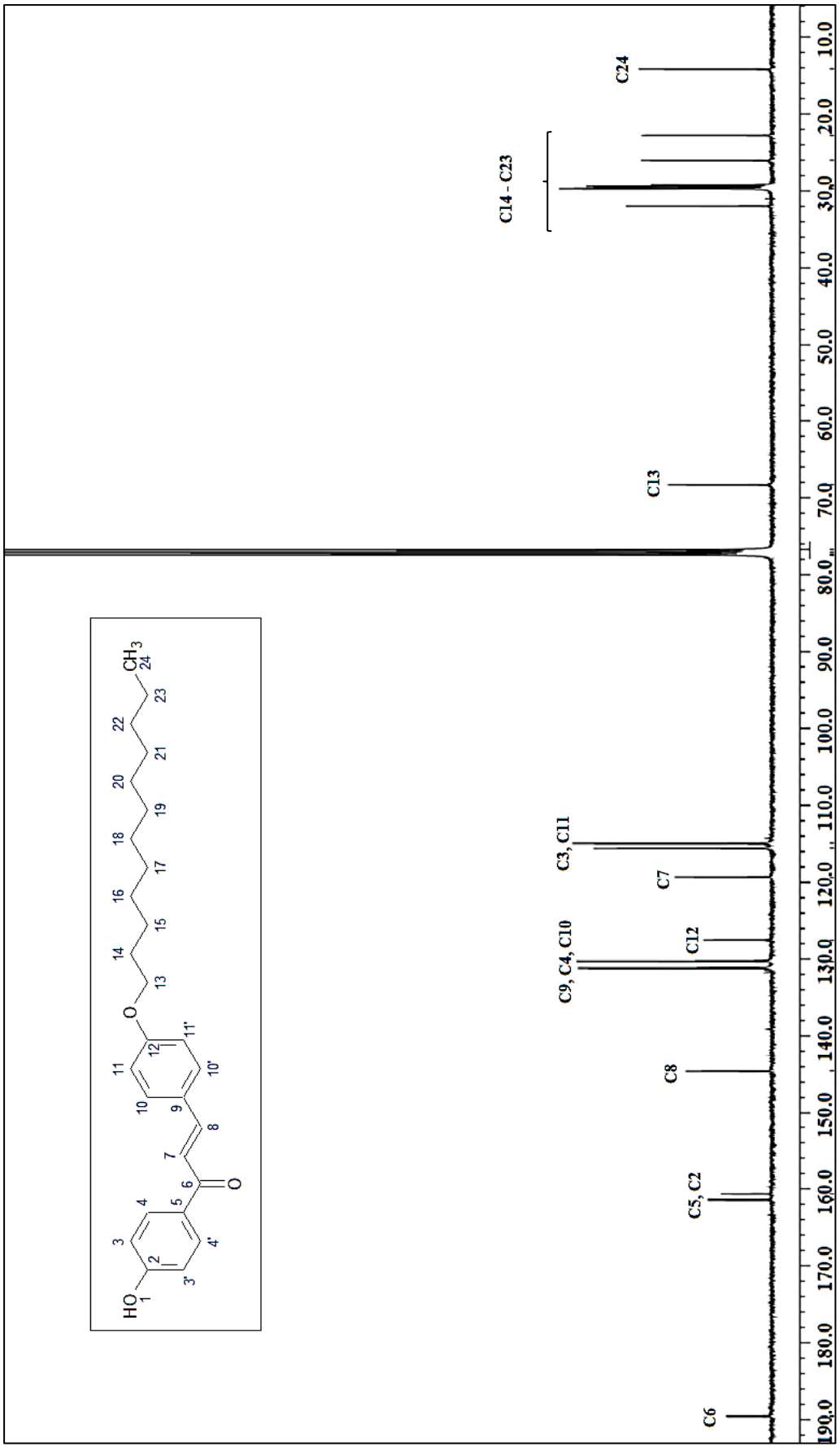

Figure 4.10: ^{13}C NMR of **DHP**

The C6 is found in the most deshielded region in ^{13}C NMR spectrum due to the highly electronegative oxygen atom directly attached to the carbon of carbonyl group of ketone. Oxygen has electron withdrawing properties thus it withdraw the electron density away from carbon toward itself. Therefore, the carbon of carbonyl group has low electron density which causes it to be deshielded. In addition, the magnetic anisotropy effect generated by phenyl and olefin π electrons further deshields the carbonyl carbon.

The signal at δ = 144.59 ppm is assigned to C8 due to its more electron poor characteristic as β-carbon in α,β-unsaturated ketone. Through resonance of α,β-unsaturated ketone, the electron density on the β-carbon would be pulled towards the carbonyl group thus making it highly deshielded compared to α-carbon. Through this resonance structure, α-carbon will be more shielded than β-carbon thus its signal appear at δ = 119.35 ppm. Another possible reason of lower electron density on β-carbon is due to anisotropic field generated by π electrons of phenyl group.

The region of δ = 161.37 – 115.00 ppm are assigned to Ar-C. It can be further classified whereby C5 and C2 signals are at δ = 161.37 and 160.55 ppm respectively. The signals for C9 and C12 appear at δ = 131.22 and δ = 127.52 ppm respectively. For C3, C4, C10 and C11, their signals are observed at δ = 115.63, 131.15, 130.32 and 115.00 ppm respectively. The assignment of signal could be done by observing the intensity of the carbon signals in the ^{13}C NMR.

For C5 and C2, their intensity is almost the same with the intensity of C9 and C12. This is due to the absence of hydrogen directly attached to the respective carbon thus there is absence of Nuclear Overhauser Enhancement (NOE) effect on that particular carbon which give rise to lower intensity signal. In C3 & C3', C4 & C4', C10 & C10' and C11 & C11', there is one hydrogen in each of the carbon atoms. Since C3 and C3' is essentially the same, there is total of two hydrogen atoms on the carbon numbered with "3". This applied to all the respective carbon which are C4, C10 and C11. When there are two hydrogen atoms present, the NOE effect would be higher compared to C2, C5, C9 and C12 thus higher intensities of carbon signals are generated.

There is one signal at δ = 68.31 ppm and this signal represent the ether bond present in the compound. The carbon directly attached to the oxygen is slightly deshielded but no as highly deshielded as carbon of carbonyl group due to electron donation effect of oxygen atom. Therefore, the carbon bonded to oxygen through ether bond has higher electron density and the signal appear at moderately shielded region.

It is observed that many signals present in the region of δ = 33.42 – 22.80 ppm and these signals represent the alkyl chain (C14 – C23). It is found that all of the signals give similar abundance. The carbon signal of methyl group in alkyl chain is found to be at the most shielded region which is at δ = 14.22 ppm.

4.3.4.2 α,ω-Bis(3-(4-dodecyloxyphenyl)-1-(phenyl-4-oxy)prop-2-en-1-one)alkane (DCnC)

All the compounds in homologous series of **DCnC** have been sent for ^{13}C NMR analysis and **DC3C** was chosen as representative and will be discussed. The structure of **DC3C** is shown in Figure 4.8 with numbering. All the data of chemical shift, δ (ppm) for **DC3C** have been tabulated in Table 4.7 and the ^{13}C NMR spectrum is shown in Figure 4.11.

Table 4.7: ^{13}C NMR data of **DC3C**

Position of C	Chemical Shift (ppm)
C19	188.87
C20	162.54
C16	161.26
C17	144.12
C23	131.60
C21	130.82
C15	130.21
C13	127.61
C18	119.38
C22	115.00
C14	114.33
C24	68.28
C12	64.55
C25	32.01
C2 – C11	29.75, 29.73, 29.68, 29.66, 29.46, 29.44, 29.25, 29.18, 26.10, 22.79
C1	14.23

$CDCl_3$ peaks observed at δ = 77.11 ppm. Carbonyl carbon was assigned at δ = 188.87 ppm. Aromatic carbon peaks are within δ = 162.54 – 114.33 ppm. Ether carbon are at δ = 68.28 – 68.55 ppm while olefinic carbon are found at δ = 119.38 and δ = 144.12 ppm. Other signals represent aliphatic carbon and all these values similar as reported by Ngaini, Fadzillah and Hussain, (2012).

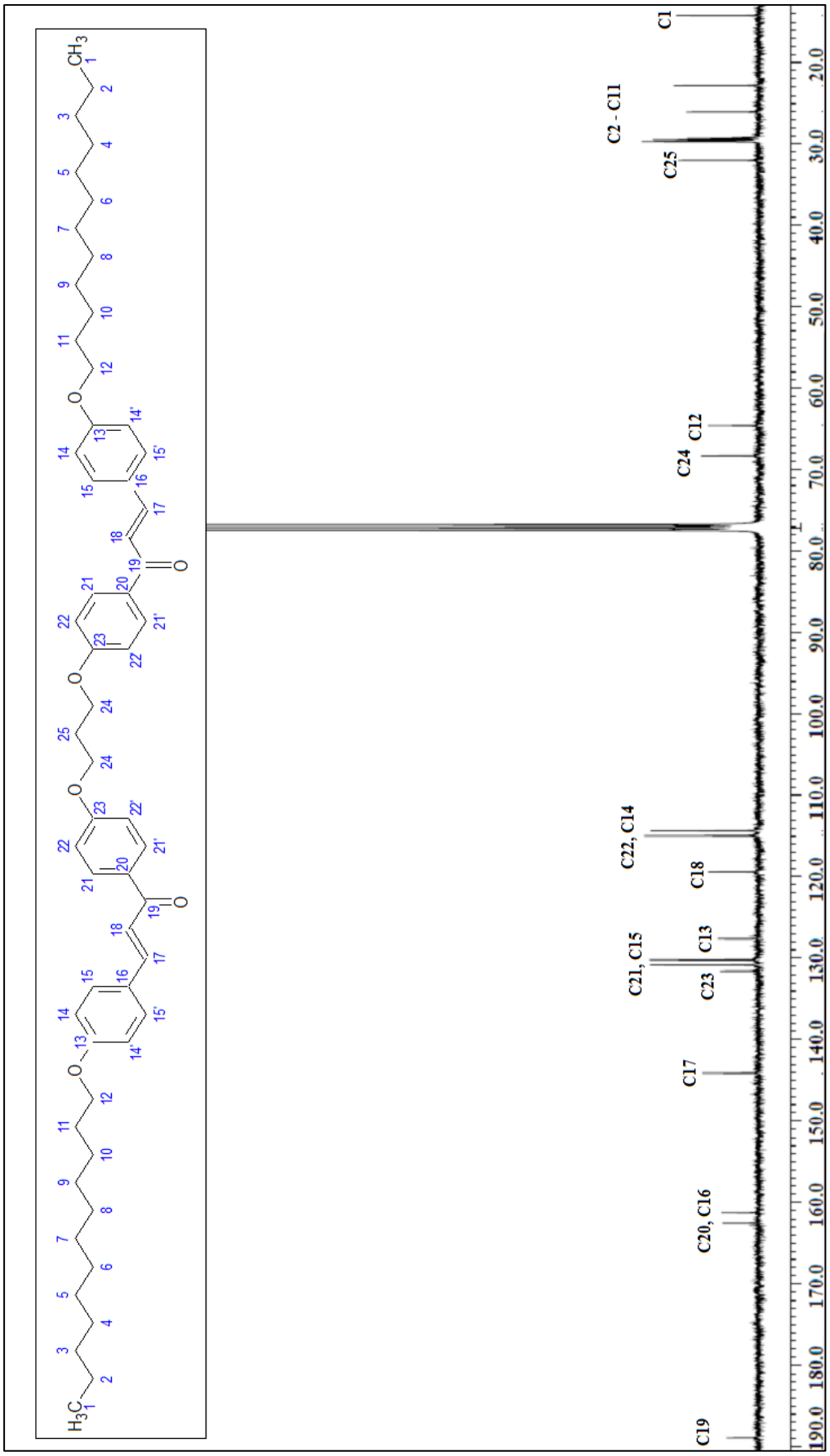

Figure 4.11: ^{13}C NMR of **DC3C**

The peaks observed in ^{13}C NMR spectrum of **DC3C** are the same as **DHP** which is explained in section 4.3.4.1**.** The only difference in these two spectrums is the presence of a new peak which represent the new ether bond form in **DC3C**. This is in agreement with the structure of **DC3C** as the formation of this compound is through the etherification of **DHP**. This new ether peak is observed δ = 68.28 ppm and ether peak of **DHP** is observed at δ = 64.55 ppm.

4.4 Thermal Properties of α,ω-bis(3-(4-dodecyloxyphenyl)-1-(phenyl-4-oxy)prop-2-en-1-one)alkane (DCnC) and 3-(4-dodecyloxyphenyl)-1-(4-hydroxyphenyl)prop-2-en-1-one (DHP)

4.4.1 DSC

All compounds in **DCnC** series and **DHP** were analysed by DSC to study their thermal properties. It is used to determine whether homologous series **DCnC** have liquid crystalline phase. DSC data upon heating and cooling cycles were tabulated in Tables 4.8 and 4.9 respectively. DSC thermogram of **DC3C** is shown in Figure 4.14 as a representative **DCnC** homologous series.

Table 4.8: Transition temperature and enthalpy changes of **DCnC** and **DHP** during heating cycle

Compounds	Transition	Temperature (℃)	Enthalpy change (kJ mol^{-1})
DC3C	Cr - I	79.08	84.79
DC4C	Cr – I	90.34	93.96
DC5C	Cr – I	83.66	87.92
DC6C	Cr – I	95.13	218.05
DHP	Cr – I	109.99	46.15

Table 4.9: Transition temperature and enthalpy changes of **DCnC** and **DHP** during heating cycle

Compounds	Transition	Temperature (℃)	Enthalpy change (kJ mol^{-1})
DC3C	I – Cr	60.44	-82.85
DC4C	I – Cr	79.02	-92.00
DC5C	I – Cr	64.25	-86.37
DC6C	I – Cr	60.39	-161.76
DHP	I – Cr	69.77	-31.83

From Tables 4.8 and 4.9, homologous series **DCnC** do not exhibit liquid crystal mesophase whether in heating or cooling cycle. All of these compounds undergo direct isotropization process and directly formed a clear isotropic liquid instead of going through liquid crystalline phases. From Table 4.8, it shows all **DCnC** series directly melted into isotropic liquid during heating cycle without any transition within the crystal region. **DC6C** has the highest melting point which is 95.13 ℃ while **DC3C** has the lowest melting point which is 79.08 ℃. During cooling cycle, all **DCnC** series crystallized directly from liquid state with **DC6C** with lowest freezing point of 60.39 ℃ and **DC4C** with the highest freezing point of 79.02 ℃.

It is observed from heating cycle, there is no obvious trend from as the number of carbon in spacer increases. However, odd – even effect of spacer is observed through graph plotted in Figure 4.12. From Figure 4.12 that **DC5C** and **DC3C** have the lower melting temperature compared to **DC4C** and **DC6C**. This shows the odd-even effect of spacer length on transition temperature. Even carbon spacer shows higher melting point due to its all-*trans* conformation whereby it proves that the molecules are likely to be linear thus it has a better packing while odd carbon spacers are prone to adapt bent shape structure (Figure 4.13). Similar observation is reported by Liao, et. al (2008) which study the effect of odd-even spacer on mesogenic compounds. Besides that, **DC6C** has a higher melting point than **DC4C**. This might be due to the increase of van der Waal forces among the alkyl chain as it is longer thus more energy is required to break this bond which leads to higher melting point.

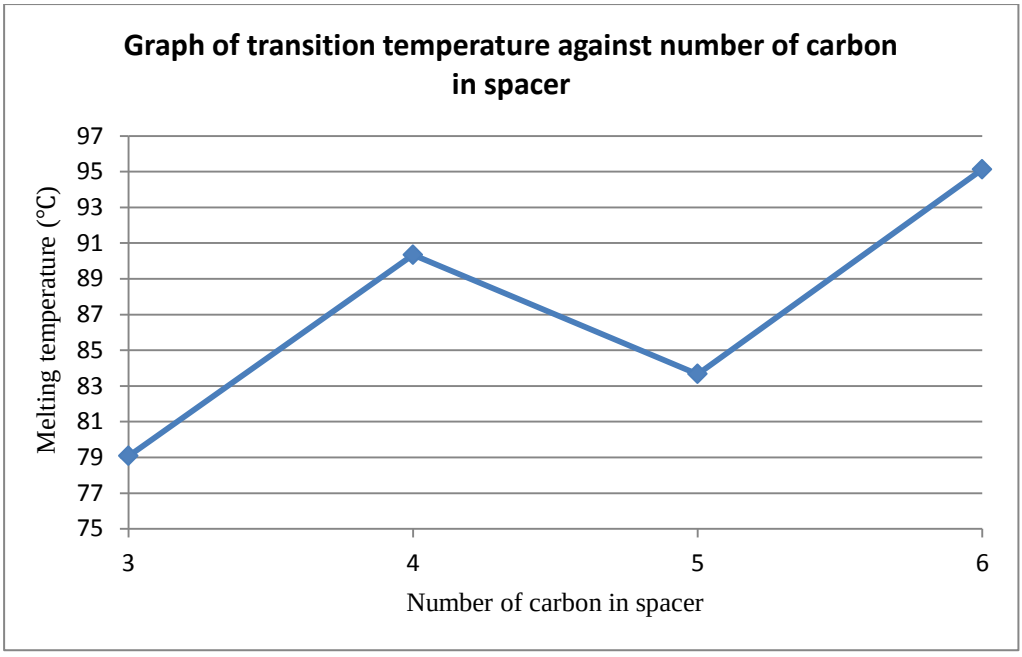

Figure 4.12: Melting temperature of **DCnC** with different number of carbon in spacer

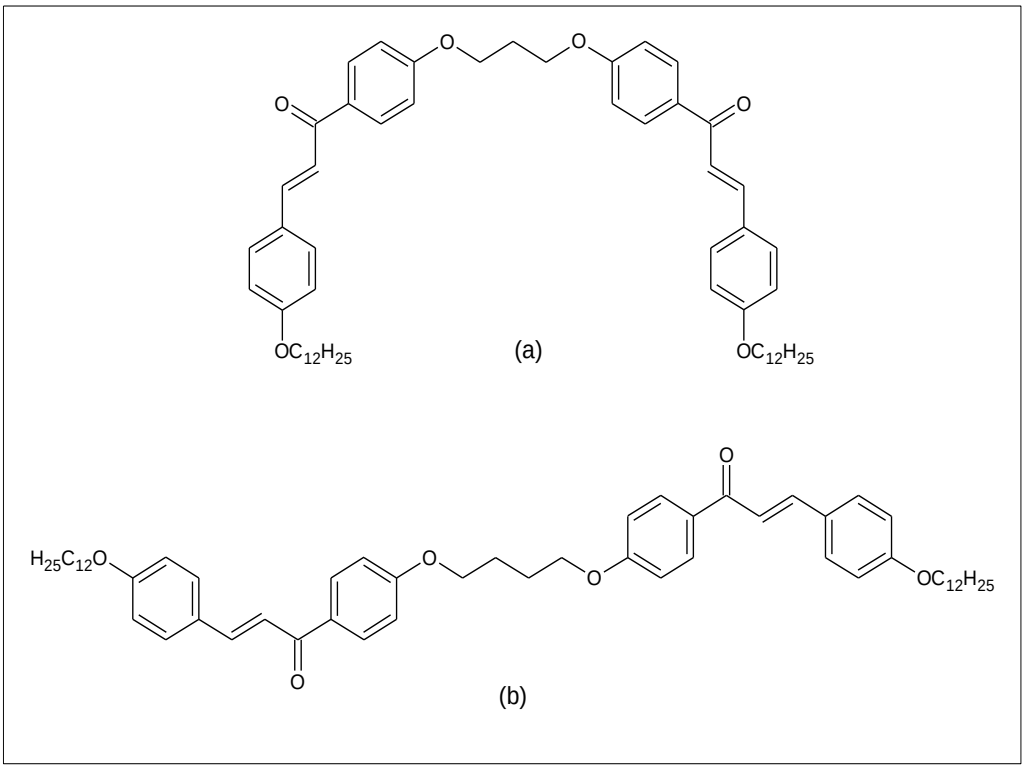

Figure 4.13: Proposed linear structure of even carbon spacer (a) and bent structure of odd carbon spacer (b) of **DCnC**

In a nutshell, the homologous series **DCnC** synthesized having enone (-CH=CH-CO-) group as a central linkage do not exhibit liquid crystal phase. This might be due to the enone group which having odd number atoms thus less conducive to mesomorphism compared to even number linkages. It is unfavourable to mesomorphism due to non-linearity which is against the main principle of liquid crystalline phase that needs to have a linear molecular axis. Besides that, the angular shape of keto group causes angle strain in the linking group which makes all chalcone derivatives less prone in exhibiting liquid crystalline phase (Thaker and Kanojiya, 2011).

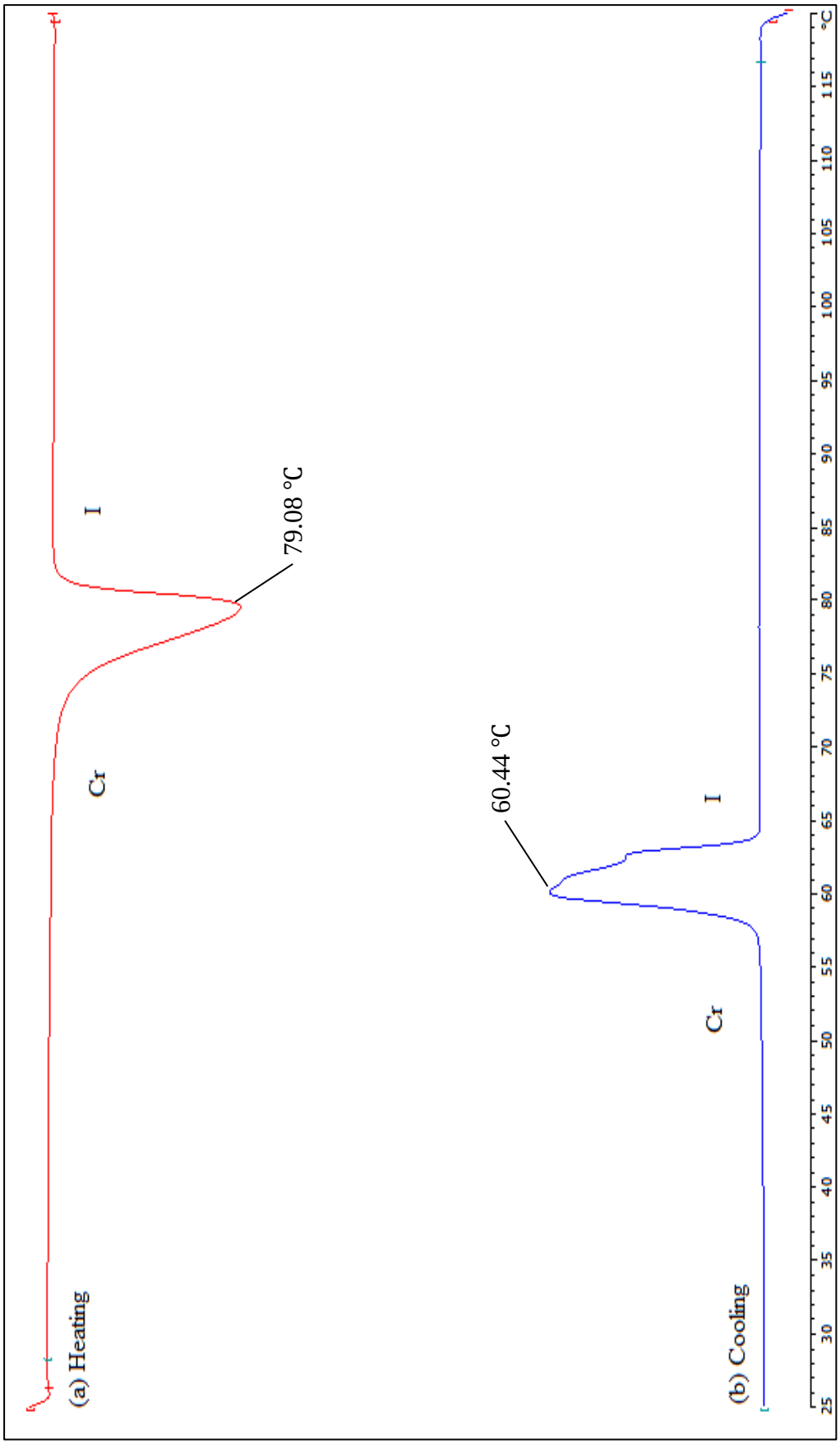

Figure 4.14: DSC thermogram of **DC3C**

4.5 Optical Properties of α,ω-bis(3-(4-dodecyloxyphenyl)-1-(phenyl-4-oxy)prop-2-en-1-one)alkane (DCnC)

4.5.1 UV – Vis Spectral Analysis

Homologous series **DCnC** were prepared in chloroform solution and analysed by UV – Vis spectrophotometry. The λ-max of the absorption peaks together with their absorptivity (ε) were tabulated in Table 4.10 The absorption bands of the compounds were studied and illustrated in Figure 4.16.

Table 4.10: UV – Vis absorption data of **DCnC**

Compounds	λ-max (nm)	Molar Absorptivity, ε (M^{-1} cm^{-1})	Literature λ-max (nm) (Shin et al., 2001)
DC3C	343.68	55,190	
DC4C	341.98	48,753	340.00
DC5C	342.60	46,545	
DC6C	342.78	44,976	

According to Figure 4.16, only one band of absorption was observed for each compound. This band of absorption could be attributed to the π-π* transition in aromatic ring, C=O group and C=C group. The π-π* transition involves the transition of π-electron from highest filled molecular orbitals (HOMO) to the lowest unoccupied molecular orbital (LUMO). However, Table 4.10 shows that **DCnC** series have very high molar absorptivity and these values suggest that intramolecular charge transfer could have taken place in the solution (Ha and Low, 2013).

Charge transfer process takes place within the molecules through the delocalization of π-electrons between donor and acceptor atoms (Ha and Low, 2013). Figure 4.15 shows the charge transfer interaction in chalcone structure and it is observed that oxygen atom from ether group act as electron donor while carbonyl group acts as electron acceptor. The lone pair on ether oxygen can donate electron to the phenyl group through resonance effect. Since carbonyl group which is an acceptor present between two phenyl groups, an extensive donor-acceptor interaction is generated. The double bond characters between two phenyl decrease while single bond order increases due to extensive donor acceptor interaction (Shin, et al., 2001).

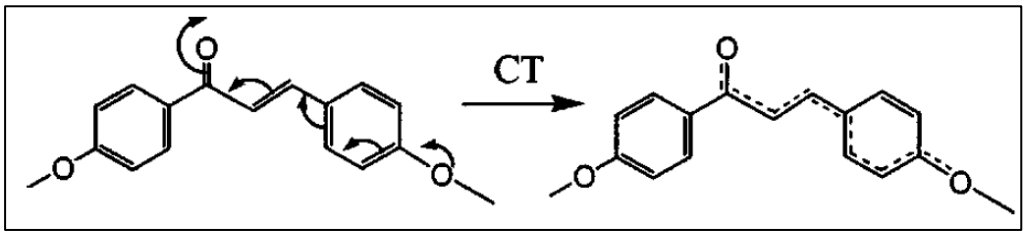

Figure 4.15: Charge transfer interaction in chalcone structure (Shin, et al., 2001).

Through comparison with literature compound, 3-(4-bromopropoxyphenyl)-1-(4-alkoxyphenyl)prop-2-en-1-one, similar results are obtained whereby as the alkyl chain increases, the intensity of peaks decreases. From Figure 4.16, the intensity of peak decreases as the spacer length increases. **DC3C** shows highest intensity and vice versa for **DC6C**. This observation proves that the steric effect of the spacer is affecting the electronic structure of **DCnC** (Shin, et al., 2001).

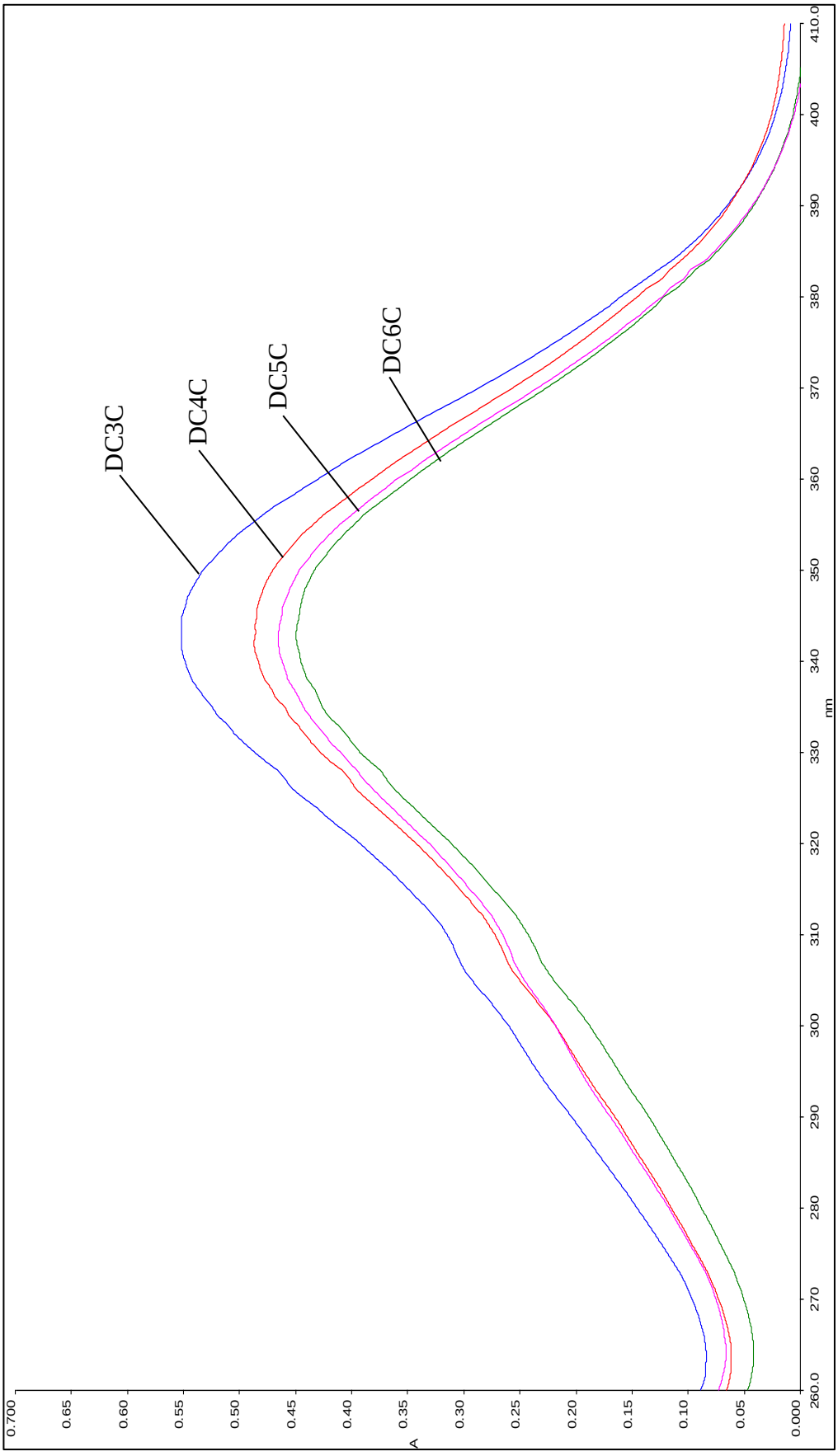

Figure 4.16: UV – Vis spectra of **DCnC**

CHAPTER 5

CONCLUSION

5.1 Conclusion

A series of dimers containing chalcone moiety, α,ω-bis(3-(4-dodecyloxyphenyl)-1-(phenyl-4-oxy)prop-2-en-1-one)alkane (**DCnC)** where n = 3, 4, 5 and 6 have been successfully synthesized and characterized. The structures of these compounds were confirmed using FTIR, ^{1}H NMR and ^{13}C NMR spectroscopic techniques. The thermal properties of these compounds were characterized by using DSC and their photophysical properties were being studied by using UV – Vis spectrophotometry.

From DSC thermogram of **DCnC** series, it was found that none of the compounds exhibit mesomorphic properties. The possible reason is the non-linearity causes by the enone group in chalcone moiety thus it is less conducive to mesomorphism. As the length of spacer increase, it is found to exhibit odd-even effect on melting point where by the even spacer has higher melting point than odd spacer. The possible reason is due to all *trans* position which resulted in better packing thus require higher energy to break the bond and lead to higher melting point. UV-Vis analysis showed that all the compounds undergo π-π* transition with strong intramolecular charge transfer character.

5.2 Recommendations for Future Study

Future study of chalcone derivatives could be done by introducing an additional linkage of phenyl ring to the chalcone.

1. To synthesize and characterize dimer containing chalcone moiety with biphenyl rings

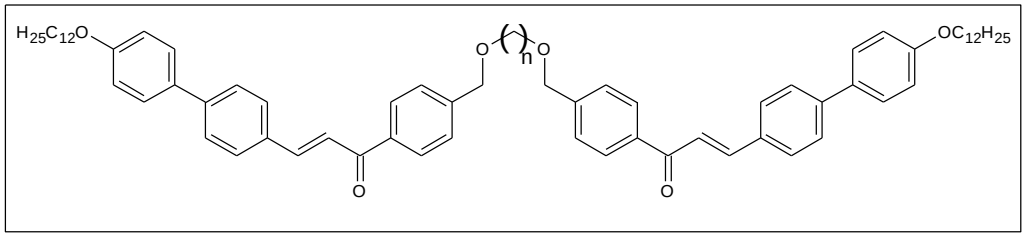

2. To synthesize and characterize dimer containing chalcone moiety with ester linkage

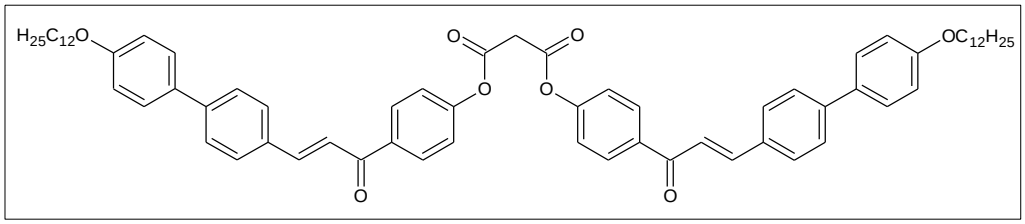

3. To synthesize and characterize dimer containing chalcone moiety with azo linkage

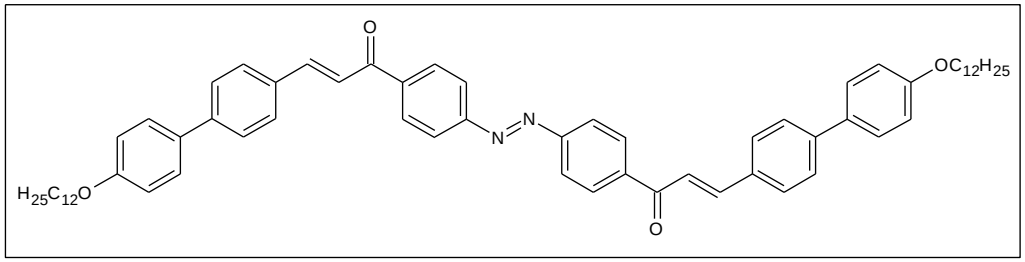

References

Adrienko, D., 2006. *Introduction to liquid crystals*. [online] Available at: <http://www2.mpip-mainz.mpg.de/~andrienk/teaching/IMPRS/liquid_crystals.pdf> [Accessed 22 May 2013].

Bhagvatiprasad, K.J., 2011. *Synthesis, characterization and mesomorphic properties of some new liquid crystalline compounds containing biphenyl moiety*. PhD. Veew Narmad South Gujarat University. Available at < http://shodhganga.inflibnet.ac.in:8080/jspui/handle/10603/3522/> [Accessed 23 December 2013].

Bong, S.H., 2011. *Synthesis and Characterisation of Schiff Base Liquid Crystals Possessing Dialkylamino Terminal Unit*. Final Year Project Thesis, BSc (Hons) Chemistry. Universiti Tunku Abdul Rahman. Available at <http://eprints.utar.edu.my/52/1/CE-0802984-2011.pdf> [Accessed 19 May 2013].

Brown, W.H., Foote, C.S., Iverson, B.L. and Anslyn, E.V., 2009. *Organic Chemistry*. 5th ed. United States of America: Brooks/Cole Cengage Learning.

Bruice, P.Y., 2009. *Organic Chemistry*. 4th ed. United States of America: Brooks/Cole Cengage Learning.

Collings, P.J., 2002. *Liquid Crystals: Nature's Delicate Phase of Matter.* 2nd ed. Oxfordshire: Princeton University Press.

Cook, A.G., Wardell, J.L., Brooks, N.J., Seddon, J.M., Felipe, A.M. and Imrie, C.T., 2012. Non-symmetric liquid crystal dimer containing a carbohydrate-based moiety, *Carbohydrate Research*, [e-journal] 360, pp. 78-83. Available through Universiti of Malaya Library website http://www.umlib.um.edu.my/. [Accessed 3 October 2013]

Devi, K. and Bharracharjee, A., 2010. A Review of Liquid Crystal Dimers, *Assam University Journal of Science & Technology: Physical Sciences and Technology*, [e-journal] 5(2), pp. 225-228. Available through Universiti of Malaya Library website http://www.umlib.um.edu.my/. [Accessed 7 October 2013]

Dierking, I., 2003. *Texture of Liquid Crystals.* Darmstadt: Wiley-VCH.

Donaldson, T., Staesche, H., Lu, Z.B., Henderson, P.A., Achard, M.F. and Imrie, C.T., 2010. Symmetric and non-symmetric chiral liquid crystal dimers, *Liquid Crystals*, [e-journal] 37(8), pp 1097-1110. Available through Universiti of Malaya Library website http://www.umlib.um.edu.my/. [Accessed 24 December 2012]

Fairchild, M.D., 2013. *Explore Mysteries of Color.* [online] Available at: <http://www.cis.rit.edu/fairchild/WhyIsColor/Questions/2-5.html> [Accessed 3 April 2014].

Fisch, M.R., 2006. *Liquid Crystals, Laptops and Life.* London: World Scientific Publishing Co. Pte. Ltd.

Gan, Y.S., 2011. *Synthesis and Characterisation of Smectic and Nematic Phases in 4-(Dimethylamino)benzylidene-4'-alkanoloxyanilines*. Final Year Project Thesis, BSc (Hons) Chemistry. Universiti Tunku Abdul Rahman. Available at <http://eprints.utar.edu.my/50/1/CE-0805471-2011.pdf> [Accessed 24 May 2013].

Guo, Y., Li, B., Yang, Y. and Wen, J., 2008. Synthesis and Mesomorphic Properties of Some Chiral Fluorinated Benzoates, *Molecular Crystal Liquid Crystal*, [e-journal] 493, pp. 57-64. Available through Universiti of Malaya Library website http://www.umlib.um.edu.my/. [Accessed 3 March 2014]

Ha, S.T. and Low, Y.W., 2013. Synthesis and Phase Transition Behaviours of New Chalcone Derivatives, *Journal of Chemistry*, pp. 1-6.

Henderson, P.A., Niemeyer, O. and Imrie, C.T., 2001. Methylene-linked liquid crystal dimer, *Liquid Crystals*, [e-journal] 28(3), pp. 463-472. Available through Universiti of Malaya Library website http://www.umlib.um.edu.my/. [Accessed 3 March 2014]

Hird, M., 2007. Fluorinated liquid crystals - properties and applications, *Chemical Society Review*, [e-journal] 36, pp. 2070-2095. Available through Universiti of Malaya Library website http://www.umlib.um.edu.my/. [Accessed 3 March 2014]

Islam, H.M.T., Shabnam, R., Howlader, B.H., Latif, M.A., Chaki, B.M. and Miah, M.A., 2012. Synthesis of Nickel (II) Complexes Using Malonodihydrazone Ligands Having Long Chain Pendent Arms, *International Journal of Chemistry*, [e-journal] 4(5), pp. 16-27. Available through Universiti of Malaya Library website http://www.umlib.um.edu.my/. [Accessed 28 December 2012]

Khoo, I.C., 2007. *Liquid Crystals.* 2nd ed. New Jersey: John Wiley & Sons.

Khor, K.X., 2011. *Synthesis and characterization of mesogenic schiff base ether*. Final Year Project Thesis, BSc (Hons) Chemistry. Universiti Tunku Abdul Rahman. Available at < http://eprints.utar.edu.my/51/1/CE-0707423-2011.pdf> [Accessed 24 may 2013].

Kropff, M.J., 2006. *Banana-shaped Liquid Crystal*. [online] Available at: < http://edepot.wur.nl/23608> [Accessed 22 March 2014].

Kumar, D., Suresh and Sandhu, J.S., 2010. An effecient green protocol for the synthesis of chalcones by a Claisen-Schmidt reaction using bismuth(III)chloride as a catalyst under solvent-free condition, *Green Chemistry Letters and Reviews,* [e-journal] 3(4), pp. 283-286. Available through Universiti of Malaya Library website http://www.umlib.um.edu.my/. [Accessed 3 May 2013]

Kundu, B., 2008. *Experimental investigations on physical properties of some novel liquid crystals with banana-shaped and rod-like molecule.* PhD. Jawaharlal Nehru University. Available at< http://dspace.rri.res.in/handle/2289/3863> [Accessed 14 November 2013].

Li, L., 2009. *Synthesis and Characterization of Siloxane-Terminated Liquid Crystals and Photochromic Fulgide Dopants for Liquid Crystal Photonics Applications.* PhD. University of Queensland. Available at< https://qspace.library.queensu.ca/bitstream/1974/1891/1/Li_Li_200905_PhD.pdf> [Accessed 17 May 2013].

Liao, C.C., Wang, C.S., Sheu, H.S. and Lai, C.K., 2008. Symmetrical dimer liquid crystals derived from benzoxazoles, *Tetrahedron*, [e-journal] 64, pp 7977-7985.Available through Universiti of Malaya Library website http://www.umlib.um.edu.my/. [Accessed 29 December 2011]

Low. Y. W. 2012. *Synthesis and characterization of chalcone derivatives.* Final Year Project Thesis, BSc (Hons) Chemistry. Universiti Tunku Abdul Rahman.

McMurry, J., 2012. *Organic Chemistry.* 8th ed. Auckland: Brooks/Cole.

Morris, S.M., 2006. *Liquid crystals for linear & non-linear photonics applications*. [online] Available at: <http://www-g.eng.cam.ac.uk/CMMPE/lcintro.html> [Accessed 3 January 2014].

Ngaini, Z., Chee, C.M. and Chin, L.L., 2013. A New Type of Banana Shape Bifunctional Monomer of Ester Chalcone, *Malaysian Journal of Fundamental and Applied Sciences*, [e-journal] 10(2), pp. 53-58. Available through Universiti of Malaya Library website http://www.umlib.um.edu.my/. [Accessed 3 October 2013]

Ngaini, Z., Fadzillah, S.M.H. and Hussain, H., 2012. Synthesis and antimicrobial studies of hydroxylated chalcone derivatives with variable chain length, *Natural Product Research*, [e-journal] 26(10), pp. 892-902. Available through Universiti of Malaya Library website http://www.umlib.um.edu.my/. [Accessed 7 February 2013]

Patil, C.B., Mahajan, S.K. and Katti, S.A., 2009. Chalcone: A Versatile Molecule, *Journal of Pharmaceutical Sciences and Research*, [e-journal] 1(3), pp 11-22. Available through Universiti of Malaya Library website http://www.umlib.um.edu.my/. [Accessed 10 March 2013]

Pavia, D.L., Lampman, G.M., Kriz, G.S. and Vyvyan, J.R., 2009. *Introduction to Spectroscopy*. 4th ed. Belmont: Brooks/Cole.

Prachar, H., Chawla, A., Sharma, A.K. and Kharb, R., 2012. Chalcone as a versatile moiety for diverse pharmacological activities, *International Journal of Pharmaceutical Sciences and Research*, [e-journal] 3(7), pp. 1913-1927. Available through Universiti of Malaya Library website http://www.umlib.um.edu.my/. [Accessed 10 March 2013]

Ramkumar, V., Anadhi, S., Kannan, P. and Gopalakrishnan, R., 2013. Synthesis, single crystal growth, characterization and comparison of two new enone shifted chalcones and their NLO behaviour, *CrystEngComm*, [e-journal] 15, pp. 2438-2449. Available through Universiti of Malaya Library website http://www.umlib.um.edu.my/. [Accessed 10 March 2013]

Rateb, N.M. and Zohdi, H.F., 2009. Atom-Efficient, Solvent-Free, Green Synthesis of Chalcone by Grinding, *Synthetic Communications*, [e-journal] 9, pp. 2789-2794. Available through Universiti of Malaya Library website http://www.umlib.um.edu.my/. [Accessed 10 March 2013]

Senthil, S., Kamalraj, V.R. and Wu, S.L., 2008. Synthesis and characterization of ferroelectric liquid crystal dimers containing thioester and carboxylate linking group in the inner side of the molecule, *Journal of Molecular Structure*, [e-journal] 886, pp. 175-182. Available through Universiti of Malaya Library website http://www.umlib.um.edu.my/. [Accessed 3 December 2013]

Shakshashiri, 2005. *Liquid Crystals*. [online] Available at: <http://scifun.chem.wisc.edu/chemweek/pdf/liquid_crystals.pdf> [Accessed 20 May 2013].

Shin, D.M., Song, D.M., Jung, K.H. and Moon, H., 2001. Photochemical Transformation of Chalcone Derivatives, *Journal of Photoscience*, [e-journal] 8(1), pp. 9-12. Available through Universiti of Malaya Library website http://www.umlib.um.edu.my/. [Accessed 24 March 2014]

Singh, S., 2002. *Liquid Crystals Fundamentals.* Danvers: World Scientific Publishing Co. Pte. Ltd.

Song, D.M., Jung, K.H. and Shin, D.M., 2002. Photochemical Behavior of Chalcone and the Phto-Alignment of Liquid Crystals with Chalcone Derivatives, *Molecular Crystal Liquid Crystal*, [e-journal] 337, pp. 117-120. Available through Universiti of Malaya Library website http://www.umlib.um.edu.my/. [Accessed 24 March 2014]

Sreedhar, N.Y., Jayapal, M.R., Prasad, K.S. and Prasad, P.R., 2010. Synthesis and Characterization of 4-Hydroxy Chalconed Using PEG-400 as a Recyclable Solvent, *Research Journal of Pharmaceutical, Biological and Chemical Sciences*, [e-journal] 1(4), pp. 480-485. Available through Universiti of Malaya Library website http://www.umlib.um.edu.my/. [Accessed 24 March 2014]

Thaker, B.T. and Kanojiya, J.B., 2011. Synthesis, Characterization and Mesophase Behavior of New Liquid Crystalline Compounds Having Chalcone as a Central Linkage, *Molecular Crystal Liquid Crystal*, [e-journal] 542, pp. 85-98. Available through Universiti of Malaya Library website http://www.umlib.um.edu.my/. [Accessed 6 May 2013]

Thaker, B.T., Patel, P.H., Vansadiya, A.D. and Kanojiya, J.B., 2009. Substitution effects on the liquid crystalline properties of thermotropic liquid crystals containing Schiff base chalcone linkages, *Molecular Crystal Liquid Crystal*, [e-journal] 515, pp. 135-147. Available through Universiti of Malaya Library website http://www.umlib.um.edu.my/. [Accessed 6 May 2013]

Walcott, K., 2013. *Types of liquid crystals.* [online] Available at: <http://www.ehow.com/list_6707420_types-liquid-crystals.html> [Accessed 23 May 2013].

Wei, Q., Yuan, X., Zhang, L., Wang , L., Yang, H. and Wang, Y., 2008. Synthesis and Mesormorphic Properties of Two Series of Laterally Flourinated Symmetric Ester Liquid Crystals, *Molecular Crystal Liquid Crystal*, [e-journal] 487, pp. 52-60. Available through Universiti of Malaya Library website http://www.umlib.um.edu.my/. [Accessed 3 March 2014]

Yeap, G.Y., Hng, T.C., Mahmood, W.A.K. and Adnan, R., 2006. Synthesis and Mesomorphic Properties of Symmetrical Dimer N,N'-Bis(3-methoxy-4-alkoxybenzylidene)-1,4-Phenylenediamine, *Molecular Crystal Liquid Crystal*, [e-journal] 452, pp. 49-61. Available through Universiti of Malaya Library website http://www.umlib.um.edu.my/. [Accessed 3 March 2014]

Yeap, G.Y., Susanti, I., Teoh, B.S. and Mahmood, W.A.K., 2005. Synthesis and phase transition in new chalone derivatives: crystal structure of 1-phenyl-3-(4'-undecylcarbonyloxyphenyl)-2-propen-1-one, *Molecular Crystal Liquid Crystal*, [e-journal] 442, pp. 133-146. Available through Universiti of Malaya Library website http://www.umlib.um.edu.my/. [Accessed 3 March 2014]

Yelamaggad, V.C., Bonde, N.L., Achalkumar, A.S., Shankarrao, D.S., Prasad, S.K. and Prakajapati, A.K., 2007. Frustrated Liquid Crystals: Synthesis and Mesomorphic Behavior of Unsymmetrical Dimers Possessing Chiral and Fluorescent Entities, *Chemisty Mater*, [e-journal] 19, pp. 2463-2472. Available through Universiti of Malaya Library website http://www.umlib.um.edu.my/. [Accessed 23 June 2013]

Yong, Y., Ahn, S., Hwang, D., Yoon, H., Jo, G., Kim, Y.H., Kim, H.S., Koh, D. and Lim, Y., 2013. ^{1}H and ^{13}C NMR spectral assignments of 2'-hydroxychalcones, *Magnetic Resonance in Chemistry*, [e-journal] 51, pp. 364-370. Available through Universiti of Malaya Library website http://www.umlib.um.edu.my/. [Accessed 17 February 2014]

APPENDICES

Appendix A1: IR spectrum of compound DC4C

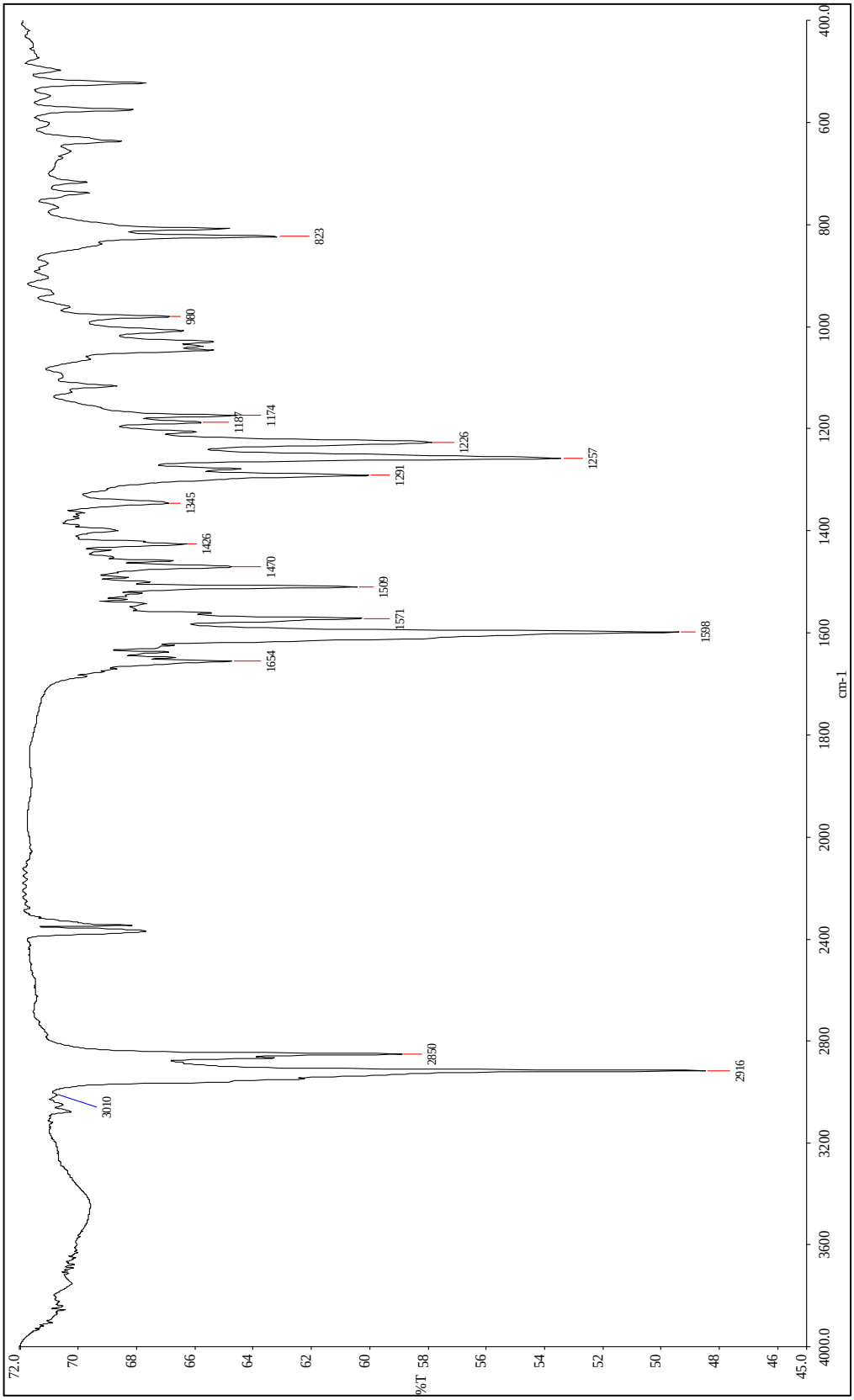

Appendix A2: IR spectrum of compound DC5C

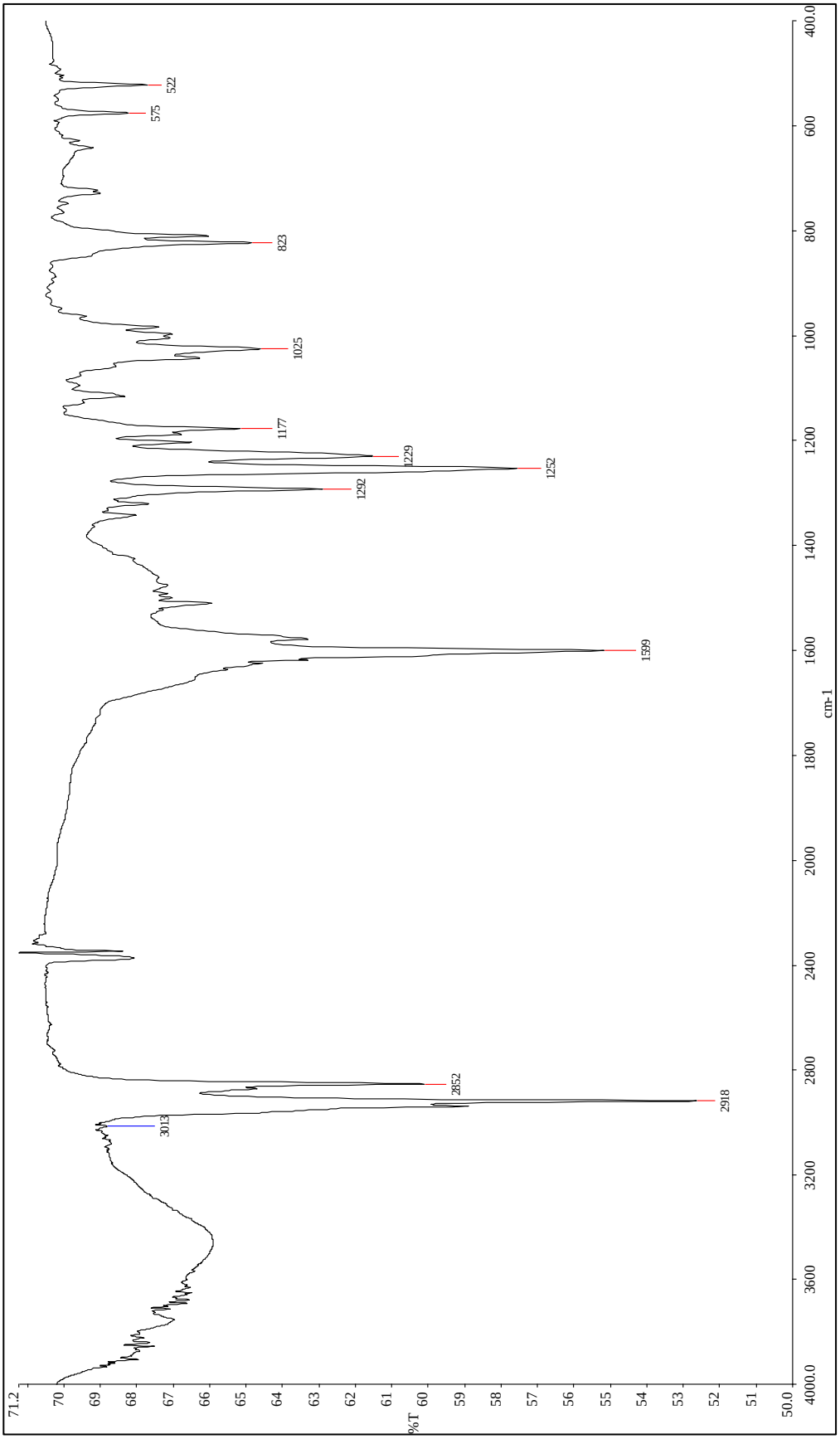

Appendix A3: IR spectrum of compound DC6C

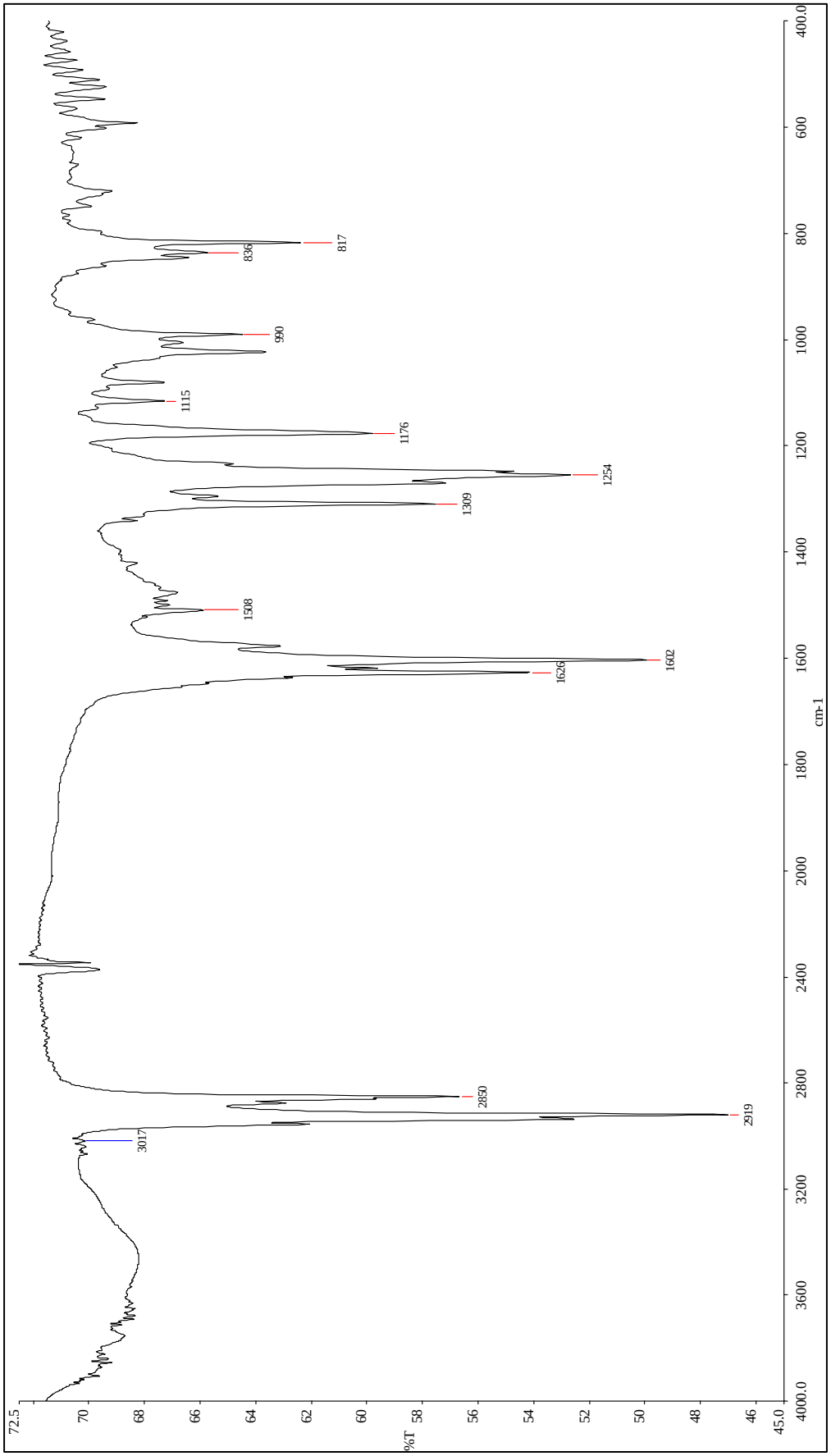

Appendix B1: ^{1}H NMR spectrum of compound DC4C

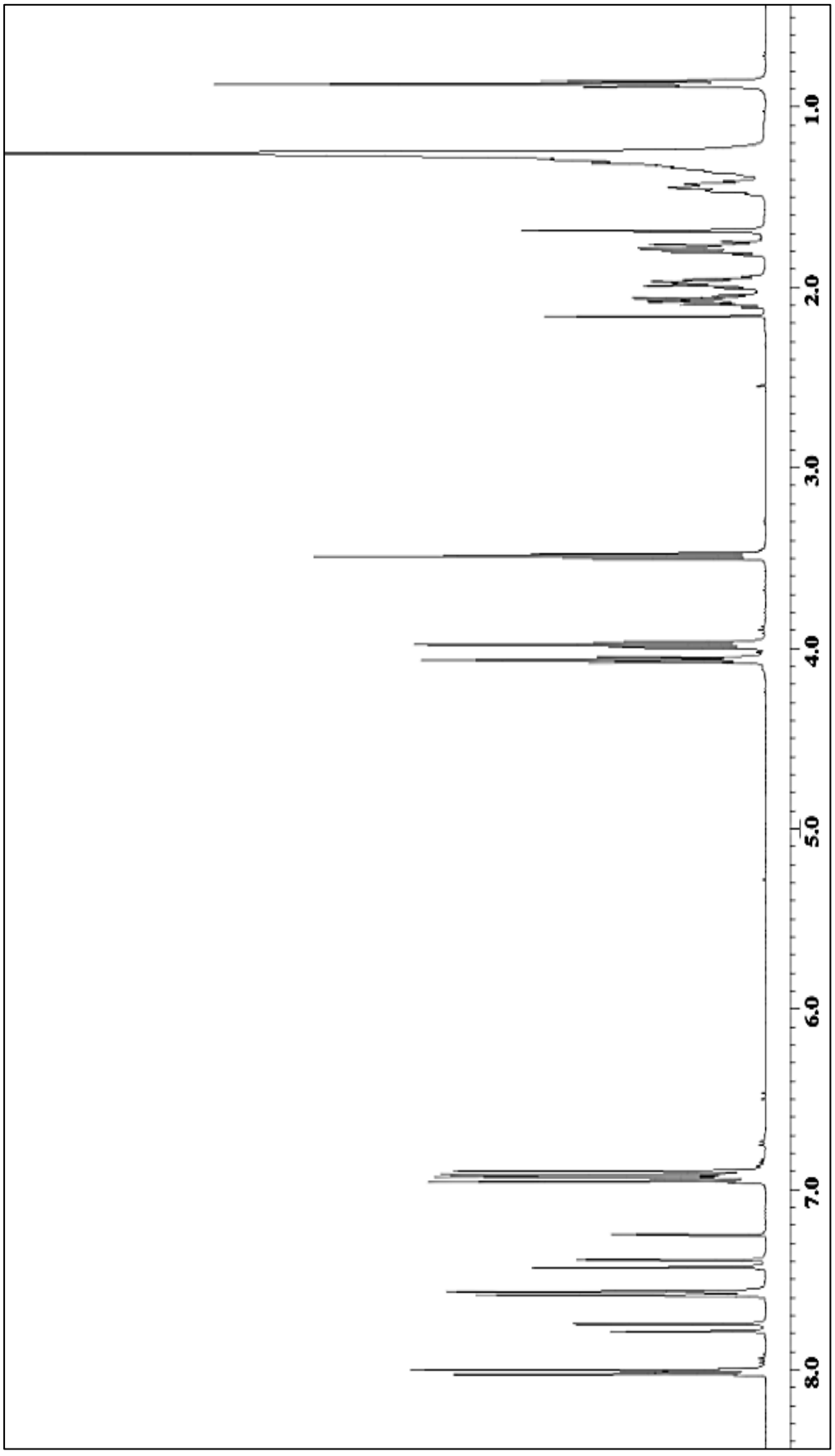

Appendix B2: ^{1}H NMR spectrum of compound DC5C

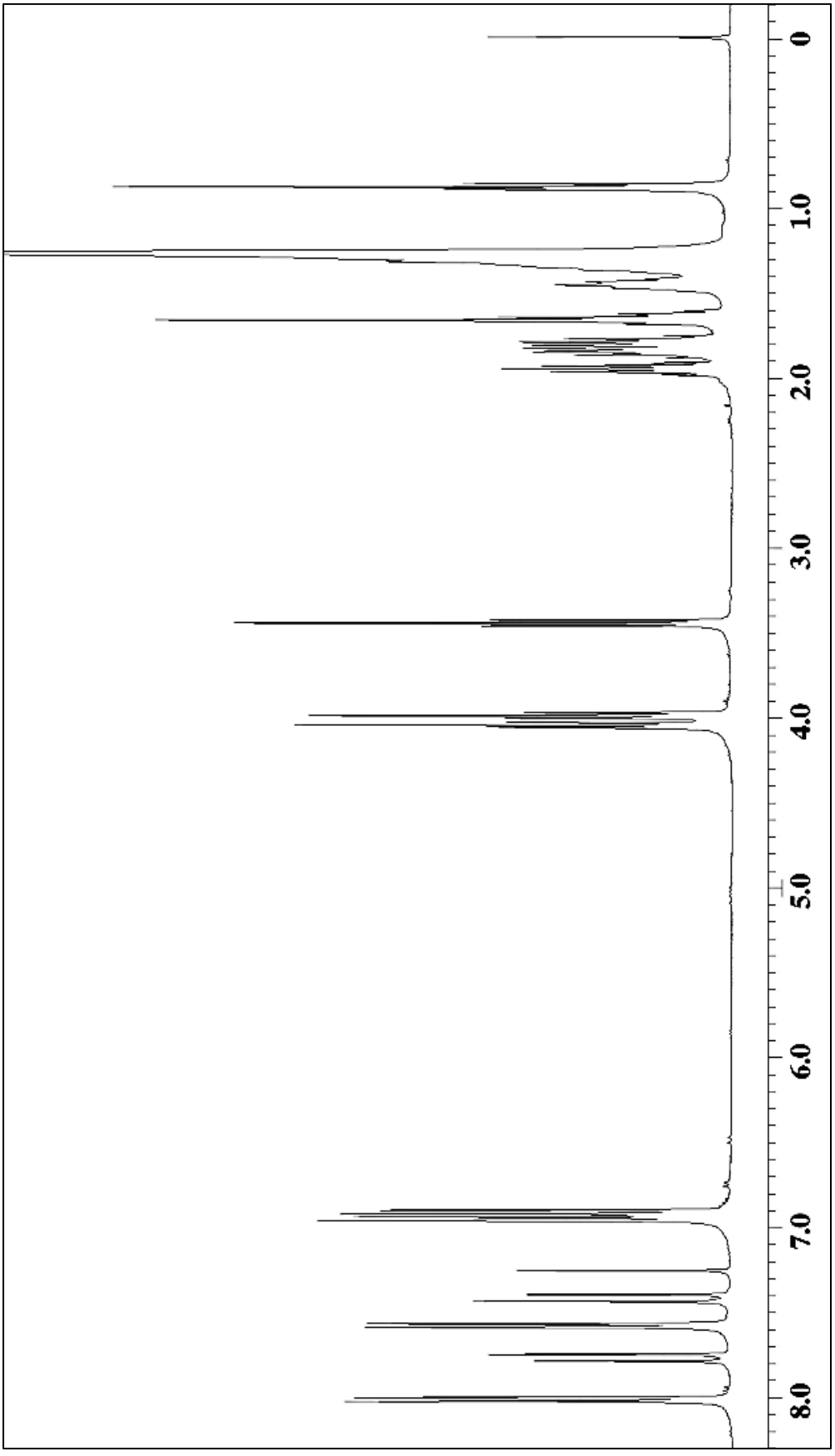

Appendix B3: ^{1}H NMR spectrum of compound DC6C

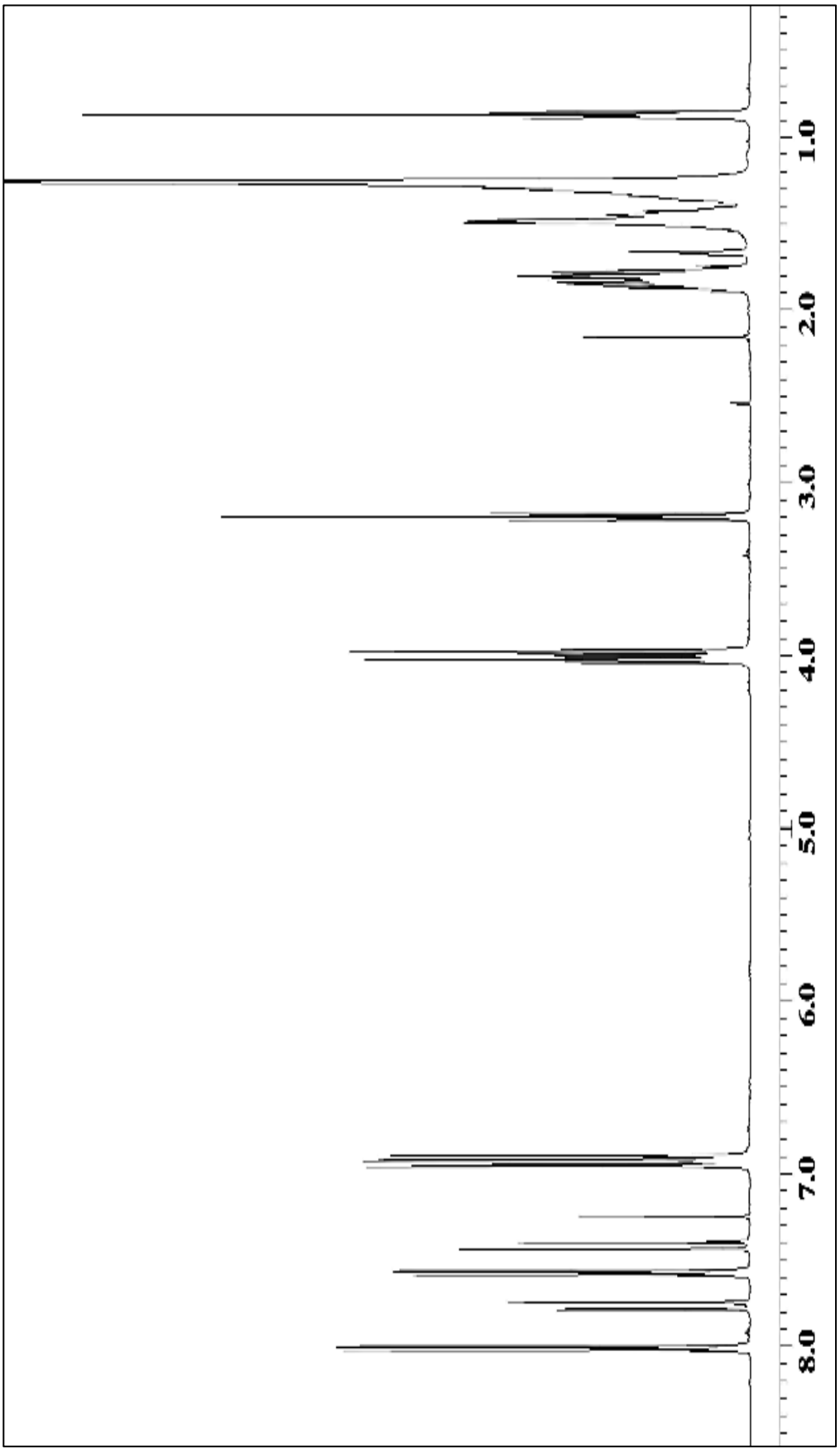

Appendix C1: ^{13}C NMR spectrum of DC4C

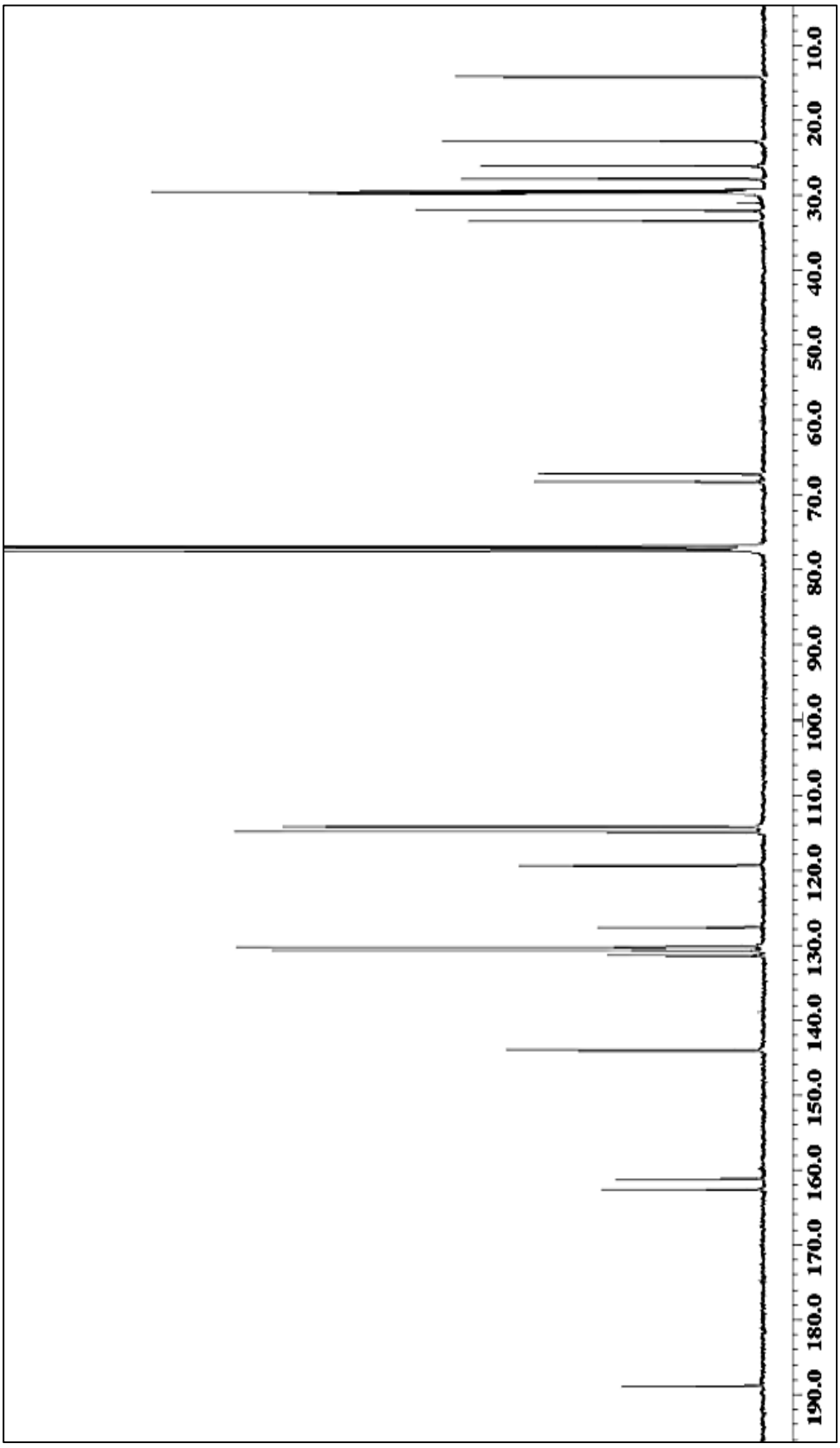

Appendix C2: ^{13}C NMR spectrum of DC5C

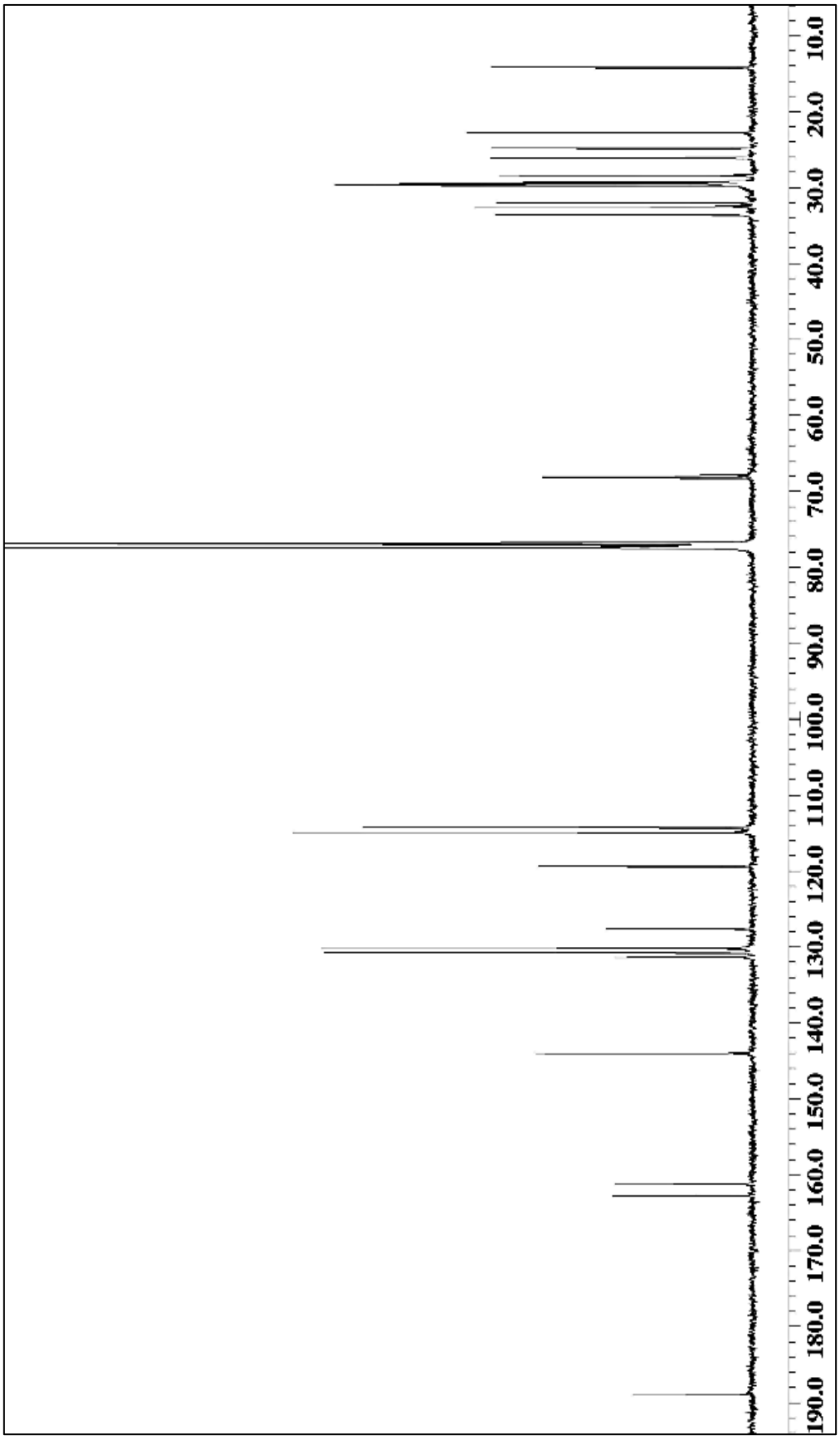

Appendix C3: ^{13}C NMR spectrum of DC6C

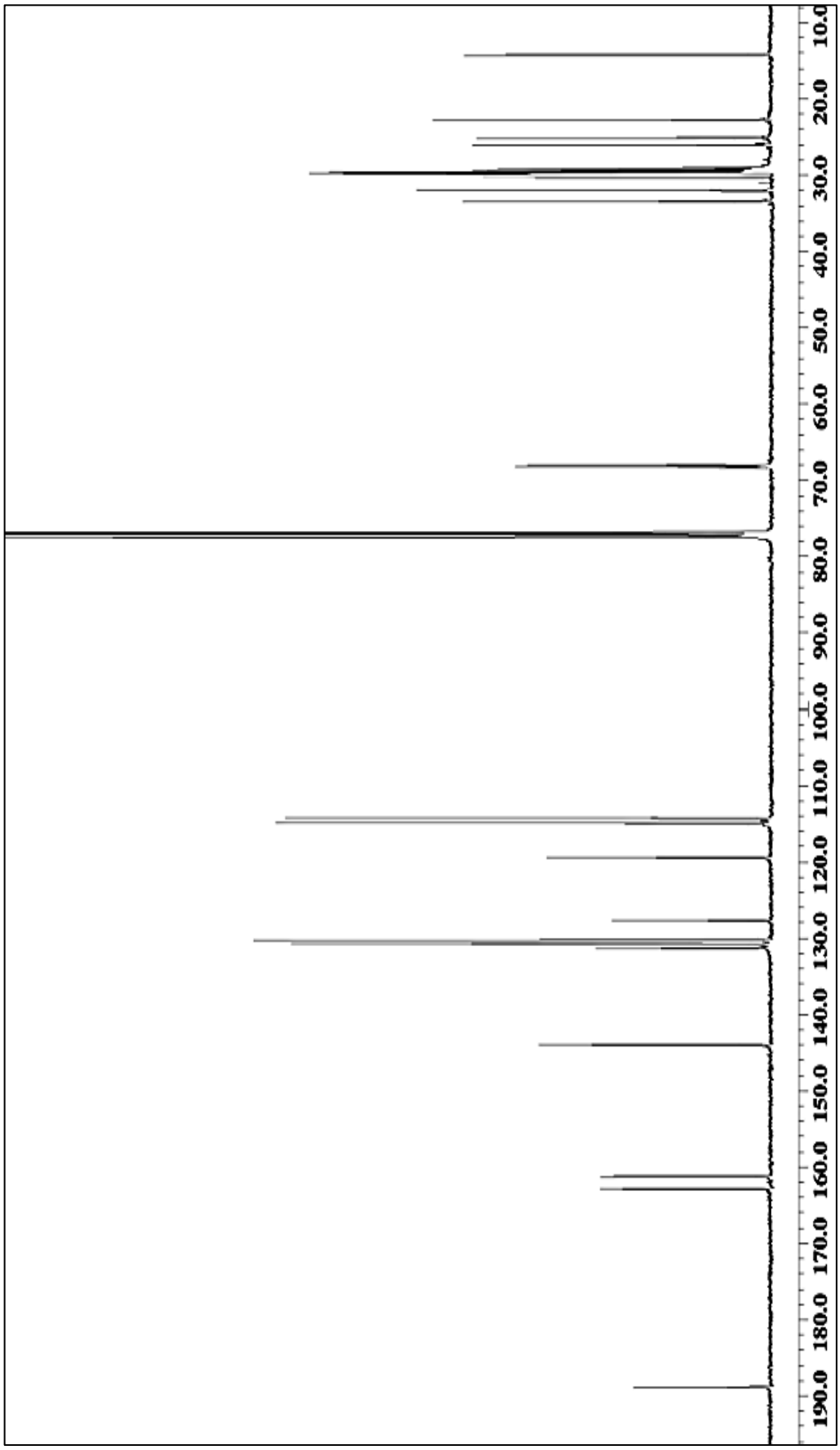

Appendix D1: DSC thermogram of compound DC4C

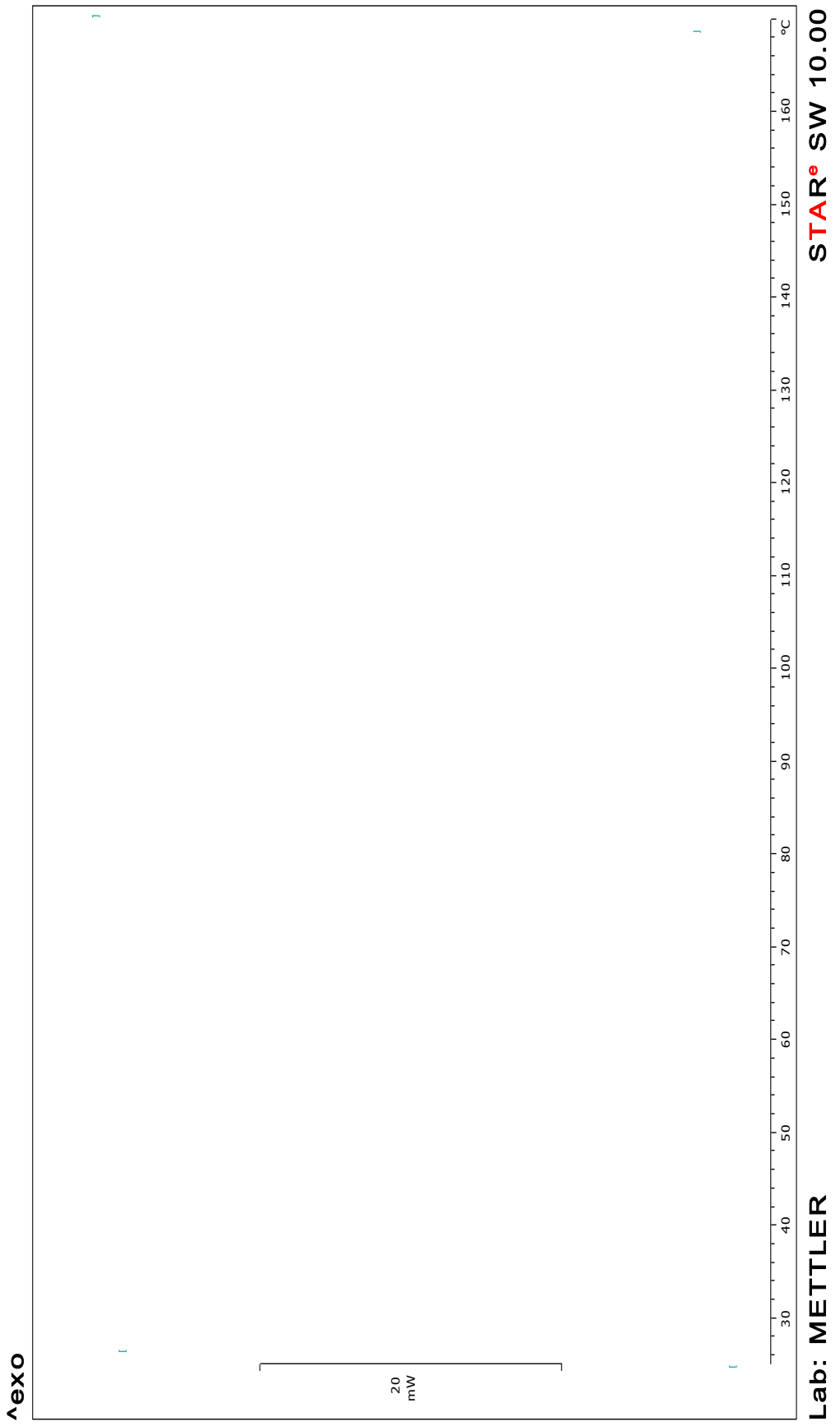

Appendix D2: DSC thermogram of compound DC5C

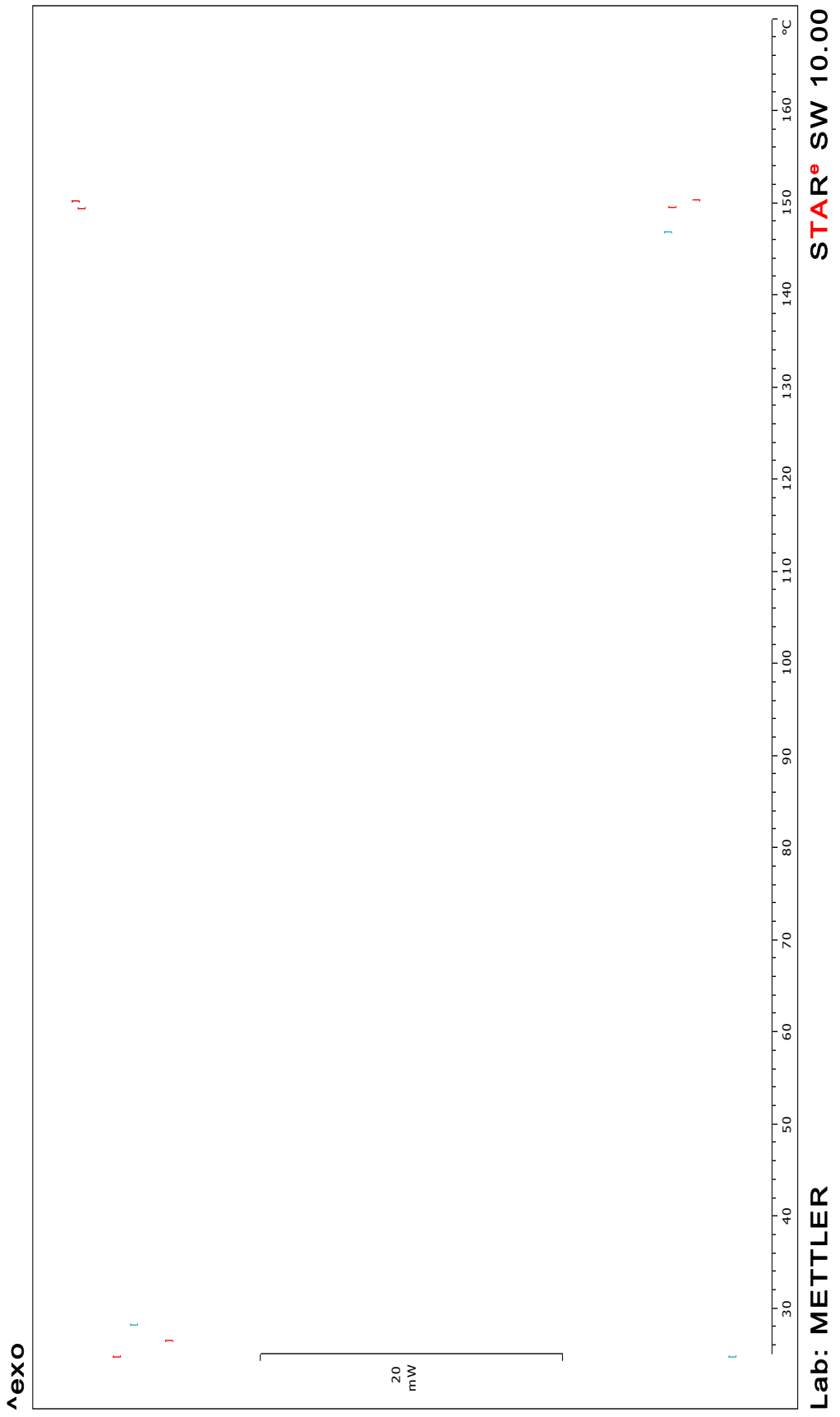

Appendix D3: DSC thermogram of compound DC6C

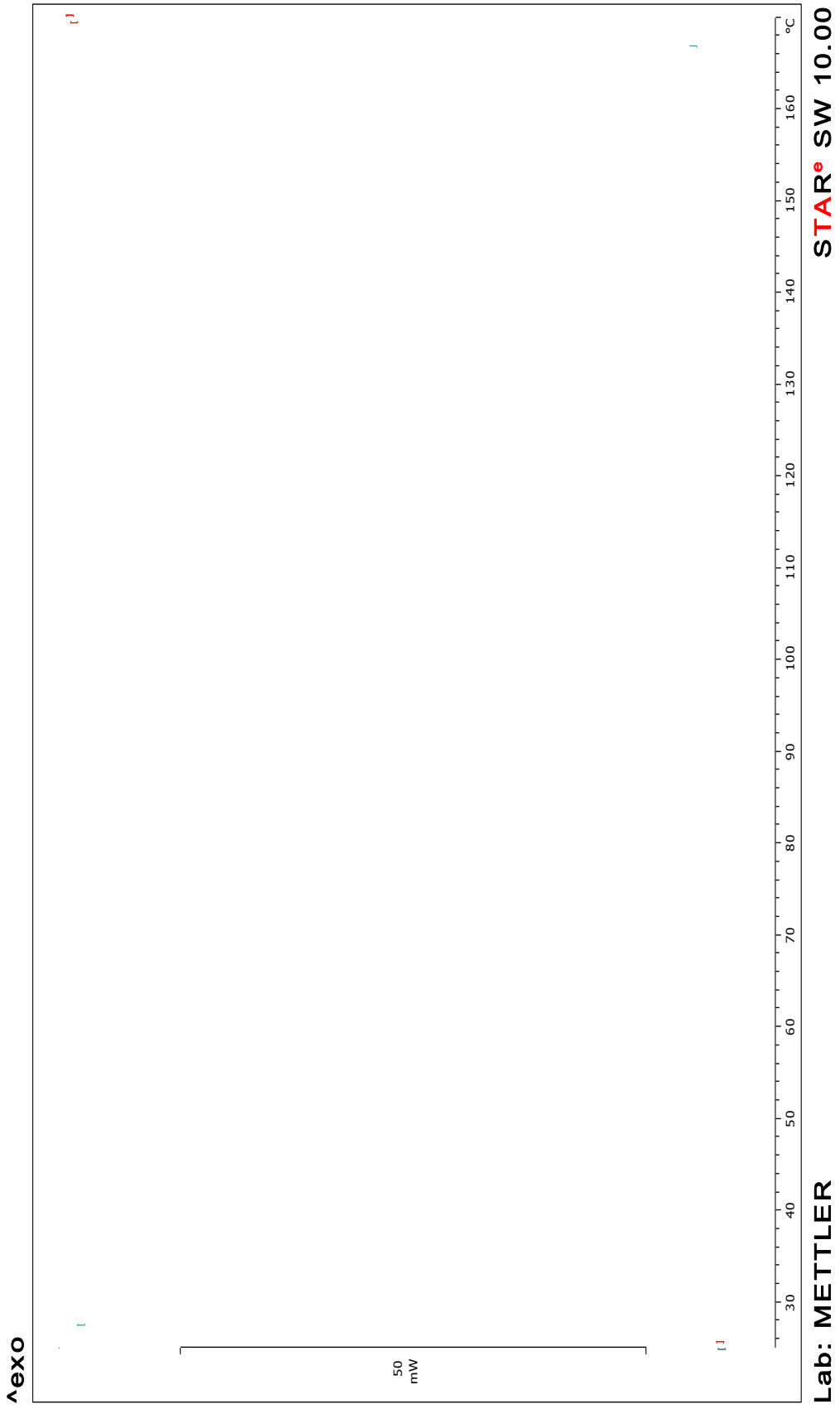

Appendix D4: DSC thermogram of compound DHP

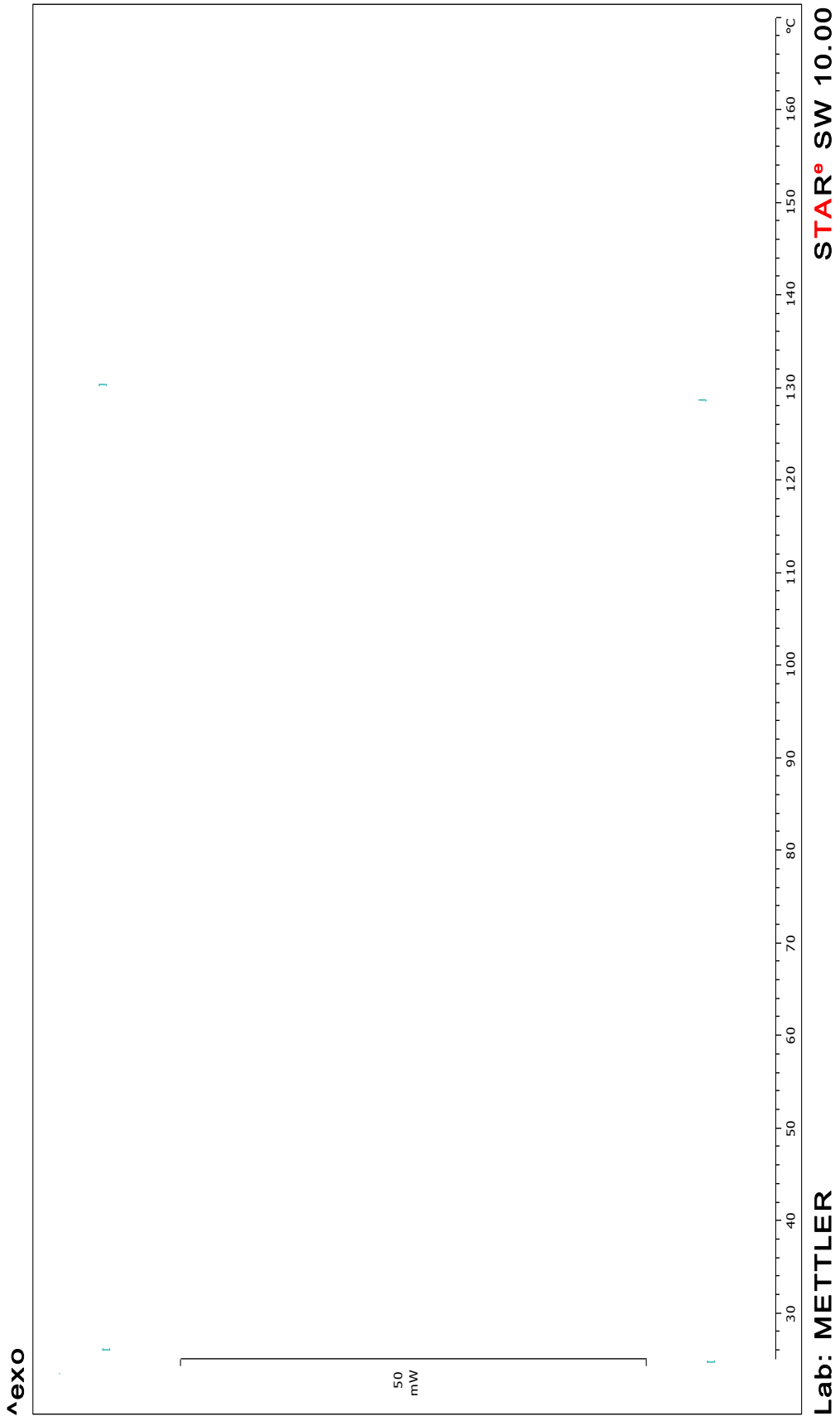

Appendix E1: UV – Vis spectrum of compound DC3C

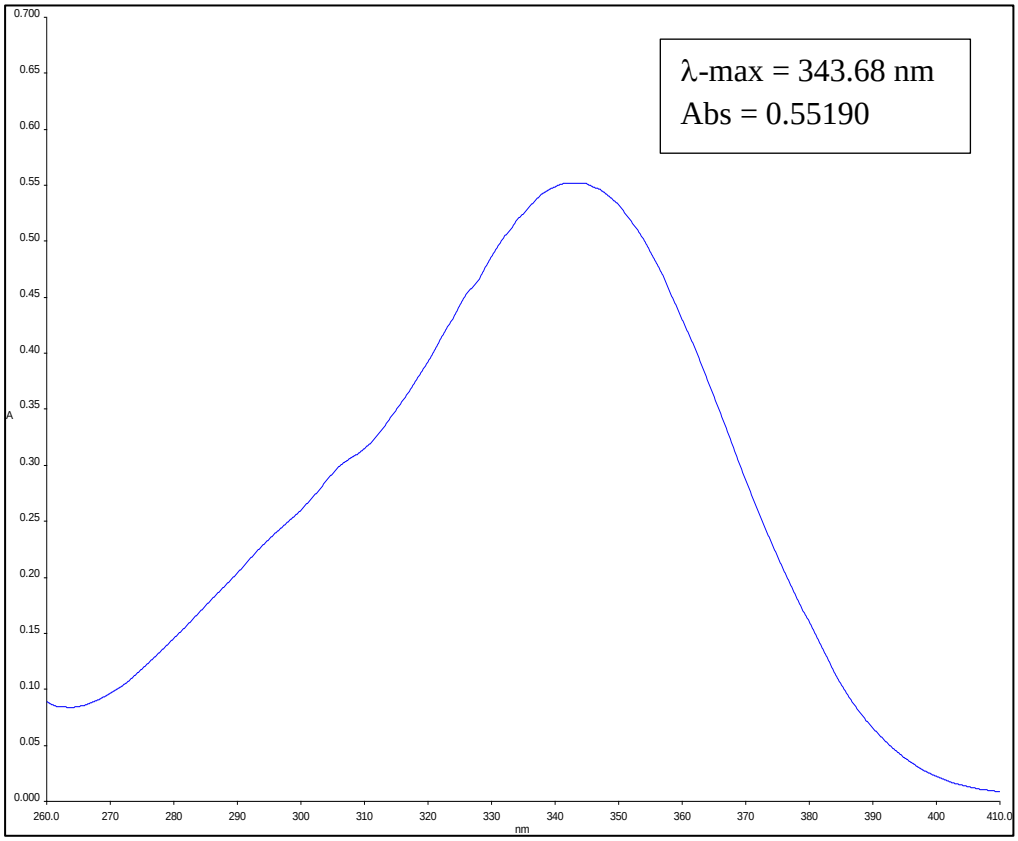

Appendix E2: UV – Vis spectrum of compound DC4C

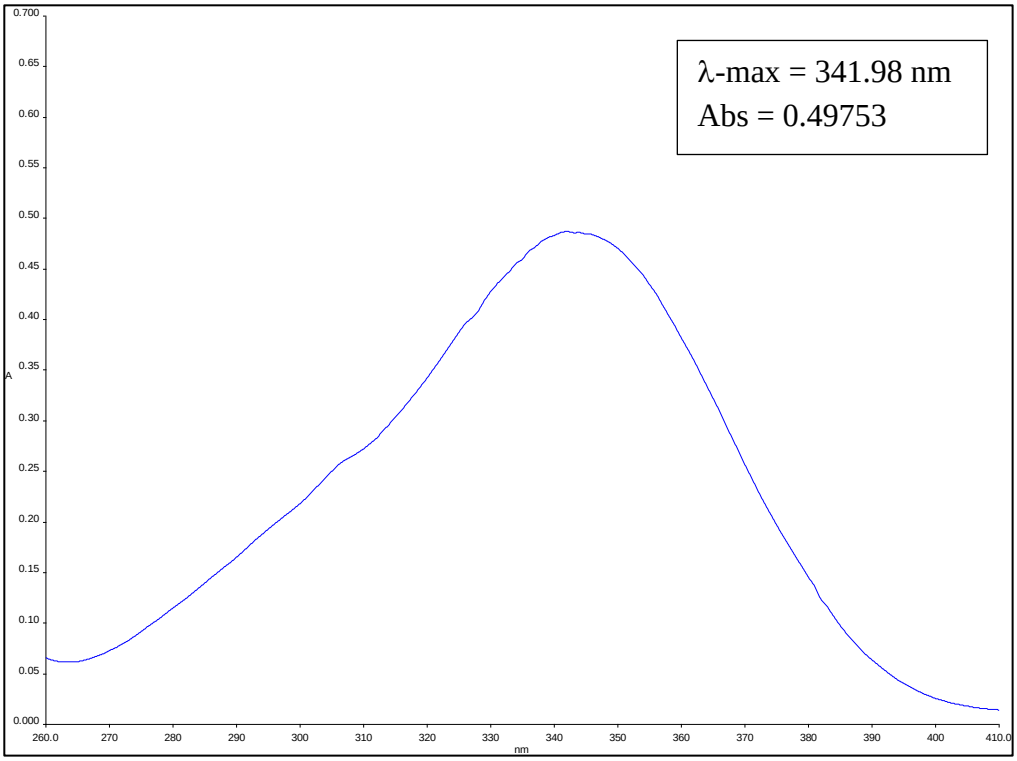

Appendix E3: UV – Vis spectrum of compound DC5C

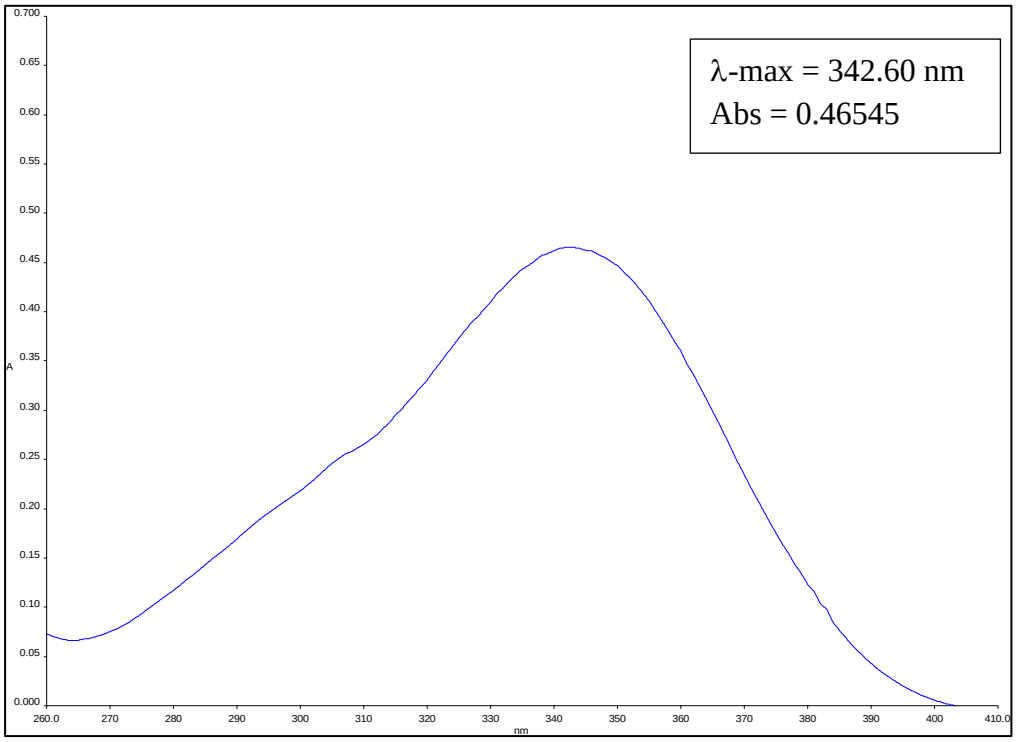

Appendix E4: UV – Vis spectrum of compound DC6C